FRACTIONAL BROWNIAN MOTION AND DYNAMIC APPROACH TO COMPLEXITY

Rasit Cakir

Dissertation Prepared for the Degree of

DOCTOR OF PHILOSOPHY

UNIVERSITY OF NORTH TEXAS

August 2007

APPROVED:

Paolo Grigolini, Major Professor
Arkadii Krokhin, Committee Member
James Roberts, Committee Member
Duncan L. Weathers, Committee Member
Floyd McDaniel, Chair of the Department of Physics
Sandra L. Terrell, Dean of the Robert B. Toulouse School of Graduate Studies

Cakir, Rasit, Fractional Brownian motion and dynamic approach to complexity. Doctor of Philosophy (Physics), August 2007, 103 pp., 42 illustrations, references, 52 titles.

The dynamic approach to fractional Brownian motion (FBM) establishes a link between non-Poisson renewal process with abrupt jumps resetting to zero the system's memory and correlated dynamic processes, whose individual trajectories keep a non-vanishing memory of their past time evolution. It is well known that the recrossing times of the origin by an ordinary 1D diffusion trajectory generates a distribution of time distances between two consecutive origin recrossing times with an inverse power law with index μ=1.5. However, with theoretical and numerical arguments, it is proved that this is the special case of a more general condition, insofar as the recrossing times produced by the dynamic FBM generates process with μ=2-H. Later, the model of ballistic deposition is studied, which is as a simple way to establish cooperation among the columns of a growing surface, to show that cooperation generates memory properties and, at same time, non-Poisson renewal events. Finally, the connection between trajectory and density memory is discussed, showing that the trajectory memory does not necessarily yields density memory, and density memory might be compatible with the existence of abrupt jumps resetting to zero the system's memory.

CONTENTS

LIST OF FIGURES

CHAPTER 1

INTRODUCTION

This thesis addresses the problem of the dynamic approach to fractional Brownian motion (FBM), for the main purpose of shedding light into some misleading opinions that have been haunting this subject, since the original work of Mandelbrot and Van Ness [1]. In fact, FBM is generally considered to be a process generating anomalous diffusion, either faster or slower than ordinary diffusion, as a consequence of infinite memory. This infinite memory is usually considered to be incompatible with the renewal properties that many physical processes, from blinking quantum dots (BQD) to the random growth of surfaces [2], are revealing with increasing theoretical and experimental evidence.

The first part of this thesis proves that memory resides in the velocity variable, whose fluctuations generate the diffusion process, whose time asymptotic properties, in turn, become indistinguishable from the FBM prescription. The space variable x, in the scaling limit, becomes a renewal variable. Studying the crossings of the space origin, $x = 0$, and recording the times at which the crossings occur, it can be proved that the space variable, x, is a time sequence that is a non-ergodic, non-Poisson process. The rigorous proof of this important property is obtained by applying to the recorded sequence a method of analysis, called aging experiment, which has been applied with success to the BQD data to prove rigorously their renewal nature. As a consequence of our analysis, the process of x-axis recrossing is proved to be renewal and non-ergodic. In conclusion, the first result proved by this thesis is that the supposedly infinite memory of FBM is the physical manifestation of ergodicity breakdown.

The second part of this thesis is a review of some work recently done in the field of random growth of interfaces and proves that the process of random growth of interfaces shares the same properties as dynamic FBM, with the coexistence of memory and renewal properties.

Finally, the third part of the thesis addresses theoretical issues concerning the formal equivalence between the generalized master equation of renewal origin and the generalized master equation of memory origin. It proves that, in spite of the formal equivalence, these processes are different and the conjecture is made that they will yield different responses to external perturbations.

CHAPTER 2

DYNAMIC APPROACH TO FRACTIONAL BROWNIAN MOTION

FBM is a random process with long memory dependence and with a defined scaling. In this chapter, a dynamic approach to FBM is proposed, to prove that despite a general conviction to the contrary this generates renewal events.

2.1. Diffusion Equation

The representation of the Brownian motion by means of probability yields,

$$\frac{\partial}{\partial t}p_B(x,t) = D\frac{\partial^2}{\partial x^2}p_B(x,t), \tag{2.1}$$

which is the normal diffusion process, where $p(x,t)$ is the probability density and D is the diffusion constant (App. A). The solution is well known.

$$p_B(x,t) = \frac{1}{\sqrt{4\pi D t}}\exp\left(-\frac{x^2}{4Dt}\right). \tag{2.2}$$

FBM can be obtained by generalizing BM as

$$p(x,t) = \frac{1}{\sqrt{4\pi D t^{2H}}}\exp\left(-\frac{x^2}{4D t^{2H}}\right), \tag{2.3}$$

where $0 < H < 1$. When $H = 1/2$, it becomes a normal diffusion process.

Let us consider a general form of the diffusion equation:

$$\frac{\partial}{\partial t}\tilde{p}(x,t) = D\left(\int_0^t d\tau \Phi_\xi(\tau)\right)\frac{\partial^2}{\partial x^2}\tilde{p}(x,t) = D(t)\frac{\partial^2}{\partial x^2}\tilde{p}(x,t), \tag{2.4}$$

where Φ_ξ is the correlation function of the stochastic noise which will be defined later. The solution of this equation is (App. B)

$$\tilde{p}(x,t) = \frac{1}{\sqrt{2\pi D < x^2(t) >}}\exp\left(-\frac{x^2(t)}{2D < x^2(t) >}\right). \tag{2.5}$$

In App. C, it is also shown that, when $t \to \infty$, $p(x,t)$ is the solution of the general diffusion equation. Since $\lim_{t\to\infty} p(x,t) = \tilde{p}(x,y)$, FBM has long time scale property.

2.2. Long Range Memory over the Stochastic Velocity

Let us consider the equation of free diffusion.

$$\frac{d}{dt}x(t) = \xi(t) \tag{2.6}$$

The Gaussian random variable ξ can be thought of the stochastic velocity of a particle with a time independent Gaussian distribution of zero average and constant variance.

$$p(\xi) = \frac{1}{\sqrt{2\pi \langle \xi^2 \rangle}} \exp\left(-\frac{\xi^2}{2\langle \xi^2 \rangle}\right). \tag{2.7}$$

The properties of the position of the particle, x, simply depend on ξ. The trajectory for a single particle is a fluctuation around zero so that $< x >= 0$. Calculation of the variance $\sigma^2 =< x^2 >$ by using $x(t) = \int_0^t \xi(t')dt' + x(0)$ gives

$$< x^2 >= \int_0^t dt' \int_0^t dt'' < \xi(t')\xi(t'') >, \tag{2.8}$$

where ξ and $x(0)$ are uncorrelated. Using the definition of the correlation function,

$$\Phi_\xi(t', t'') \equiv \frac{< \xi(t')\xi(t'') >}{< \xi^2 >}. \tag{2.9}$$

Eq. 2.8 turns into (App. D)

$$< x^2 >= 2 < \xi^2 > \int_0^t dt' \int_0^{t'} dt'' \Phi_\xi(t''). \tag{2.10}$$

In case of ordinary BM, $\xi(t)$ is uncorrelated random variable so $\Phi_\xi(t) = \delta(t)$, which gives

$$< x^2 >= 2 < \xi^2 > t. \tag{2.11}$$

Since there is no dissipating force, x is growing with $\sqrt{t}$ because of the fluctuation.

In FBM, $\Phi_\xi(t)$ is no longer a delta function. Since FBM has long range memory, the auto-correlation of ξ is chosen as power law. If we calculate the variance, $< x^2 >= \int_{-\infty}^{\infty} x^2 p(x, t)dx$, using Eq. 2.3, we obtain (App. E)

$$< x^2(t) >= 2Dt^{2H}. \tag{2.12}$$

For $H = 1/2$, $< x^2(t) >= 2Dt$, which gives $D =< \xi^2 >$.

Let us go back to Eq. 2.10 for FBM. The second derivative of it is

$$\frac{d^2}{dt^2} < x^2 >= 2 < \xi^2 > \Phi_\xi(t). \tag{2.13}$$

The function $\xi(t)$ is a stochastic process with power law correlation, $\Phi_\xi(t) \propto 1/t^\beta$. Let us take the derivative of Eq 2.12.

$$\frac{d^2}{dt^2} < x^2 >= 2D2H(2H-1)t^{2H-2} = 2 < \xi^2 > \Phi_\xi(t) \propto 1/t^\beta. \tag{2.14}$$

The relation between the scaling and the power law correlation of ξ is obtained as

$$\beta = 2 - 2H \tag{2.15}$$

and the coefficient becomes negative when $H < 1/2$. The general form of the correlation function becomes

$$\Phi_\xi(t) \propto \begin{cases} 1/t^\beta & \text{for } 1 > H > 1/2, \text{ super-diffusion;} \\ \delta(t) & \text{for } H = 1/2, \text{ normal diffusion;} \\ -1/t^\beta & \text{for } 0 < H < 1/2, \text{ sub-diffusion.} \end{cases} \tag{2.16}$$

When $H > 1/2$, x diffuses faster than the normal diffusion, which is called *super-diffusion*. Because of the positive correlation of ξ, particles tend to diffuse in the same direction. And when $H < 1/2$, x diffuses slower than the normal diffusion, which is called *sub-diffusion*. For $H \neq 1/2$, $\xi(t)$ has long range memory that is the reason of the anomalous diffusion.

2.3. Scaling

The scaling from the probability distribution function is defined as δ by

$$p(x, t) = \frac{1}{t^\delta} F\left(\frac{x}{t^\delta}\right), \tag{2.17}$$

where F is an arbitrary function. So Eq. 2.3 gives the scaling $\delta = H$. Diffusion entropy (DE) calculations determine the scaling through the property (App. F):

$$S(t) = -\int p \ln(p) dx = A + \delta \ln(t). \tag{2.18}$$

The scaling can also be determined using the variance. The variance is defined as

$$< x^2 >= \int_{-\infty}^{\infty} x^2 p(x,t) dx. \tag{2.19}$$

From App. E, we get

$$< x^2 >= 2Dt^{2H}. \tag{2.20}$$

Since the scaling is an asymptotic property, variance and DE will reach the scaling regime when $t \to \infty$. In this work, scaling will be represented as H.

2.4. Renewal Properties

2.4.1. *Recrossing Times*

The renewal properties of FBM will be first shown by the recrossing times of $x(t)$ and $\xi(t)$. Recrossing times of a function f is the time distance τ between successive time value when $f(t) = 0$. Let us first make the critical assumption, which will be checked numerically, that in the scaling regime of Eq. 2.17 the process is renewal, which means that recrossing times of $x(t)$ are statistically independent.

The trajectory $x(t)$, which at $t = 0$ starts from $x = 0$, contributes to the probability $p(0, t)$, due to successive recrossing of the x axes at later times. The rate of occurrence of recrossing times is the density at the origin and it can be written as follows (Eq. 2.3):

$$R(t) = p(0,t) \propto 1/t^H. \tag{2.21}$$

The distribution of recrossing times will be assumed to be given by the power law

$$\psi(\tau) = (\mu - 1)\frac{T^{\mu-1}}{(T+\tau)^{\mu}}, \tag{2.22}$$

where T is a constant that defines the time scale. Let us find the relation between μ and H. The rate of occurrence of recrossing times is the summation of all possible recrossing times that occur n times with the last occurring exactly at time t.

$$R(t) = \sum_{n=1}^{\infty} \psi_n(t). \tag{2.23}$$

With this equation, it is assumed that at this time at least one collision occurs after the initial time. Using (App. G)

$$\hat{\psi}_n(u) = (\hat{\psi}(u))^n, \tag{2.24}$$

Eq. 2.23 can be rewritten as

$$\hat{R}(t) = \sum_{n=1}^{\infty} \hat{\psi}_n(u) = \sum_{n=1}^{\infty} \left(\hat{\psi}(u)\right)^n. \tag{2.25}$$

Because of the normalization, $\int_0^\infty \psi(t)dt = 1$, with $u > 0$, $\hat{\psi}(u) = \int_0^\infty exp(-ut)\psi(t)dt$ is a number smaller than 1. Therefore, Eq. 2.25 yields

$$\hat{R}(t) = \frac{\hat{\psi}(u)}{1 - \hat{\psi}(u)}. \tag{2.26}$$

Using power law assumption and from Eq. H.5 in App. H, we have

$$\lim_{u\to 0} \frac{\hat{\psi}(u)}{1 - \hat{\psi}(u)} \approx \frac{1 - \Gamma(2-\mu)T^{\mu-1}u^{\mu-1}}{1 - (1 - \Gamma(2-\mu)T^{\mu-1}u^{\mu-1})} \approx \frac{1}{\Gamma(2-\mu)T^{\mu-1}u^{\mu-1}} \propto u^{1-\mu}. \tag{2.27}$$

Comparing Eq. 2.21 and Eq. 2.27, and using $\mathcal{L}[t^{-H}] = \Gamma(1-H)u^{H-1}$, we get

$$u^{H-1} \propto u^{1-\mu}. \tag{2.28}$$

so for long time scale

$$H = 2 - \mu. \tag{2.29}$$

This relation has been originally derived using FBM theory, and therefore it was considered to imply trajectory memory on x. We will see that this is not so.

2.4.2. *Renewal Aging*

The renewal properties of FBM can also be shown by the aging calculation. To see what is aging, let us look at Fig. 2.1. The time distances τ_i are from the distribution of recrossing times, $\psi(\tau)$.

Consider an ensemble number of the trajectory $x(t)$. Each of the time values of $x(t) = 0$ is considered as an event. If the observation starts at $t = 0$, which is also an event, the time until next event is τ_1. So this time is selected from the distribution, $\psi(\tau)$. But, if the observation starts from an arbitrary time $t_a > 0$, which is not necessarily an

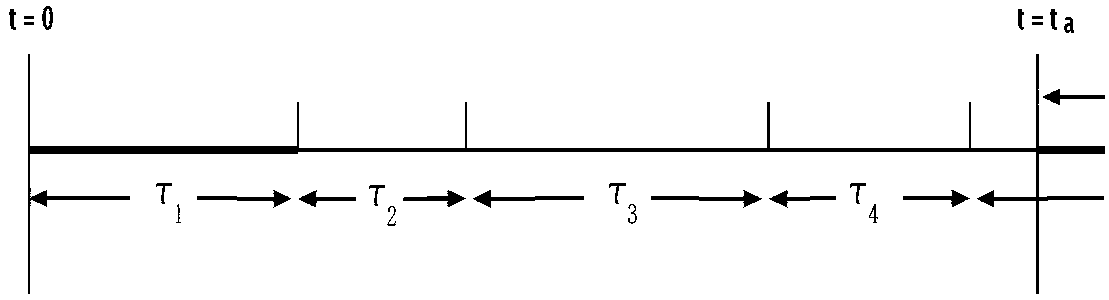

Figure 2.1. Aging experiment.

event, the time until next event is τ_1^a. If the distribution of this time, $\psi_a(\tau)$, is different from $\psi(\tau)$, then the recrossing times have an aging property.

Aging can be considered as the change of the system towards equilibrium. $\psi_a(\tau)$ would give the renewal aging if x(t) could reach equilibrium. But when $t_a \to \infty$, $\psi_a(\tau)$ will approach renewal aging distribution.

The analytical form of it is given by [9]

$$\psi_a(\tau) = \psi(t, t_a) = \sum_{n=0}^{\infty} \int_0^{t_a} \psi_n(\tau)\, \psi(t-\tau)\, d\tau. \tag{2.30}$$

It can be again explained from Fig. 2.1. The ensemble has been prepared at $t = 0$. The last nth event just before t_a has happened exactly at time τ, where $0 < \tau < t_a$. The number of events, n, can be any integer 0 to infinity. The probability $\psi_n(\tau)$ is the probability for n events to happen with the last one at time τ. After that the $(n+1)$st event will happen at $t > t_a$, with probability $\psi(t-\tau)$.

This expression is exact but it is not quite useful for practical purposes. It is more convenient to use an approximated expression [10]. Let us write Eq. 2.30 as

$$\psi(t, t_a) = \int_0^{t_a} P(\tau)\, \psi(t-\tau)\, d\tau, \tag{2.31}$$

where

$$P(\tau) = \sum_{n=0}^{\infty} \psi_n(\tau). \tag{2.32}$$

The meaning of $P(\tau)$ is the probability of an event to occur at t. The Laplace transform of $P(\tau)$ has been done for $1 < \mu < 2$. Using App. G, Eq. 2.26 and Eq. 2.27,

$$\hat{P}(u) = \sum_{n=0}^{\infty} \hat{\psi}_n(u) = \sum_{n=0}^{\infty} (\hat{\psi}(u))^n = \frac{1}{1-\hat{\psi}(u)} \approx \frac{1}{\Gamma(2-\mu)T^{\mu-1}u^{\mu-1}}. \tag{2.33}$$

The inverse Laplace transform simply is

$$P(t) \approx \frac{1}{\Gamma(2-\mu)T^{\mu-1}} \frac{1}{\Gamma(\mu-1)} \frac{1}{t^{2-\mu}} \tag{2.34}$$

and finally Eq. 2.30 becomes

$$\psi(t, t_a) \approx \frac{1}{\Gamma(2-\mu)T^{\mu-1}\Gamma(\mu-1)} \int_0^{t_a} \frac{1}{t^{2-\mu}}\ \psi(t-\tau)\ d\tau. \tag{2.35}$$

In the numeric calculations, $P(t)$ is considered as constant; therefore

$$\psi(t, t_a) \approx N \int_0^{t_a} \psi(t-\tau)\ d\tau \tag{2.36}$$

is used to compare the simulation results.

2.5. Non-ergodicity

The correlation of $x(t)$ can be obtained from the variance. (App. I)

$$\Phi(t, t_0) = \frac{< x(t)x(t_0) >}{< x^2(t_0) >} = \frac{1}{2}\left(\left(\frac{t}{t_0}\right)^{2H} + 1 - \left(\frac{t}{t_0} - 1\right)^{2H}\right) \tag{2.37}$$

Let us put $t \to t$ and $t_0 \to -t$. Eq. 2.37 becomes

$$\frac{< x(t)x(-t) >}{< x^2(t) >} = 1 - 2^{2H-1} \tag{2.38}$$

When, $H = 1/2$, for BM, Eq. 2.38 becomes zero and it is non-zero otherwise. This has been considered a non-Markovian process with the well known property of non-decaying correlations between future and past [5][6]. And, this property has been accepted as the memory of individual trajectories because it is zero for BM and nonzero for $H \neq 1/2$. In fact, Eq. 2.38 is misleading. If we look at Eq. 2.37, we see that $\Phi(t, t_0) = 1$ for

$H = 1/2$, which means that the equation being constant doesn't mean memory. Fig. 2.2 shows that there is positive correlation for all of the three cases.

The reason is that the average over ensembles does not afford information about the trajectory $x(t)$, because $x(t)$ is not *ergodic*. Since the correlation function in Eq. 2.37 depends on the initial time t_0, we have

$$\Phi(t, t_0) \neq \Phi(|t - t_0|), \tag{2.39}$$

which means $x(t)$ is not stationary. For a single trajectory $x(t)$ tends to be usually positive or negative but we know that $< x >= 0$ so we cannot use the equivalence of time and ensemble averages. The average over the trajectory time keeps changing and does not give the ensemble average. Eq. 2.38 does not depend on the trajectory memory. It depends on the non-ergodic nature of the process. The numerical calculations, indeed, show that $x(t)$ is *renewal*, implying that the trajectory does not have memory.

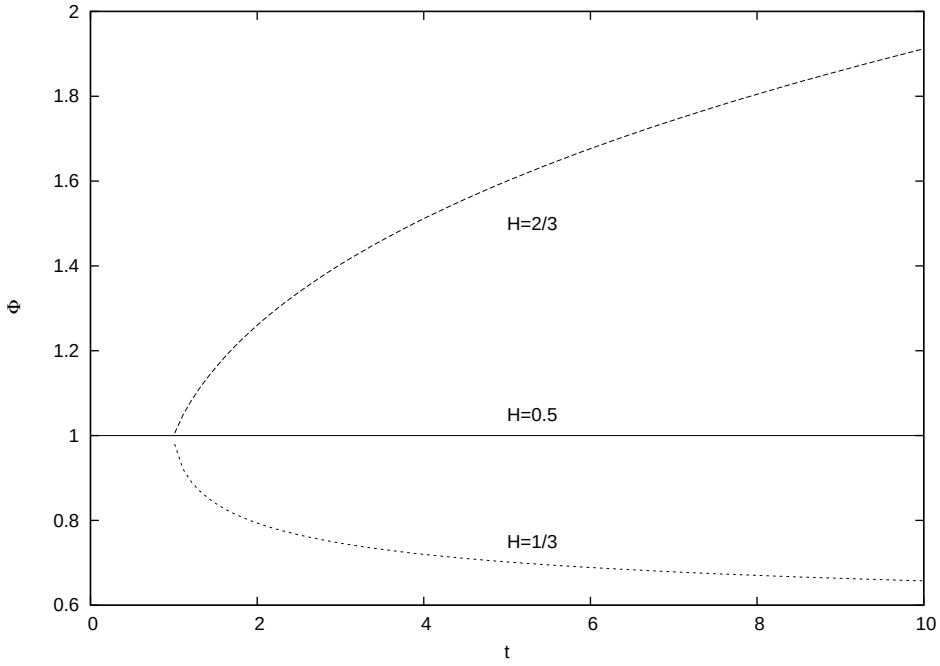

Figure 2.2. The correlation of $x(t)$ for normal diffusion, sub- diffusion and super-diffusion. $t_0 = 1$.

CHAPTER 3

NUMERICAL CALCULATIONS

3.1. Renewal and Cooperation Model

The Renewal and Cooperation (RC) model is is based on the equation

$$\dot{x} = \xi(t). \tag{3.1}$$

The stochastic variable $\xi(t)$ has a long-range correlation, $< \xi(t)\xi(t') >= \xi_0^2 \Phi_\xi(t - t')$. The long-range properties of the variable $\xi(t)$ are determined by cooperation. The variable x is responsible for renewal.

Let us illustrate first the cooperative and memory properties of the RC model. $\xi(t)$ is derived from the non-Ohmic bath [3]

$$\xi(t) = \sum_i c_i \left[x_i(0) \cos \omega_i t + v_i(0) \omega_i^{-1} \sin \omega_i t \right]. \tag{3.2}$$

Here $x_i(0)$ and $v_i(0)$ are randomly selected from the canonical distribution $\exp[-(\omega_i^2 x_i^2 + v_i^2)/k_B T)]/Z$, and $c_i^2 = \omega_i^{\beta-1}$.

Let us assume that the frequencies ω_i range from $\omega_0 = 0$ to ω_D and let us divide the interval $[0, \omega_D]$ into N small intervals as

$$\omega_i = \frac{i}{N} \omega_D. \tag{3.3}$$

The average on the Gibbs ensemble, since different oscillators are uncorrelated, yields

$$\langle \xi(t)\xi(t') \rangle = \sum_i c_i^2 \left[\left\langle x_i^2(0) \right\rangle \cos(\omega_i t) \cos(\omega_i t') + \frac{\langle v_i^2(0) \rangle}{\omega_i^2} \sin(\omega_i t) \sin(\omega_i t') \right]. \tag{3.4}$$

The adoption of the canonical condition yields

$$\left\langle v_i^2 \right\rangle = \omega_i^2 \left\langle x_i^2 \right\rangle = k_b T. \tag{3.5}$$

Thus, Eq. 3.4 becomes

$$\langle \xi(t)\xi(t')\rangle = k_b T \sum_i \frac{c_i^2}{\omega_i^2}\cos\omega_i(t-t'). \tag{3.6}$$

Using the relation $\overline{\cos(\omega_i t)\cos(\omega_i(t+\tau))} = \overline{\sin(\omega_i t)\sin(\omega_i(t+\tau))} = \frac{\delta_{ij}}{2}\cos(\omega_i t)$, the correlation function of $\xi(t)$, making the time average, becomes

$$\overline{\xi(t)\xi(t+\tau)} = \lim_{T\to\infty}\frac{1}{T}\int_0^T \xi(t)\xi(t+\tau)dt = \sum_{i=1}^{N}\frac{c_i^2}{2}[x_i^2 + \frac{v_i^2}{\omega_i^2}]\cos(\omega_i\tau), \tag{3.7}$$

which is the same result as Eq. 3.6.

The normalized correlation function is

$$\Phi_\xi(|t-t'|) = \frac{\sum_i \frac{c_i^2}{\omega_i^2}\cos\omega_i(t-t')}{\sum_i \frac{c_i^2}{\omega_i^2}}. \tag{3.8}$$

It is straightforward to show that the correlation function $\Phi_\xi(t)$ has the following asymptotic: [4]

$$\lim_{t\to\infty}\Phi_\xi(t) = \lim_{t\to\infty}\frac{<\xi(0)\xi(t)>}{<\xi^2>} \propto \frac{\mathrm{sign}(1-\beta)}{t^\beta}. \tag{3.9}$$

The cooperation is controlled by the parameter β. As we have seen, $c_i^2 \propto \omega_i^{\beta-1}$. Thus $\beta = 1$ is equivalent to assigning the same statistical weight to all the frequencies. The adoption of either $\beta > 1$ or $\beta < 1$ is equivalent to establishing a form of cooperative motion, which yields a strong departure from the white noise condition. Eq. (3.9) shows that the non-Ohmic condition $\beta \neq 1$ leads to either a positive (for $0 < \beta < 1$) or negative (for $1 < \beta < 2$) power law tail of the correlation function. [3, 4] It is important to stress that when $\beta > 1$, the long-time tail generates a negative area which is exactly compensated by the fast decay at the origin, so as to ensure that in the Laplace dominion $\hat{\Phi}(u)|_{u=0} = 0$.

The dynamical RC model of Eq. 3.2 does not yield a very efficient algorithm to create a fluctuation whose correlation function has the same asymptotic property as Eq. 3.9. Because of the term $\cos\omega_i t$ in the summation, it takes too long time to converge to the power law function. Fig. 3.1 shows the correlation function of Eq. 3.8 for the sub-diffusion and super-diffusion case for $N = 10^7$ oscillators. For this reason, two other

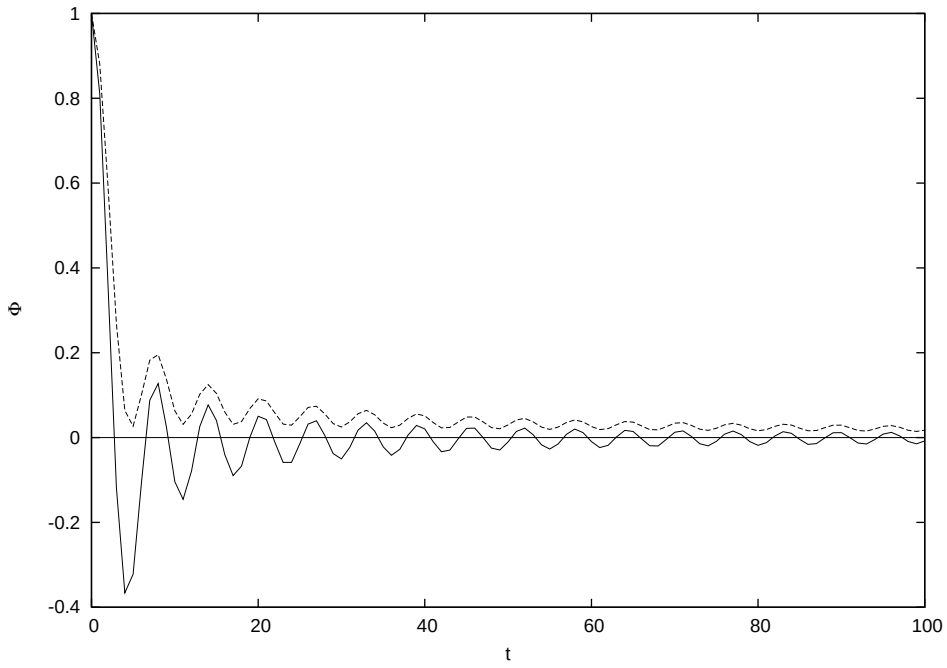

Figure 3.1. The correlation function of $\xi(t)$ for sub-diffusion case (dashed), $H = 1/3$, and super-diffusion case (solid), $H = 2/3$, using the RC model for $N = 10^7$.

kinds of algorithms are used to generate FBM. The first one is the Fourier algorithm [7]. It starts from the correlation functions. and then obtains the trajectories. Later, to check these results, the same properties are obtained again with the Voss algorithm [11]. In the first algorithm, it is possible to generate a trajectory as long as required. But the correlation function has to have a cut-off value. The second algorithm gives limited trajectories while their correlation functions result with no cut-off value.

3.2. The Fourier Algorithm

In the numerical simulations, the discrete time series, $t_n = n = 1, 2, 3, \ldots$ are used to generate the random variable $\xi(n)$ with correlation function Eq. 2.16, having either a positive or negative tail, using the algorithm [7]

$$\xi(n) = \sum_{m=-\infty}^{\infty} \mathcal{R}_{m+n}\, \mathcal{Z}_m \tag{3.10}$$

and

$$\mathcal{Z}_m = \frac{2}{\pi} \int_0^{\pi/2} \sqrt{\mathcal{F}(y)} \cos(2my)dy. \tag{3.11}$$

Here, $\mathcal{R}_n$ are Gaussian random numbers with $< \mathcal{R}_n >= 0$ and $< \mathcal{R}_n^2 >= 1$, and $\mathcal{Z}_m = \mathcal{Z}_{-m}$. The function $\mathcal{F}(y)$ is determined through its Fourier series,

$$\mathcal{F}(y) = 1 + 2\sum_{k=1}^{\infty} \Phi_\xi(k)\cos(2ky). \tag{3.12}$$

Starting from the correlation function Φ_ξ and using the above algorithm, the series $\xi(n)$ and the diffusion trajectory

$$x(n) = \sum_{k=1}^{n} \xi(k) \tag{3.13}$$

are easily generated.

For the super-diffusion case, Φ_ξ is chosen as

$$\Phi_\xi(t) = \left(\frac{T}{T+t}\right)^\beta \tag{3.14}$$

where

$$\beta = 2 - 2H = 2/3$$
$$H = 2/3$$
$$T = 1$$

The correlation function starts from one and is positive since super-diffusion requires positive correlation.

For the sub-diffusion case, Φ_ξ is chosen as

$$\Phi_\xi(t) = \frac{1}{b}\left(\frac{T\Gamma e^{-\Gamma t}}{\beta - 1} - \left(\frac{T}{T+t}\right)^\beta\right) \tag{3.15}$$

where

$$\beta = 2 - 2H = 4/3$$
$$H = 1/3$$
$$T = 1$$
$$b = (T\Gamma + 1 - \beta)/(\beta - 1) = 2$$
$$\Gamma = 1 > (\beta - 1)/T$$

The correlation function starts from one and it has a negative tail since sub-diffusion requires negative correlation. Note that the parameter values are close so as to ensure $\int_0^\infty \Phi_\xi(t)dt = 0$ for sub-diffusion. In fact, the negative value is unphysical and it would produce ordinary diffusion in the long time limit.

The index k in Eq. 3.12 goes to 1000 and also m in Eq. 3.10 is in the range $-1000 < m < 1000$ so the correlation functions are cut at $t = 1000$. At the end, the stochastic x and ξ values are obtained for required time values.

These analytical forms of Φ_ξ in Eq. 3.14 and 3.15, and the results from the algorithm are compared in Fig. 3.2 and Fig. 3.3. They are plotted in normal and log-log scales to see the values in short and long times.

Variance and DE calculations in Figs. 3.4, 3.6, 3.5 and 3.7 yield the correct slopes, approaching the expected scaling values, until the cut-off time. After that they show that normal diffusion is obtained.

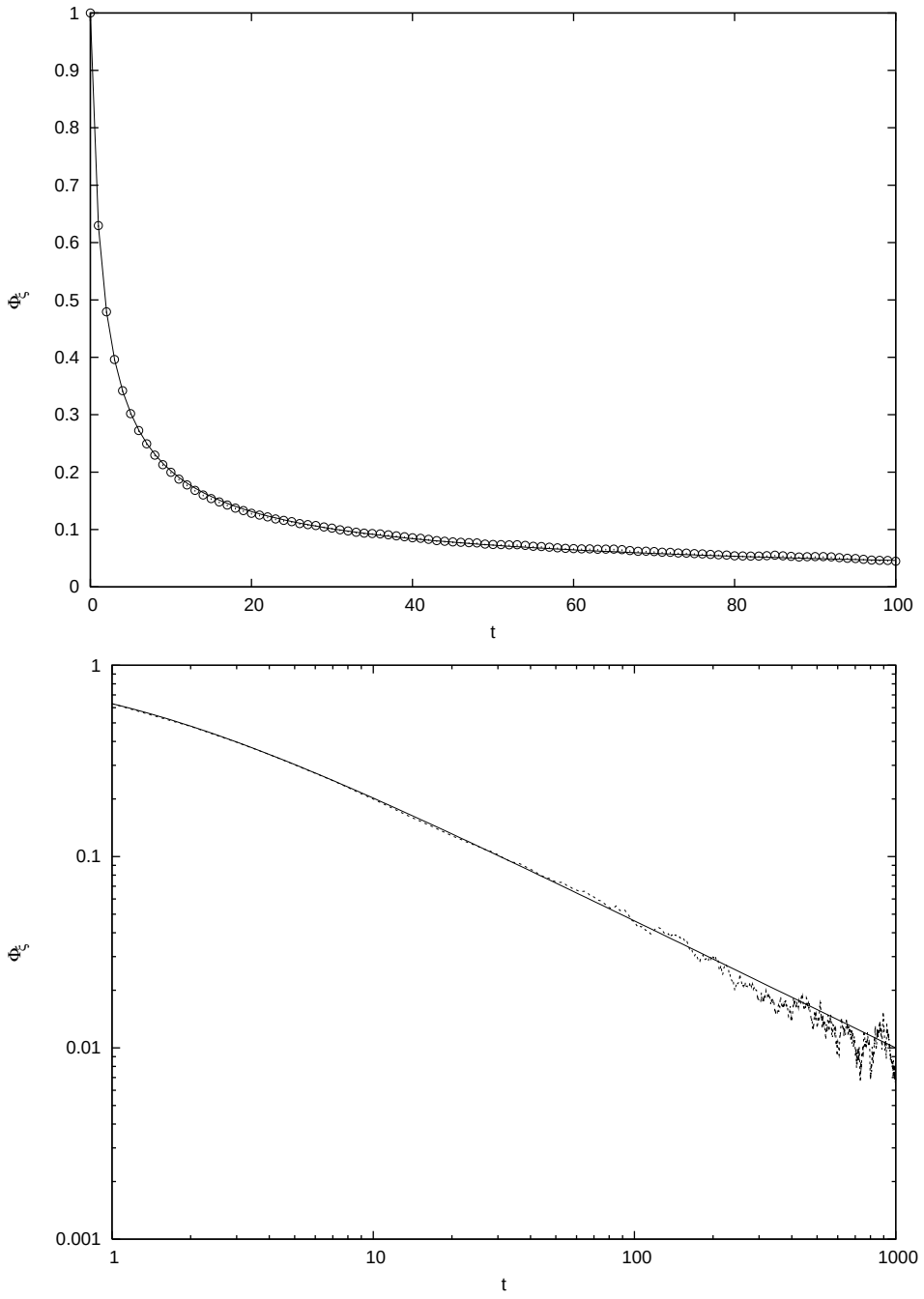

Figure 3.2. The correlation function of $\xi(t)$ for the super-diffusion case, $H = 2/3$ in normal (top) and log-log (bottom) scale. The analytical forms are solid lines and the correlations from the algorithm are circles and dashed line.

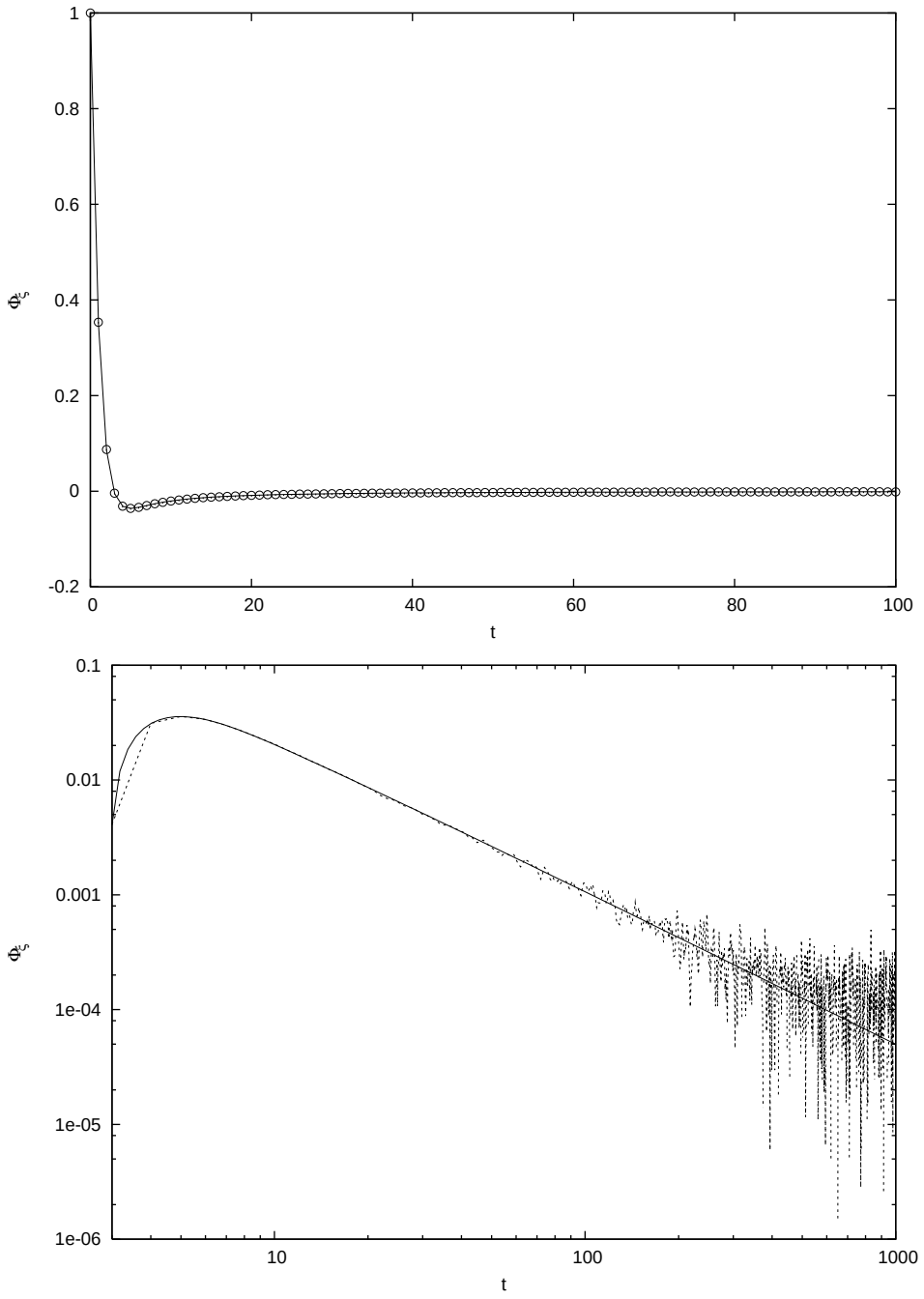

Figure 3.3. The correlation function of $\xi(t)$ for the sub-diffusion case, $H = 1/3$ in normal (top) and log-log (bottom) scales. The analytical form are solid lines and the correlations from the algorithm are circles and dashed line.

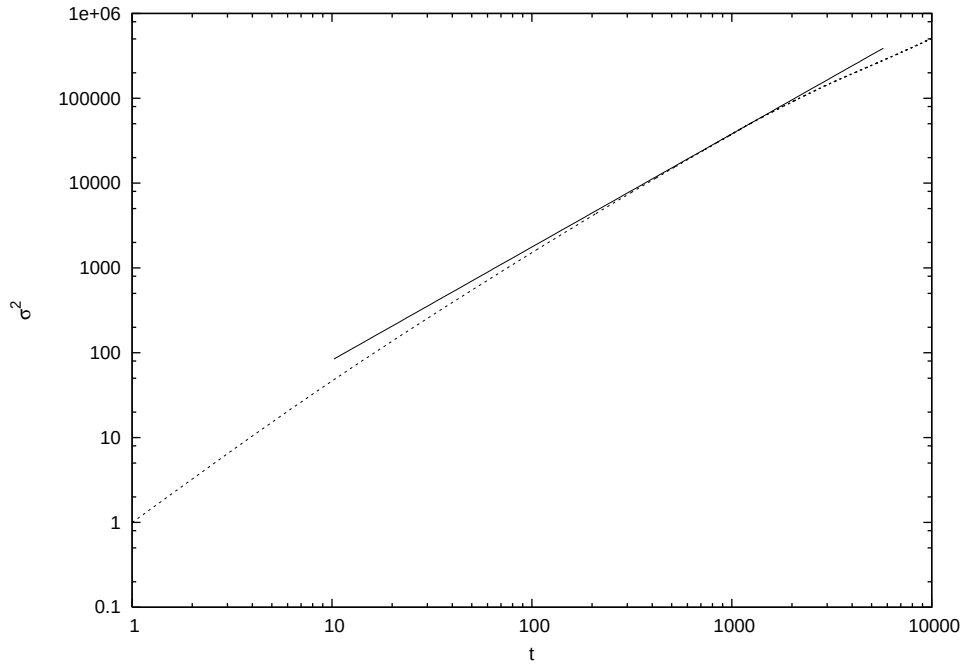

Figure 3.4. Variance for the super-diffusion case, $H = 2/3$ (dashed). The solid lines is $3.8x^{4/3}$.

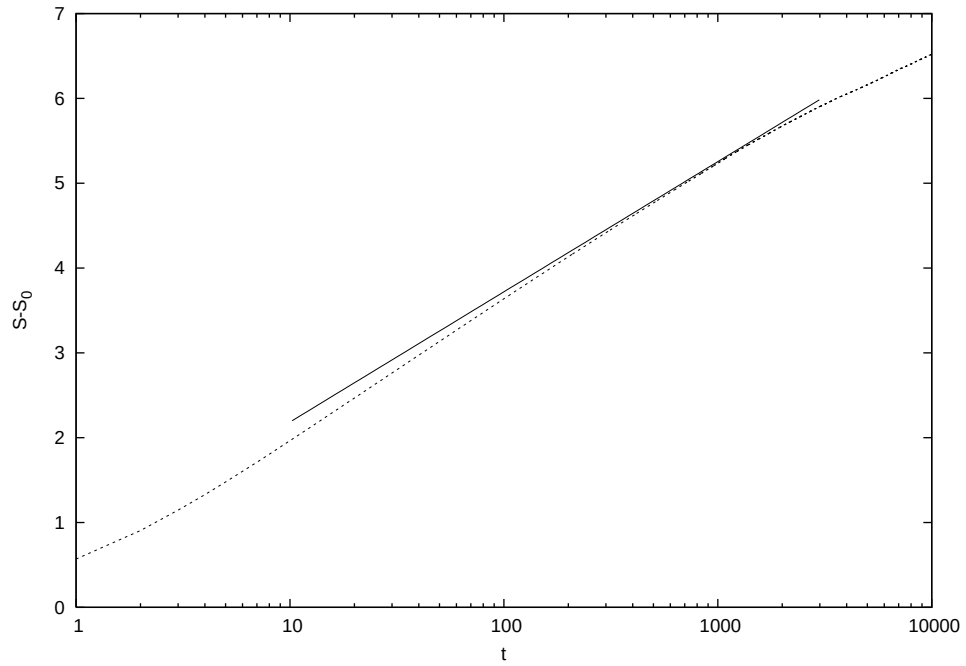

Figure 3.5. Diffusion entropy for the super-diffusion case, $H = 2/3$ (dashed). The solid lines is $0.6666\log(x) + 0.65$.

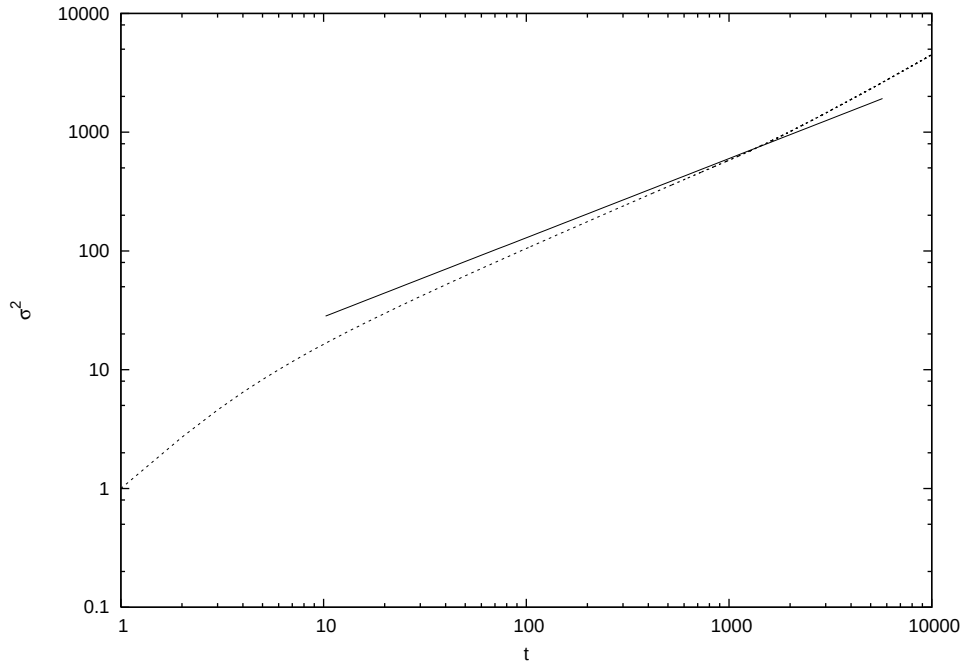

Figure 3.6. Variance for the sub-diffusion case, $H = 1/3$ (dashed). The solid lines is $6x^{2/3}$.

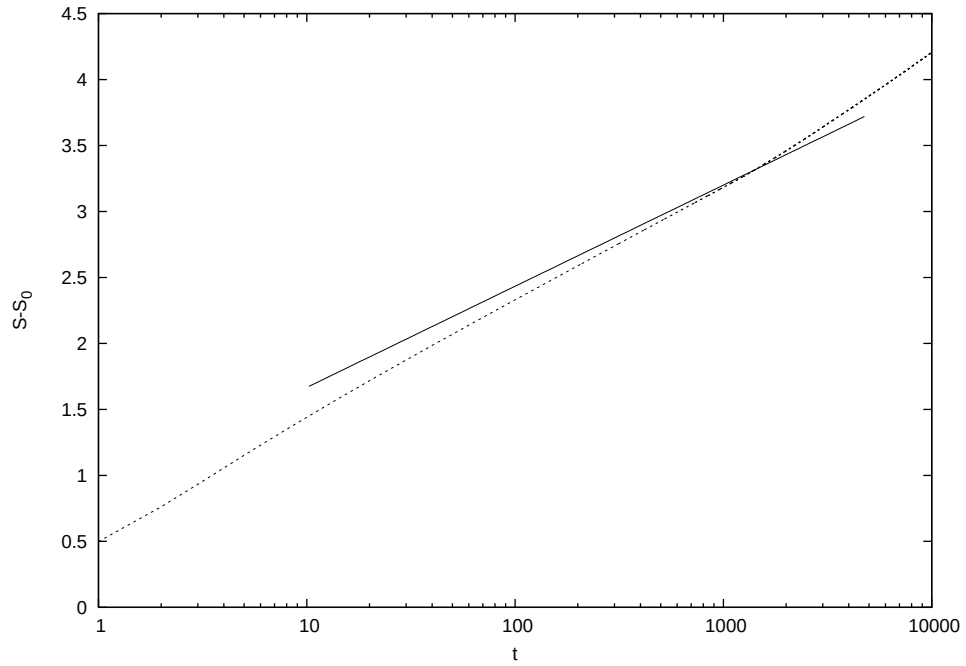

Figure 3.7. Diffusion entropy for the sub-diffusion case, $H = 1/3$ (dashed). The solid lines is $0.333\log(x) + 0.9$.

The numerical results in Fig. 3.8 show that distribution of recrossing times of $x(t)$ reaches a power law for larger time values and recrossing times are delta correlated as shown in Fig. 3.9.

The aging properties are calculated using Eq. 2.36 and are also obtained by aging experiment as in Fig. 2.1. Fig. 3.10 shows the survival probabilities, $\Psi_a(\tau)$, of recrossing times of $H = 1/3$ and $H = 2/3$ for $t_a = 100$ and $t_a = 0$, where

$$\Psi_a(\tau) = \Psi(\tau, t_a) = 1 - \int_0^\tau \psi(\tau, t_a) = \int_\tau^\infty \psi(\tau, t_a) \tag{3.16}$$

For the case of $\xi(t)$, the distribution of recrossing times is exponential, which is shown in Fig. 3.11. There is also correlation of recrossing times in Fig. 3.12 due to the memory on the trajectory $\xi(t)$. They are also plotted in log scale to see the oscillatory decrease in power law.

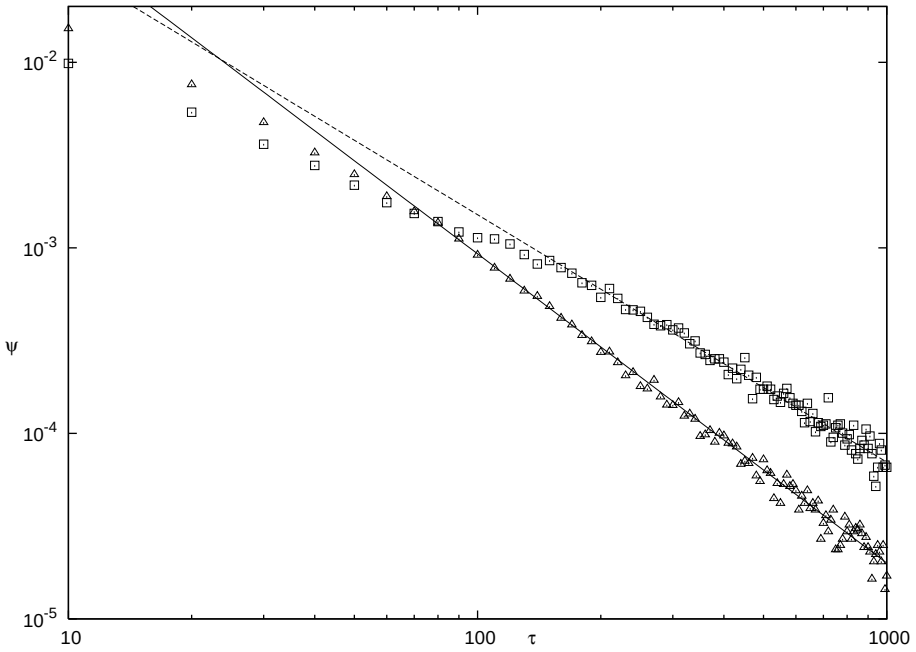

Figure 3.8. The distributions of recrossing times of $x(t)$ for $H = 1/3$ (triangle) and for $H = 2/3$ (square). The former and the latter conditions fit solid line $2\tau^{-5/3}$ and dashed line $0.7\tau^{-4/3}$

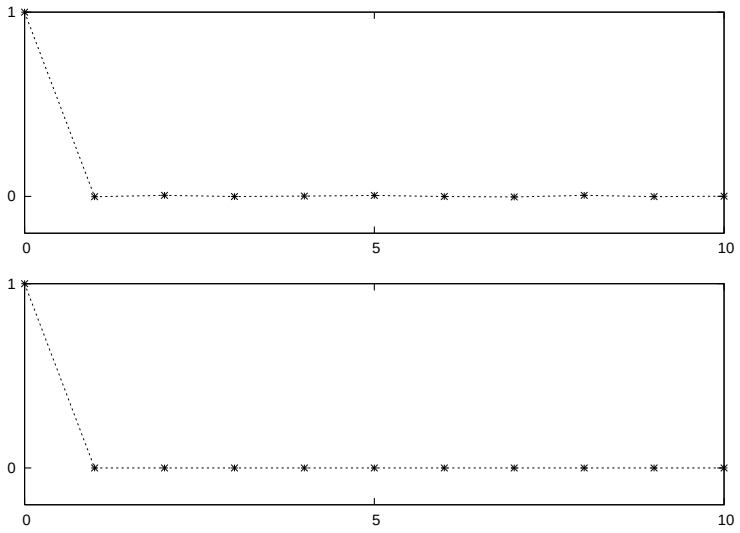

Figure 3.9. Correlation functions of recrossing times of $x(t)$ for $H = 1/3$ (top) and $H = 2/3$ (bottom).

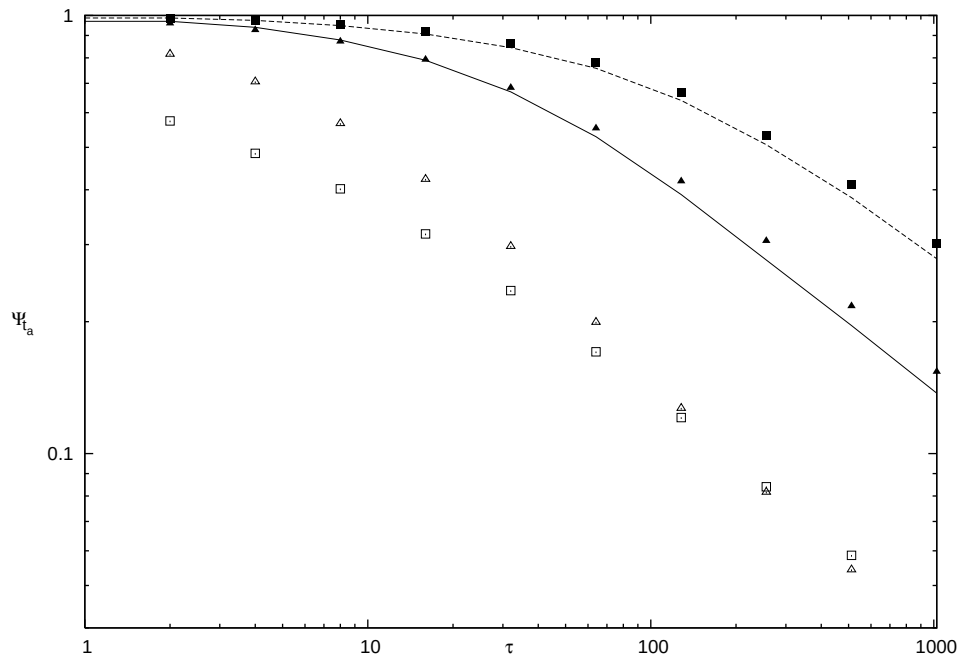

Figure 3.10. Survival probabilities of renewal aging of recrossing times of $x(t)$ for $t_a = 100$. Aging experiment for $H = 1/3$ as full triangle and for $H = 2/3$ as full square and analytical forms of Eq. 2.35 for $H = 1/3$ as solid line and for $H = 2/3$ as dashed line are compared. The normal distributions are also shown ($t_a = 0$) for $H = 1/3$ as empty triangle and for $H = 2/3$ as empty square.

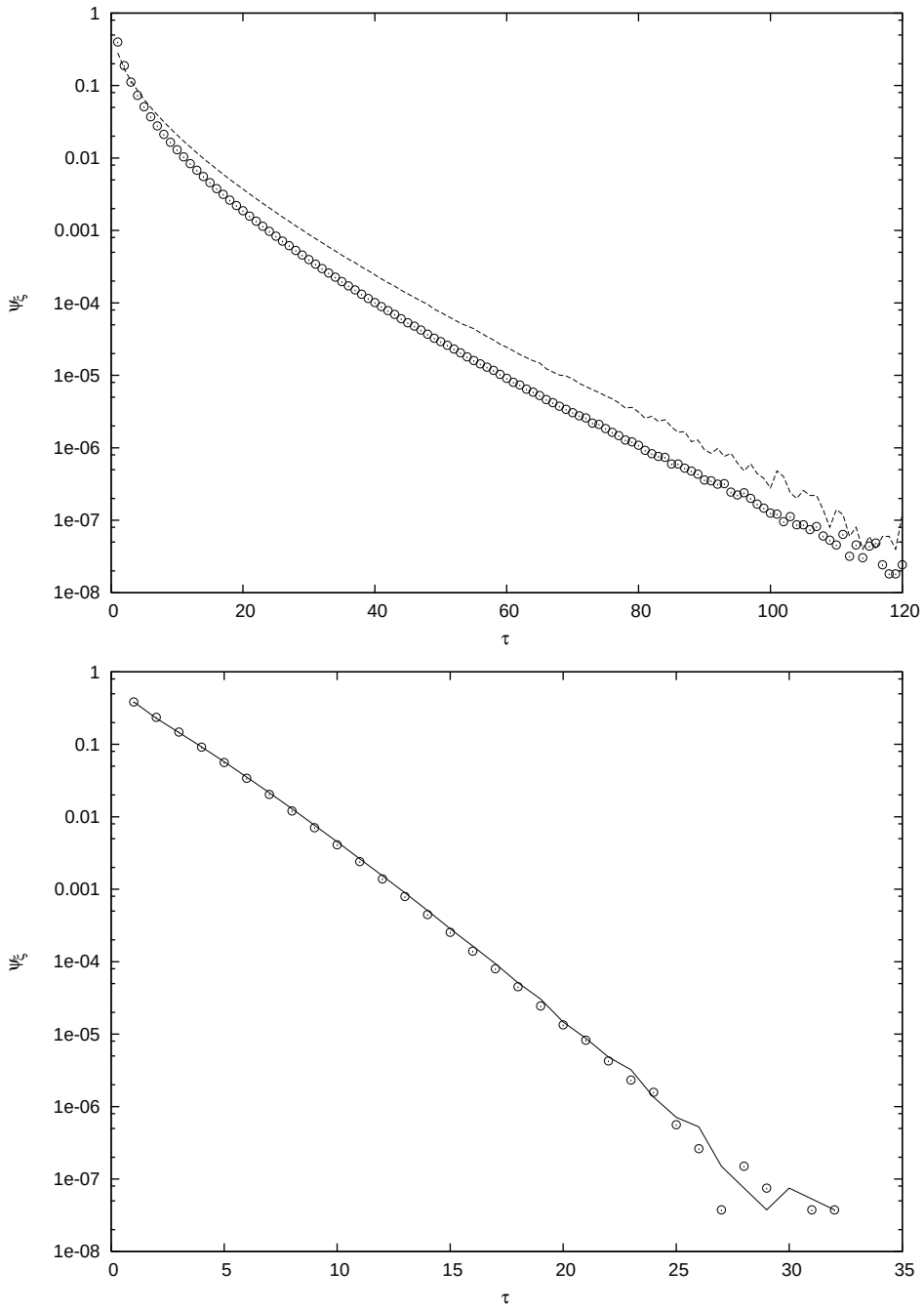

Figure 3.11. The distributions of recrossing times of $\xi(t)$ for $H = 2/3$ (above) and for $H = 1/3$ (below), fitting dashed line $0.01exp(-0.1\tau)$ and solid line $0.4exp(-0.3\tau)$.

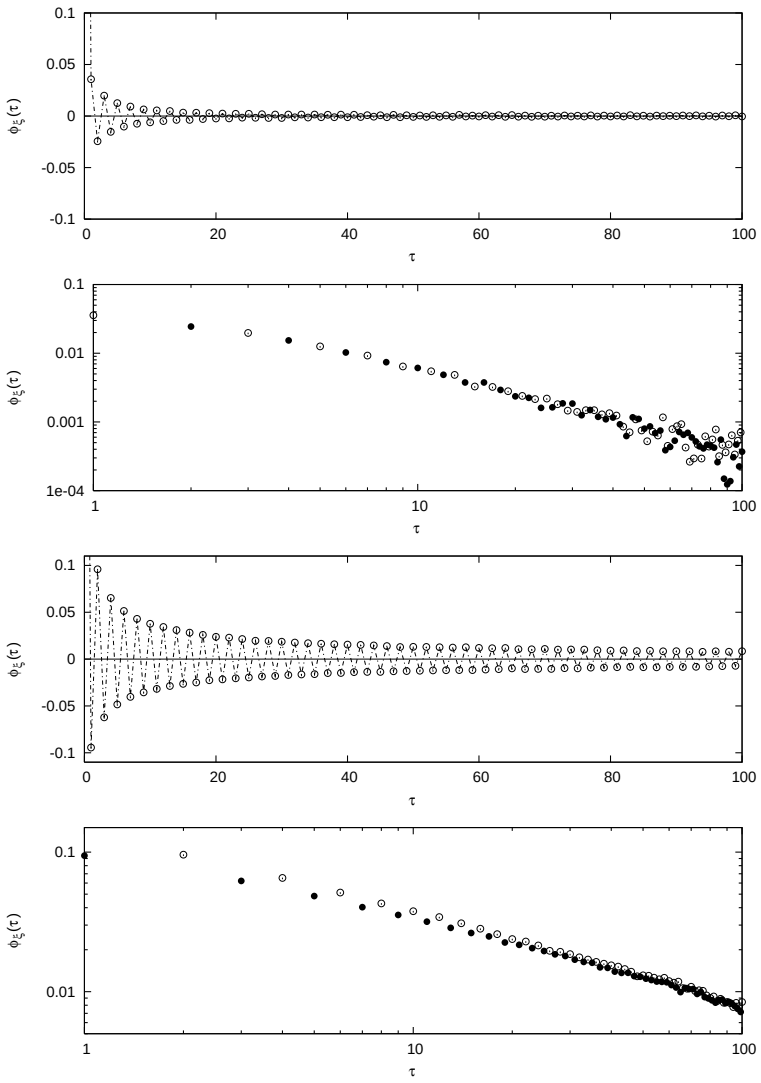

Figure 3.12. Correlation functions of recrossing times of $\xi(t)$ for $H = 1/3$ (first) and $H = 2/3$ (third). Also in log-log scale, for $H = 1/3$ (second) and $H = 2/3$ (fourth) of positive values and absolute of negative values in reversed vertical scale.

3.3. The Voss Algorithm

FBM is also generated by the Voss algorithm [11] to compare the same properties. But it doesn't give as many numbers as the previous algorithm. It gives the values of $x(t)$ for $t = 0, 1, 2, \ldots, 2^m$ where m is an integer. The process takes m steps. To get the results close to FBM, m must be large enough.

Fig. 3.13 shows the process for $m = 3$. In step zero, all x values are zero. In the first step, random x values are given for initial time $t = 0$, middle time $t = 4$ and final time $t = 2^m = 8$ and the average of each couple of x values are written to the middle times $t = 2$ and $t = 6$ as shown in the figure. In the second step, random numbers are added to the all previously calculated x values and again averaged values are calculated between those times. And in the final step $m = 3$, random numbers are added to all times $t = 0, 1, 2, \ldots, 2^m$.

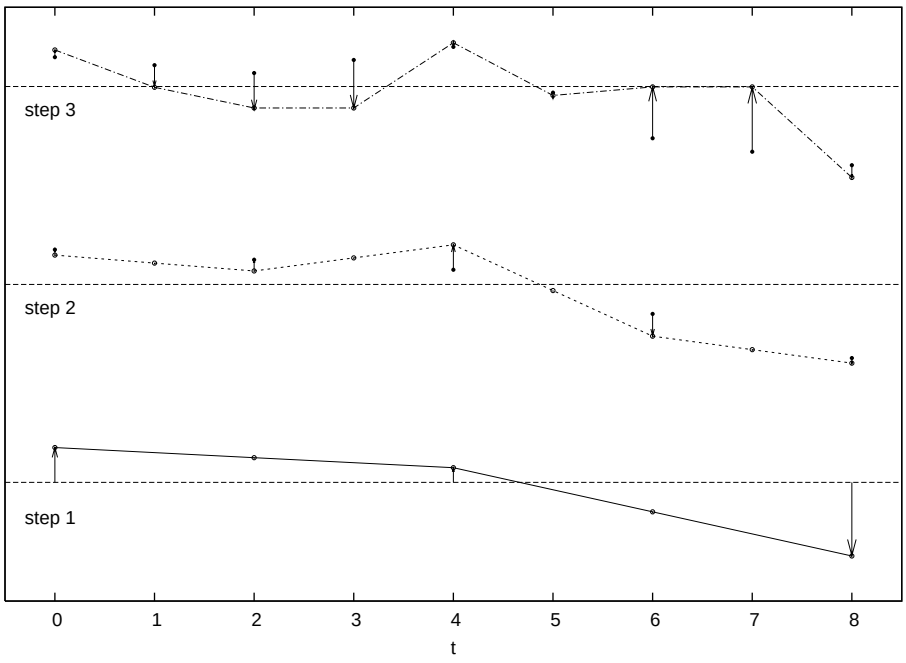

Figure 3.13. Voss algorithm for $m = 3$. The arrows are the magnitudes of random numbers.

In each step i, a set of random numbers $\{\mathcal{R}_i\}$ are produced from Gaussian distribution with zero mean. The variance for the step i is

$$\sigma_i^2 = \left(\frac{1}{2^H}\right)^{i-1} \tag{3.17}$$

If $\mathcal{R}$ is a Gaussian random number with unit variance then $\mathcal{R}_i = \sigma_i \mathcal{R}$ is a Gaussian random number with σ_i variance.

Fig. 3.14 shows the development of $x(t)$ for each step for $m = 8$, from step 1 at bottom to step 8 to top.

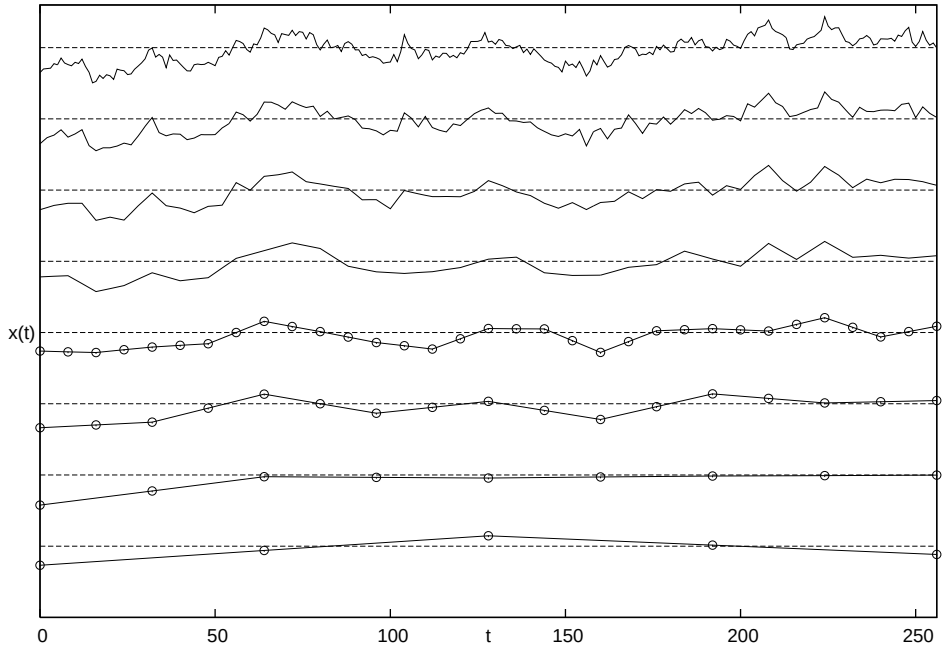

Figure 3.14. The development of $x(t)$ for $m = 8$.

The simulations are done for $m = 24$. The stochastic velocity, $\xi(t) = x(t) - x(t-1)$ is obtained for $H = 0.333$ and $H = 0.666$. The slopes of the correlation function of ξ are as expected in Eq. 2.15. This algorithm uses Gaussian random numbers but no correlation function to produce the diffusion, but the velocity turns out to be correlated. Fig. 3.15 show the correlation functions of ξ for both the super-diffusion and the sub-diffusion in linear and log-log scale. In this algorithm, reaching to the scaling regime is faster then the previous one.

Fig. 3.17 shows again that the distribution of the recrossing times of $x(t)$ is power law with the slope in Eq. 2.29. Because the number of data that can be obtained in Voss algorithm is limited, this plot has more fluctuation. And later, in Fig. 3.18, we see that recrossing times are uncorrelated. The recrossing times of ξ is distributed exponentially and are correlated as seen in Figs. 3.19 and 3.20.

The aging experiment was possible only for the sub-diffusion because there was not enough number of recrossing times for the super-diffusion. Fig. 3.21 show that there is renewal aging for $H = 1/3$.

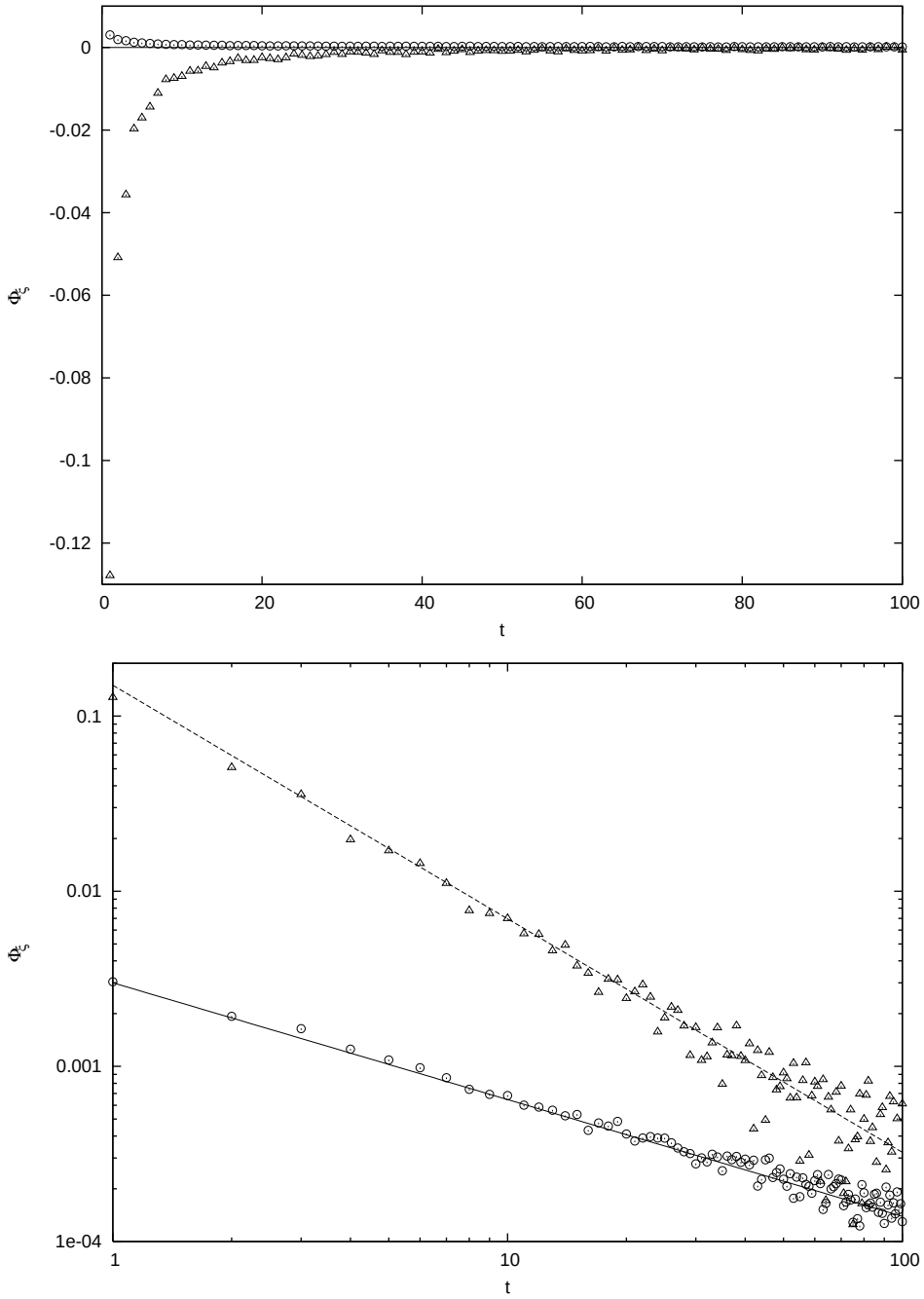

Figure 3.15. The correlation functions of the super-diffusion, $H = 2/3$, (circles) and the sub-diffusion, $H = 1/3$, (triangles) for both normal (upper) and log-log (lower) scales.

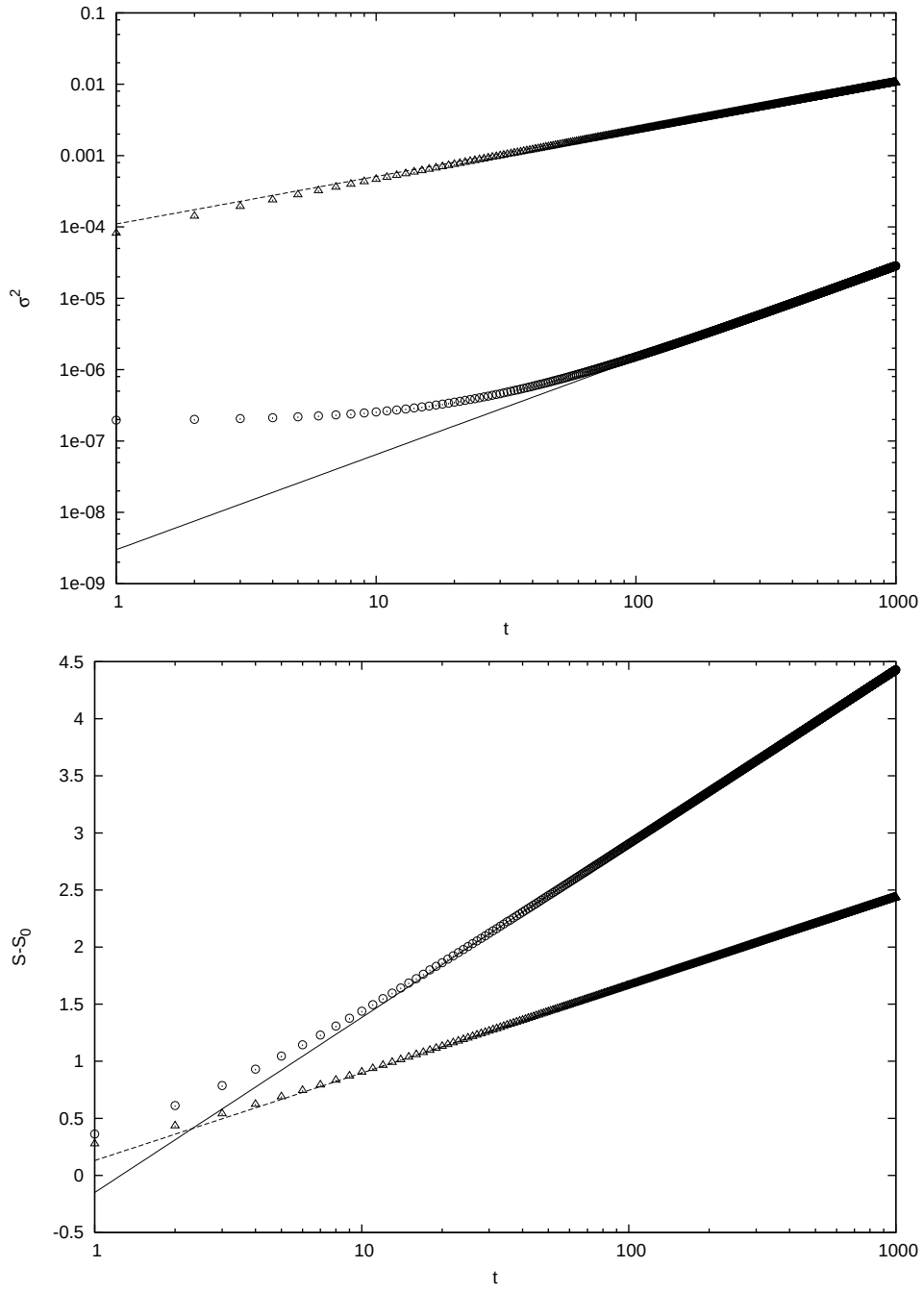

Figure 3.16. Variance (upper) and DE (lower) of the super-diffusion, $H = 2/3$, (circles) and the sub-diffusion, $H = 1/3$, (triangles).

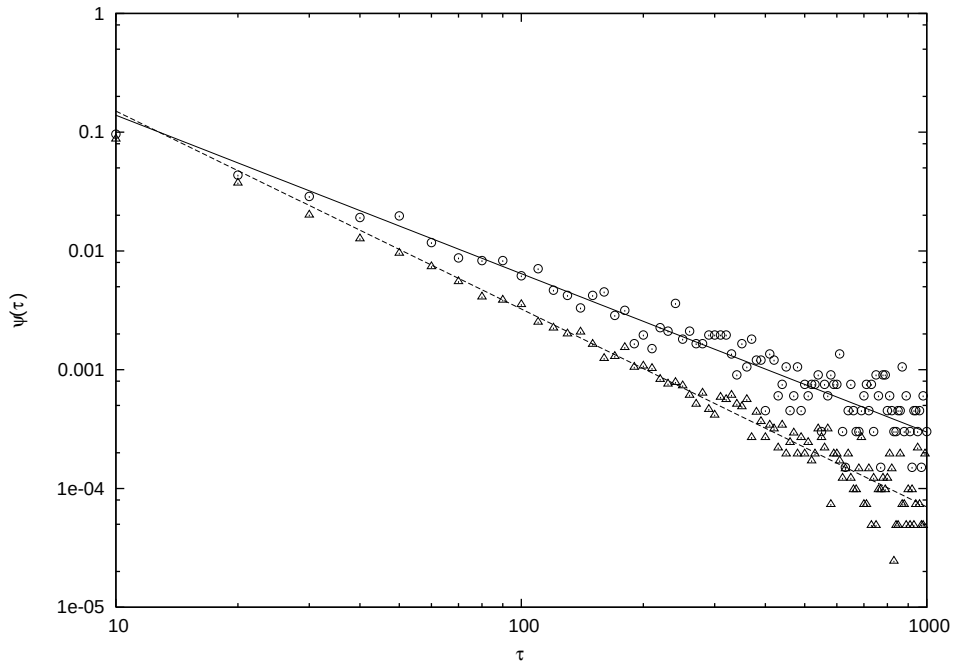

Figure 3.17. Distributions of recrossing times of x for the super-diffusion, $H = 2/3$, (circles) and the sub-diffusion, $H = 1/3$, (triangles).

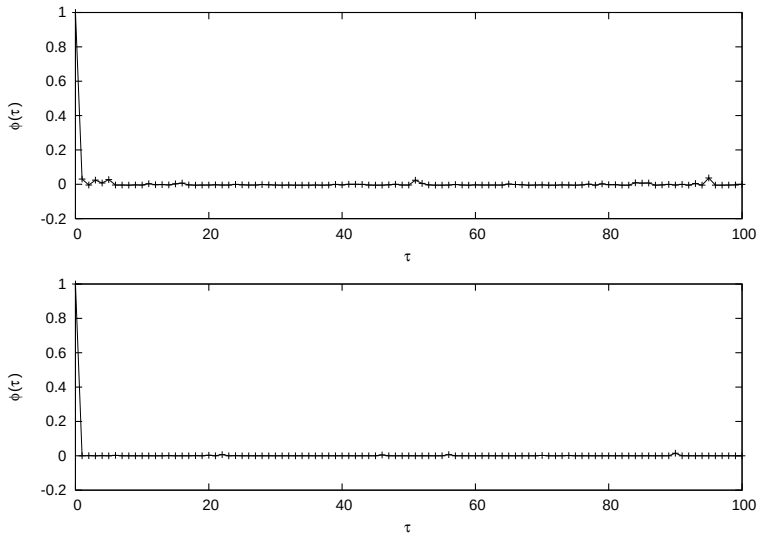

Figure 3.18. The correlation functions of recrossing times of x for the super-diffusion, $H = 2/3$, (upper) and the sub-diffusion, $H = 1/3$, (lower).

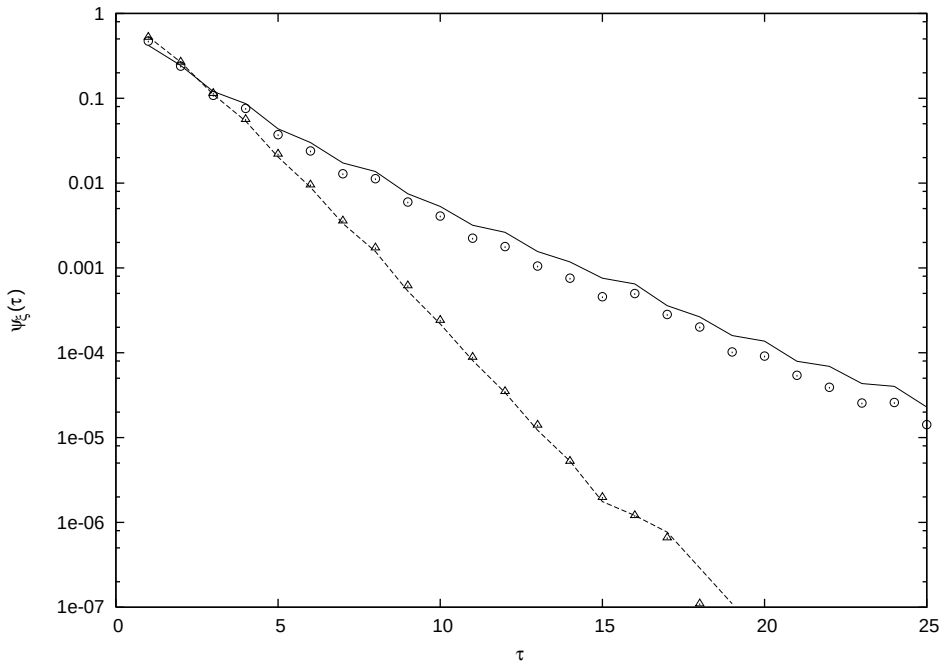

Figure 3.19. Distributions of recrossing times of ξ for the super-diffusion, $H = 2/3$, (circles) and the sub-diffusion, $H = 1/3$, (triangles).

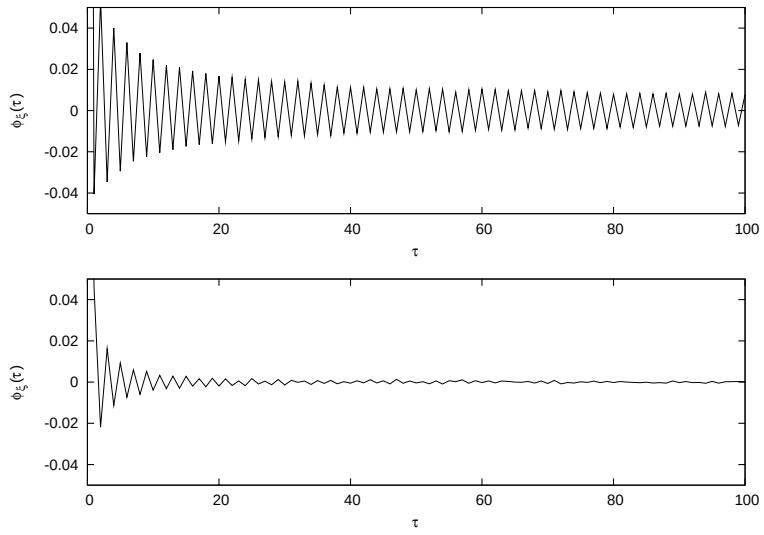

Figure 3.20. The correlation functions of recrossing times of ξ for the super-diffusion, $H = 2/3$, (upper) and the sub-diffusion, $H = 1/3$, (lower).

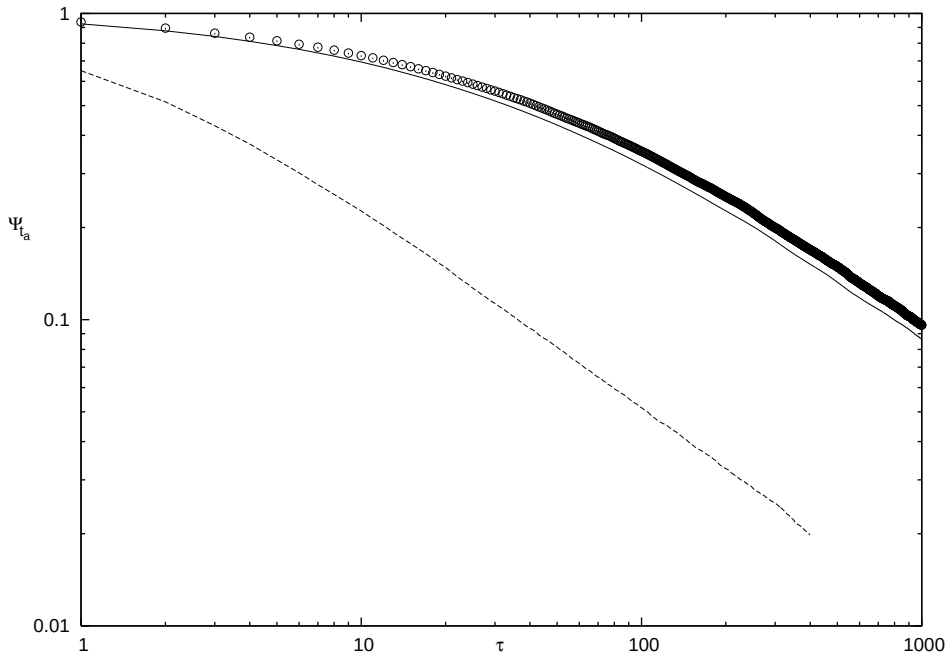

Figure 3.21. Aging of the recrossing times of x for the sub-diffusion for $H = 1/3$.

CHAPTER 4

RANDOM SURFACE GROWTH

The model of ballistic deposition (BD) is a simple way to establish cooperation among the columns of a growing surface. It can be used as a model for the birth of cooperation in complex systems. This model will show that the birth of complexity is associated with both memory and renewal property. (See the RC model of chapter 2.) It generates memory properties and non-Poisson renewal events. The variable generating memory can be regarded as the velocity of a particle driven by a bath with the same time scale, and the variable generating renewal processes is the corresponding diffusional coordinate.

Fig. 4.1 is fully adequate to illustrate how the model works for the (1+1)-dimension case. At any time step, $n = 1, 2, \ldots$, a particle drop randomly on one of the L columns.

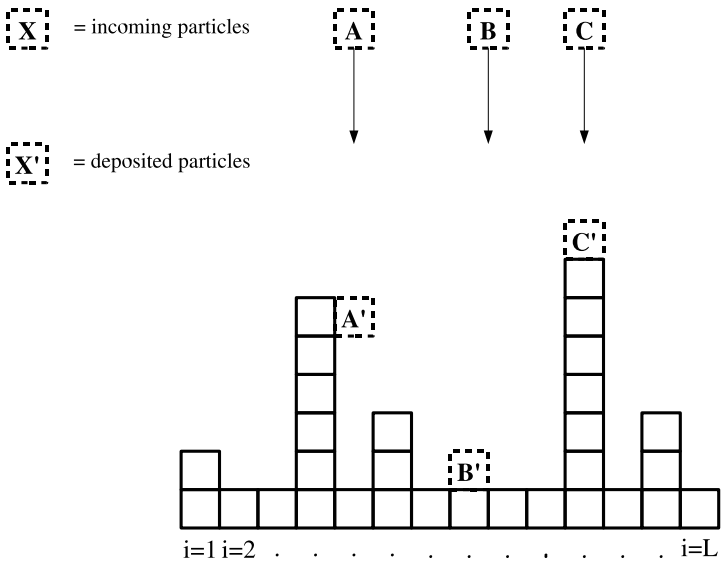

Figure 4.1. Model of ballistic deposition. The particle B settles at the top of an earlier particle of the same column, given the fact that there are no particles at a higher level in the two nearest neighbor columns. The particle A sticks to the right side of the left nearest neighbor column rather than at the top of a particle in the same column at a lower level.

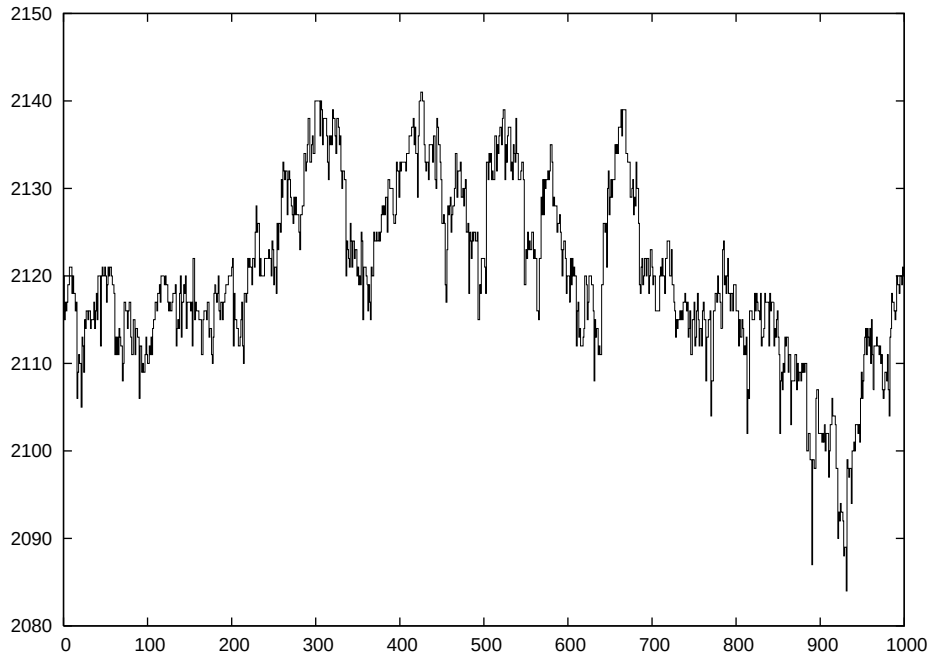

Figure 4.2. The surface for $L = 1000$.

The particles fall down in sequence to settle either at the bottom of the column or at the top of an earlier selected particle that by chance fell down in the same column. However, if the height of one of the two nearest neighbor columns is higher than the selected column, the particle sticks to the side of the highest particle of this neighbor column. There are also periodic boundary conditions to decrease the effect of limited surface size. The particle falling to the column L will be affected by the first column and vice versa. Fig. 4.2 shows an example surface for $L = 1000$ that is the surface size in the calculations.

Actually, this side sticking action corresponds to a transverse transport of information, through which the column under study is informed about the height of the surrounding columns. Thus, examining the time evolution of a single column is equivalent to studying the behavior of a single individual and to assessing to what an extent it reflects the properties of the whole society. It will be shown that the cooperation among the different columns generates memory and this memory generates renewal effects.

4.1. Collective Properties

The variable $y(t)$ is defined by

$$y(t) \equiv h(t) - < h(t) >_c, \tag{4.1}$$

where h(t) is the height of the selected column and $< h(t) >_c$ denotes the average over all the sample columns. A graph of $y(t)$ can be seen in Fig. 4.3.

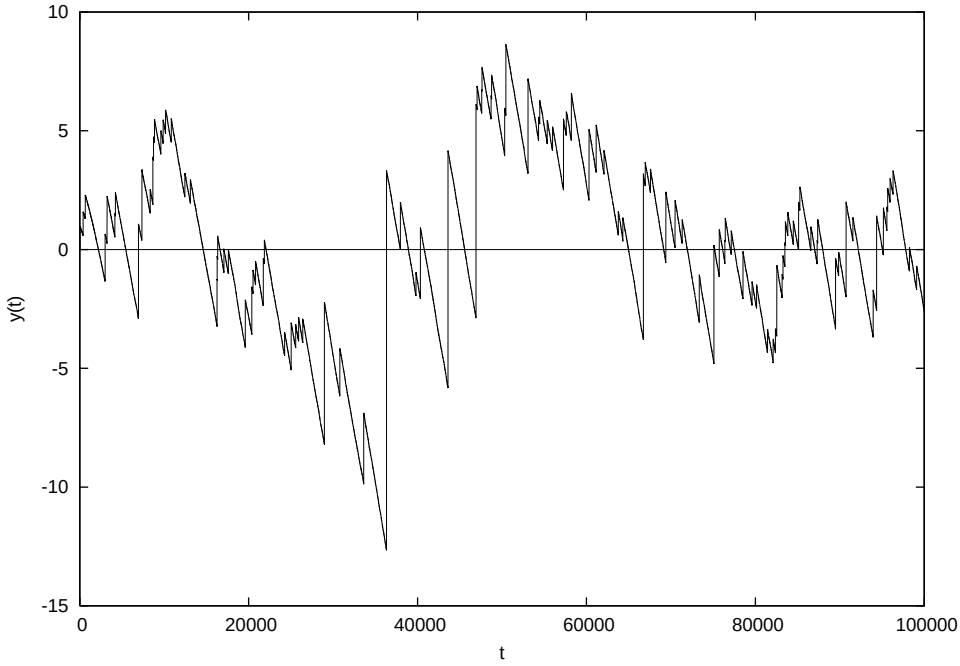

Figure 4.3. $y(t)$ for $L = 1000$.

In the earlier work of Ref. [2] it was argued that the regression of the variable y to the origin $y = 0$ is a renewal process and its standard deviation was shown to obey the anomalous prescription.

$$\sigma(t) \propto t^{\beta} \tag{4.2}$$

Here again, the same properties is shown. Actually, for $L \to \infty$ the power index β is expected to fit the Kardar-Parisi-Zhang (KPZ) prediction, $\beta = 1/3$ [12]. The calculations are done for the limited surface size of $L = 1000$, and consequently give the value $\beta \approx 0.28$.

The standard deviation of $y(t)$

$$\sigma(t) = \left\langle (y(t) - \langle y(t) \rangle)^2 \right\rangle^{1/2} \tag{4.3}$$

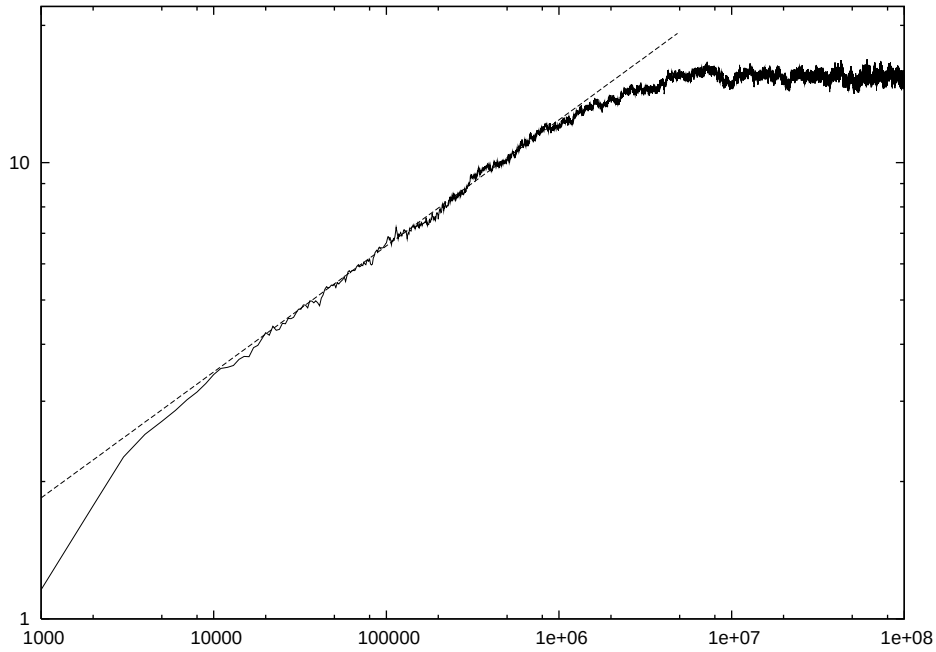

Figure 4.4. Standard deviation of $y(t)$. The dashed line is $0.273t^{0.276}$

is shown in Fig 4.4, which obeys the Eq. 4.2. The constant value after $t \approx L^2 = 10^6$ is the saturation effect which is due to the limited size of the surface.

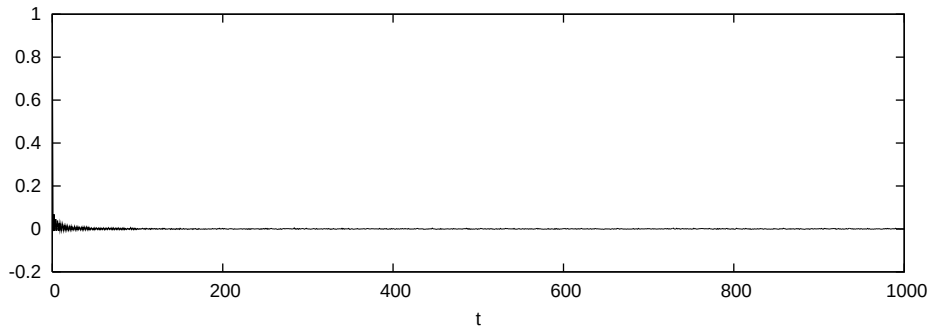

Figure 4.5. Correlation function of recrossing times of $y(t)$ for $L = 1000$.

In Fig. 4.5, it was expected the recrossings of $y(t)$ to have zero correlation but it shows some oscillation for the initial time, which is a sign of memory on trajectory $y(t)$. However, Fig. 4.6 confirms the renewal nature of the y-process, thereby providing further support for the theoretical approach to the stochastic growth of a single column and for the adoption of the renewal theory to derive the crucial relation $\beta = 2 - \mu$. So the numerical results of Fig. 4.6 for $\mu = 1.72$ give $\beta = 0.28$. This same power index will be derived from the memory properties of a single column.

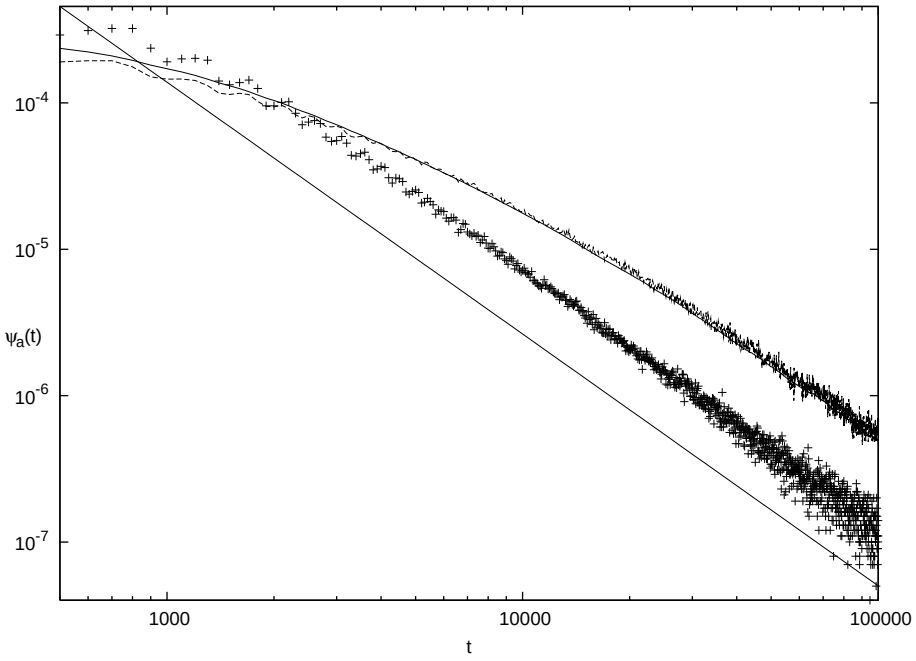

Figure 4.6. Probability distribution of waiting times of $y(t)$ are shown with $(+)$ when there is no aging. The straight solid line is $20\ x^{-1.72}$. Probability distribution of aged waiting times are dashed curve for experimental and solid curve for theoretical calculation.

4.2. Properties of the Jumps

Because of the side-sticking effect, when one particle arrives, the height of the column increases by a quantity that can be also much greater than 1. If $\xi(t)$ is the height increase of the column, and this quantity is 0 when no particle arrives, and a number equal to 1 or larger when a particle arrives. The height of the column at a give time t is given by

$$h(t) = \sum_{n=0}^{t} \xi_n, \tag{4.4}$$

with $\xi_0 = 0$.

It is well known that the time distance between the arrival of one particle in this column and the next has the Poisson time distribution [13]

$$\psi(\tau) = \lambda \exp(-\lambda\tau), \tag{4.5}$$

where

$$\lambda = \frac{1}{L}. \tag{4.6}$$

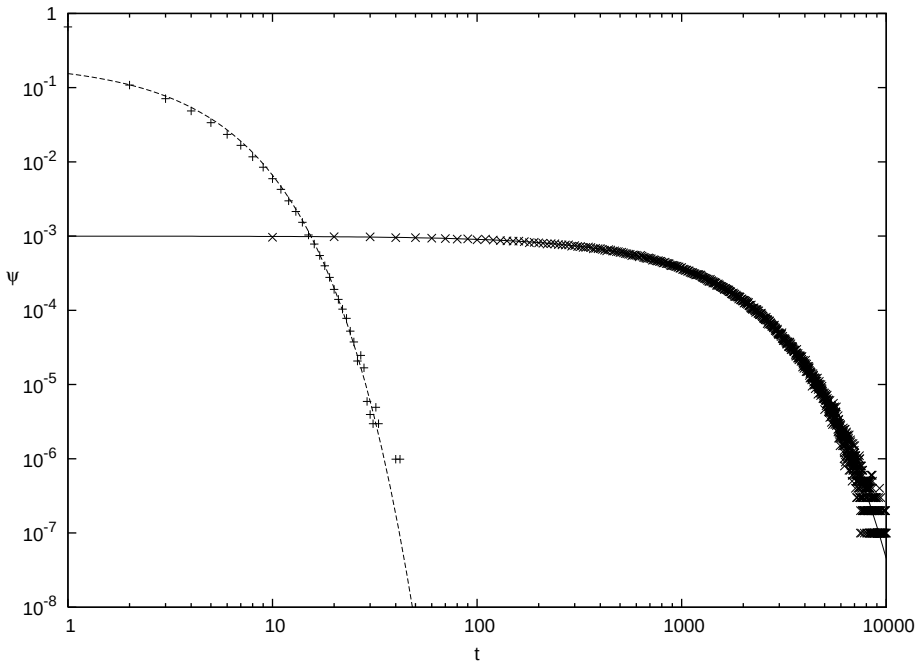

Figure 4.7. Probability distribution of jumps, ξ, (+), fitting to dashed line 0.22 $exp(-0.35\ t)$; and waiting times of jumps, (x), fitting to solid line 0.001 $exp(-0.001\ t)$. L = 1000

Fig. 4.7 illustrates the distribution density $\psi(\tau)$ and $\psi(\xi)$, and prove that the latter distribution, as well as the former, is an exponential,

$$\psi(\xi) = a\exp(-b\xi). \tag{4.7}$$

On the basis of these results one would be tempted to conclude that the single column process is Poisson. It is not so because the fluctuation $\xi(t)$ has memory, in spite of its exponential distribution. This memory is a consequence of the process of transverse transport of information, and it can be considered a signature of cooperation.

To show the memory on ξ, we need to see that the correlation function of xi has a non-zero value. However, it can be seen in the the top graph in Fig 4.8 that there is no correlation, unlike what is expected. To understand this, the correlation function is calculated again only for the values of $\xi > 1$ as seen in the bottom graph in Fig. 4.8. In that case, it is possible to obtain non-zero values. The reason for this is that $\xi > 1$ values can only be obtained by the sticking rule, which is the source of memory, while

the values of $\xi = 1$ include mostly the totally random depositions that are not due to the sticking rule. This causes the correlation to get lost.

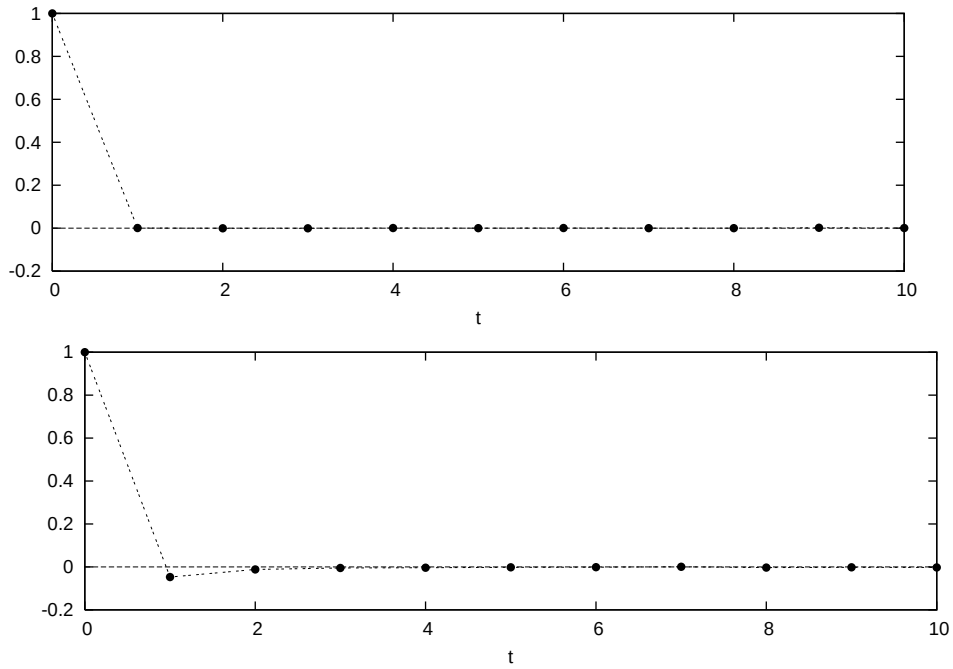

Figure 4.8. Correlation function of jumps, in ballistic deposition for $L = 1000$ and for $\xi > 0$ (top) and $\xi > 1$ (bottom).

4.3. Single Column Properties

The statistical analysis that led us to Eqs. 4.5 and 4.7 would suggest that the anomalous growth property of the interface as a whole is annihilated by the observation of a single column. Let us now define the variable that is the signature of the memory properties generated by the BD model. This is the variable $\tilde{\xi}(t)$ defined by

$$\tilde{\xi} \equiv \xi(t) - \bar{\xi}, \tag{4.8}$$

where the symbol $\bar{\xi}$ denotes a time average. The time average is calculated with very a long but finite sequence of $\xi(t)$.

$$\bar{\xi} = \frac{\sum_{t=1}^{T_{max}} \xi(t)}{T_{max}}. \tag{4.9}$$

To assess the memory properties created by cooperation, the variable

$$x(t) = \sum_{t'=1}^{t} \tilde{\xi}(t') \tag{4.10}$$

will be considered as the diffusion variable. Fig 4.9 shows the plot of $x(t)$ for $L = 1000$.

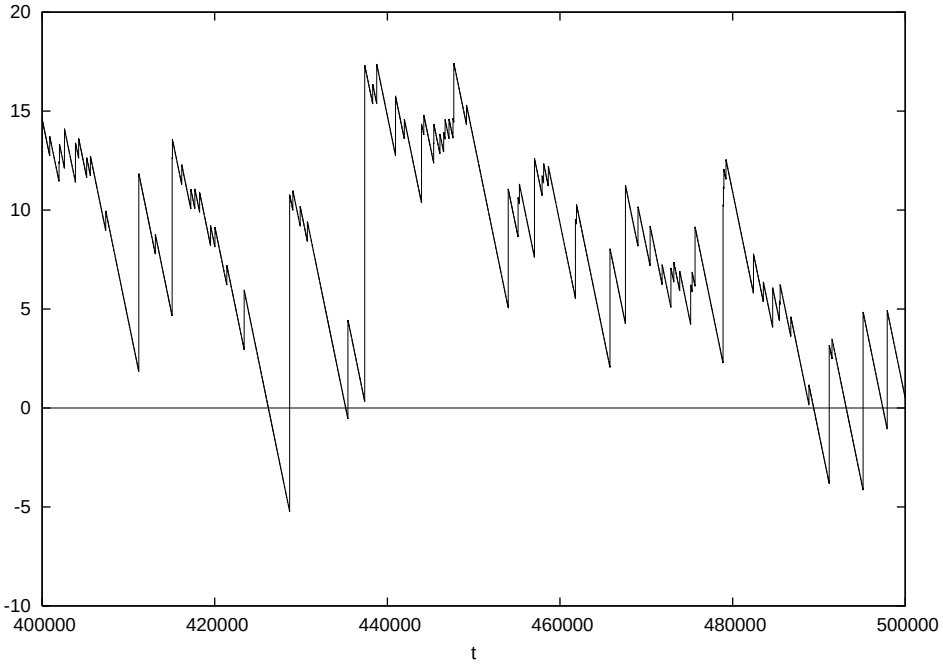

Figure 4.9. $x(t)$ for $L = 1000$.

It is evident that the single column reflects the complex behavior of the whole surface, see Eq. 4.2. Fig. 4.10 shows that this prediction is fulfilled with $\beta = 0.288$.

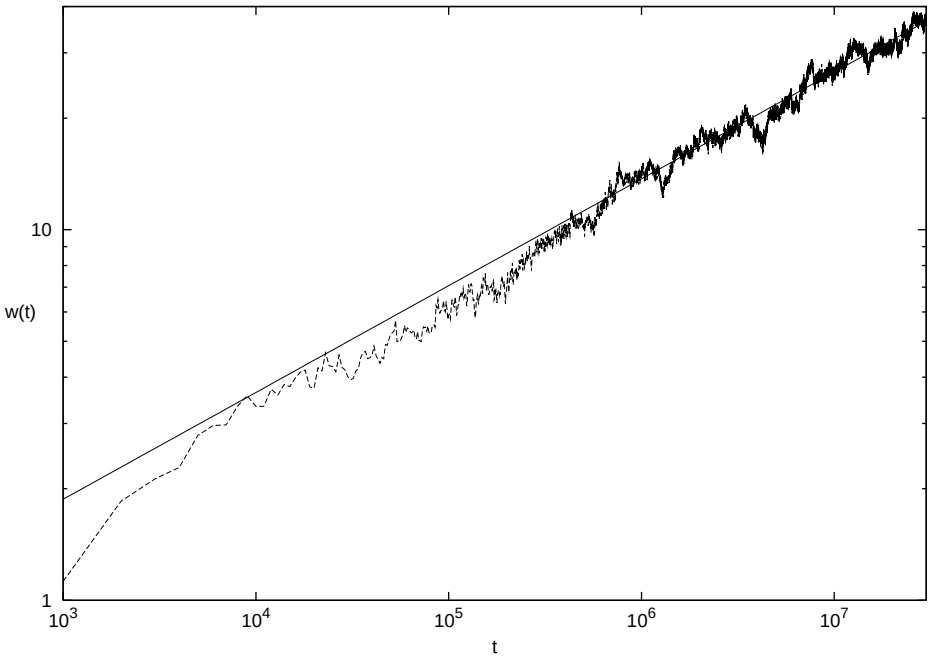

Figure 4.10. Standard deviation of x is shown with dashed line for $L = 1000$. The solid line is $0.256\ x^{0.288}$

To see the effect of the saturation, the standard deviation is also calculated for smaller surface size, $L = 200$, in Fig, 4.11. For $L = 1000$, the time range is not enough to see the effect and it was not technically possible to get more values. When it reaches saturation, it turns to normal diffusion, changing the slope towards to 0.5, but still this process takes some time; although the slope is increasing, it is still not half.

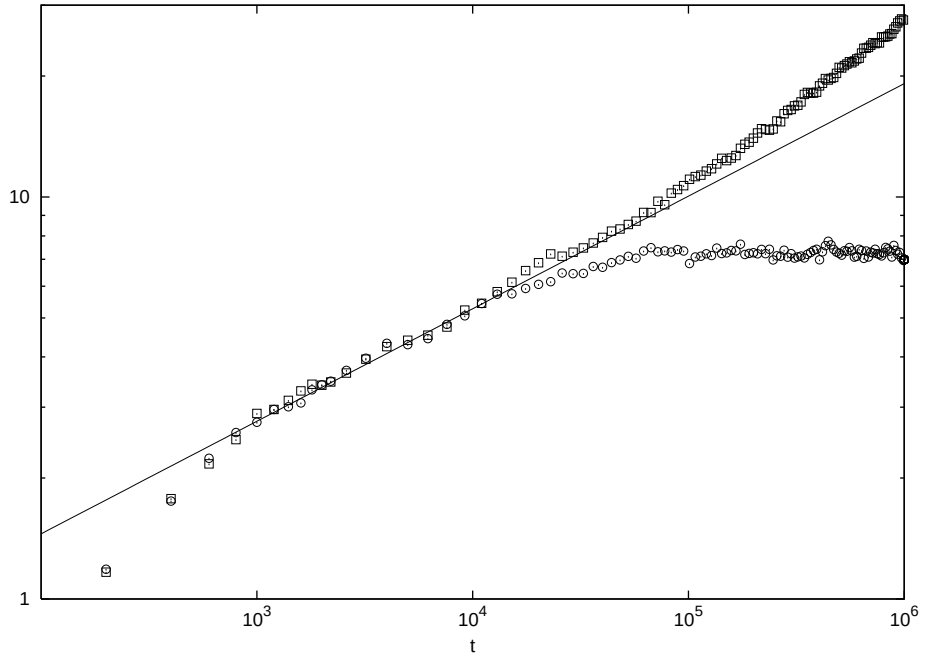

Figure 4.11. Standard deviation of x (square) and y (circle) for $L = 200$. The solid line is $0.4t^{0.28}$.

The renewal properties of $x(t)$ is shown in Figs. 4.12 and 4.13 with zero correlation function and renewal aging as expected.

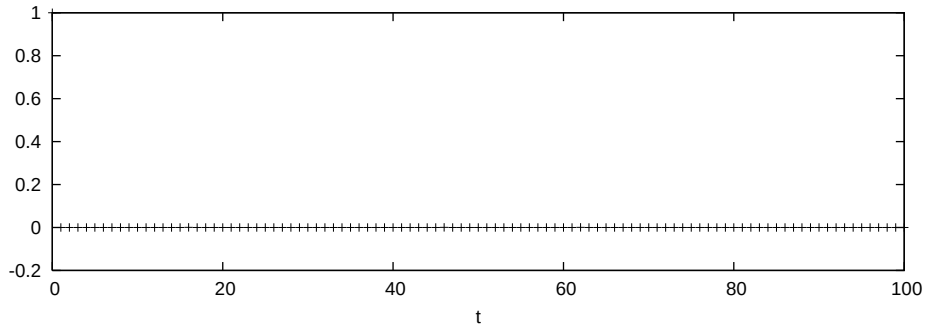

Figure 4.12. Correlation function of recrossing times of $x(t)$ for $L = 1000$.

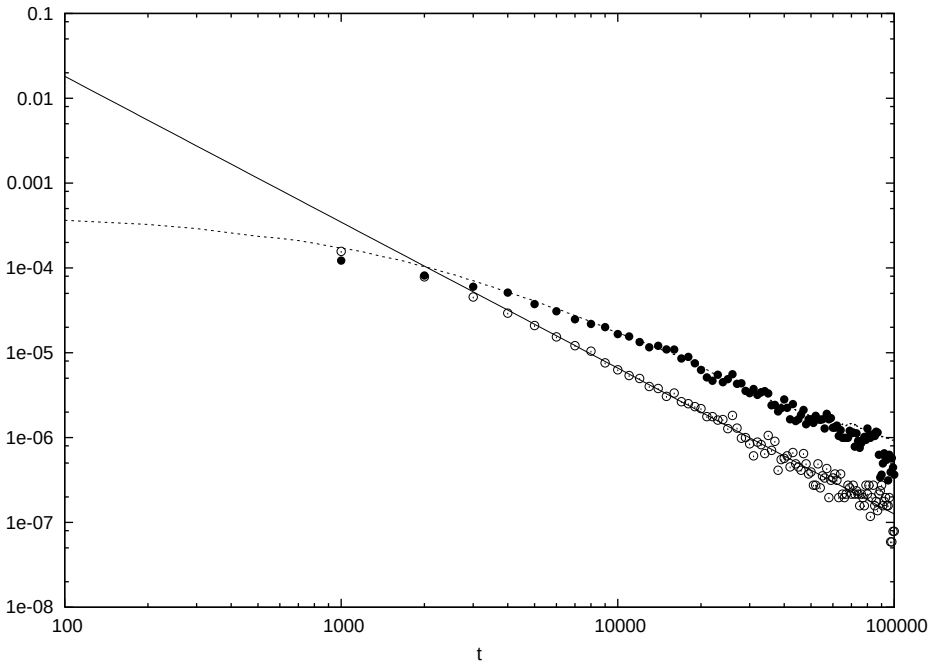

Figure 4.13. Probability distribution of waiting times of $x(t)$ are shown with empty circles when there is no aging. The straight solid line is 50 $x^{-1.72}$. Probability distribution of aged waiting times are full circles for experimental and dashed line for theoretical calculation.

Under the stationary assumption, It was proved that (Eqn. 2.13)

$$\frac{d^2}{dt^2} < x^2(t) > \propto \Phi_{\tilde{\xi}}(t), \tag{4.11}$$

where $\Phi_{\tilde{\xi}}(t)$ denotes the equilibrium correlation function of the fluctuation $\xi(t)$.

The diffusion process has anomalous scaling defined by β, with $\beta < 1/2$. By differentiating Eq. 4.11 with respect to time, it is possible to establish a connection with the time asymptotic properties of $\Phi_{\tilde{\xi}}(t)$. Due to the fact that $\beta < 1/2$, the correlation function $\Phi_{\tilde{\xi}}(t)$ must have a negative tail, namely that

$$\lim_{t\to\infty} \Phi_{\tilde{\xi}}(t) = -\frac{constant}{t^{\psi}}, \tag{4.12}$$

with

$$\psi = 2 - 2\beta. \tag{4.13}$$

This property establishes a closer connection with the earlier work of FBM, where the variable responsible for memory yields a correlation function with a negative tail. In

the case of FBM the correlation function is known theoretically, so that it is possible to move from the correlation function to the variance time evolution using Eq. 4.11. In the present case, there is no analytical approach to obtain the equilibrium correlation function of $\tilde{\xi}(t)$. It's numerical derivation, as pointed out by Eq. 4.11, would be equivalent to differentiating twice the variance, which is numerically a source of big errors. In, fact, the numerical approach to the equilibrium correlation function yields a negative tail, as shown in Fig. 4.14, but the assessment of the correct power requires rich statistics and excessive computational time. The standard deviation of $x(t)$ gets close to the correct slope after around $t = 10^4$ but the correlation function was possible to obtain until that time.

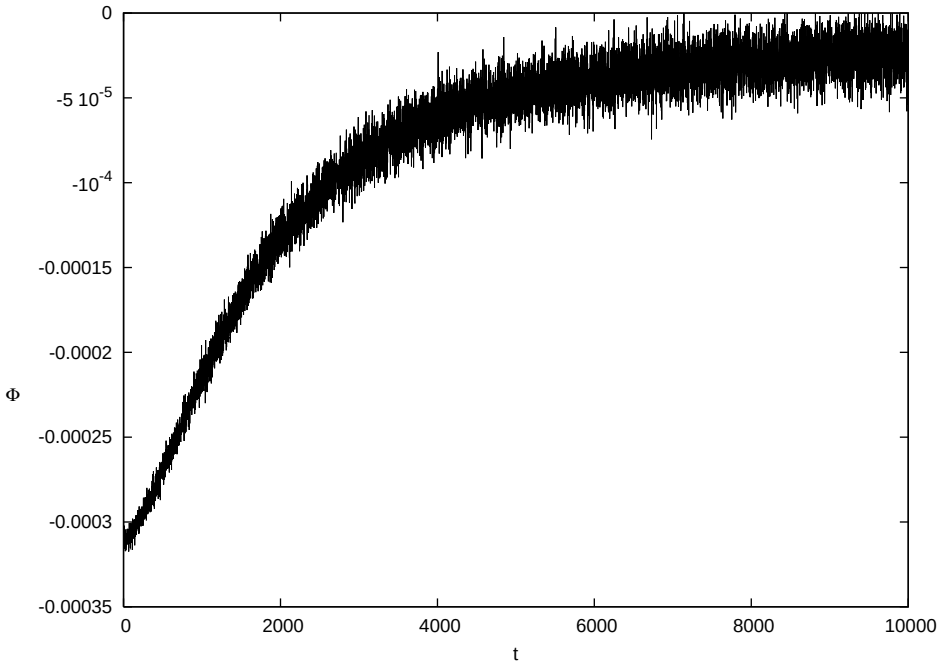

Figure 4.14. Correlation function of $\tilde{\xi}(t)$ for $L = 1000$.

This chapter shows how to reconcile a perspective based on memory with one based on renewal non-Poisson processes. To a first sight, these two visions can be perceived as being incompatible. For instance, the adoption of the FBM theory adopted by some authors to account for persistency [14, 15, 16] seems to conflict with the renewal approach. On the contrary, in accordance with the results of chapter 2, this paper shows that the cooperative nature of the BD model generates memory and, consequently, anomalous

diffusion. However, the origin recrossings of the variable y are renewal, in the same way as the diffusion variable generated by the long-memory fluctuations used to generate dynamically FBM exhibit a renewal character.

CHAPTER 5

TRAJECTORY AND DENSITY MEMORY

This chapter discusses the connection between trajectory and density memory. The first form of memory is a property of a stochastic trajectory, whose stationary correlation function shows that the fluctuation at a given time depends on the earlier fluctuations. The density memory is a property of a collection of trajectories, whose density time evolution is described by a time convoluted equation showing that the density time evolution depends on its past history. It will be shown that the trajectory memory does not necessarily yield density memory, and that density memory might be compatible with the existence of abrupt jumps resetting to zero the system's memory.

In literature it seems to be widely accepted that density and trajectory memory are equivalent. However, there are good reasons to not share this conviction. In the last few years, there has been an increasing interest for the diffusion equations emerging from the perspective of *continuous time random walk* (CTRW) [27]. Since the fundamental work of Kenkre, Shlesinger and Montroll [28], it is well known that the CTRW generates, for the time evolution of density, the same time convoluted structure as the methods of Refs. [17, 18, 23, 24]. According to the earlier definitions, this is density memory, and the expected equivalence between trajectory and density memory is clearly violated, if we keep in mind that the CTRW is a process based on jumps, whose occurrence resets to zero the system's memory. To make this aspect more evident, the derivation of CTRW from the diffusion equation will be shown in Section 5.1:

$$\frac{\partial}{\partial t}p(x,\,t) = D\int_0^t d\tau\Phi(\tau)\frac{\partial^2}{\partial x^2}p(x,\,t-\tau). \tag{5.1}$$

Eq.5.1 has the earlier mentioned time convoluted structure, thereby implying that the time evolution of the probability density $p(x,\,t)$ depends on the earlier times $t-\tau$: this explains why it is called density memory. What about trajectory memory? As earlier

pointed out, there is no such memory here, due to the occurrence of memory erasing jumps.

Now, let us point out another aspect conflicting with the naive conviction that trajectory and density memory are equivalent. Let us go back to the chapter 2 of FBM, or, more precisely, to the dynamic approach to FBM, to generate the following generalized diffusion equation

$$\frac{\partial}{\partial t}p(x,t) = D\left(\int_0^t d\tau \Phi(\tau)\right)\frac{\partial^2}{\partial x^2}p(x,t). \tag{5.2}$$

Note that the function $\Phi(t)$ in this case is the correlation function of ξ, and it has fat tails, indicating the existence of trajectory memory. Yet, the diffusion equation does not have the time convoluted structure of Eq. 5.1. The work of Ref. [31] shows that the emergence of the time-convolutionless structure of Eq. 5.2, to compare to the time-convolution structure of Eq. 5.1, is determined by the fact that the stochastic variable $\xi(t)$ is Gaussian in the case of Eq. 5.2. In the recent work of Ref. [32] Kenkre noticed that, although the two equations might yield the same second moment, the higher moments are not identical and that Eq. 5.2 cannot produce the transition from merely diffusive to merely wave-like motion, whereas Eq. 5.1 does.

The main purpose here is to shed some light into the confusion concerning the relations between these two kinds of memory. The solution of the very elusive problem of establishing the trajectory properties behind Eq. 5.1, when this equation generates super-diffusion, will also be shown. The trajectory properties of this equation are well known in the sub-diffusional case [33], but in the super-diffusion case its correct interpretation in terms of CTRW does not exist [34] and there are good reasons to believe that in this case Eq. 5.1 is incompatible with a CTRW origin. In line with [34], the trajectory memory picture that explains the dynamical origin of Eq. 5.1 in the super-diffusion case will be studied.

This process can be simply described by a particle doing random jumps to left or right. In one dimension, the equation of motion is

$$\frac{d}{dt}x = \xi, \tag{5.3}$$

where ξ is $+1$ or -1 randomly and time is discrete. Let us imagine a sequel of events described by

$$\mathbf{p}(n) = \mathbf{M}^n\mathbf{p}(0). \tag{5.4}$$

The symbol $\mathbf{p}$ denotes a vector with infinite components p_i fitting the normalization condition

$$\sum_{i=-\infty}^{\infty} p_i = 1. \tag{5.5}$$

The initial condition is when at $n = 0$, only the site $i = 0$ is occupied and all the other sites are empty. At each time step the particle makes a transition from the site $i = 0$ to other sites, depending on the form of the matrix $\mathbf{M}$. In this paper, $\mathbf{M}$ has the following specific form

$$\mathbf{M} \equiv \sum \frac{1}{2}(|i><i+1| + |i+1><i|). \tag{5.6}$$

The choice of this quantum-like formalism is done to avoid the cumbersome matrix notation, and it does not imply any departure from the classical condition. For instance, since at $t = 0$ only the site $i = 0$ is occupied,

$$\mathbf{M}\mathbf{p}(0) = \mathbf{M}|0>= \frac{1}{2}(|1> + <-1|), \tag{5.7}$$

which means that the particle at the first step will jump with equal probability from the site $i = 0$ to the two nearest neighbor sites $|1>$ and $|-1>$. It should be easy to consider transition matrices with a different form.

For an individual trajectory, the position $x(n)$ of the particle after n steps will be

$$x(n) = \sum_{i}^{n} \xi_i. \tag{5.8}$$

The time distance between two consecutive jumps is fixed and equal to t_u. The spatial distance between two nearest neighbor sites is fixed and is equal to a.

Let us do the experiment with many particles, moving from the same initial site $i = 0$. The position $x(n)$ will correspond to a given site with index i. Let us count how many particles are found in this site and call n_i the number of particles occupying this site, and we divide this number by the total number of trajectories, N. This will give the relation

$$\frac{n_i}{N} = p_i(n) =< i|\mathbf{M}^n|\mathbf{p}(0) > . \tag{5.9}$$

With this equivalence between stochastic trajectories and a probabilistic description in mind, the first conclusion is that Eq. 5.9 represents the probability distribution of this set of random walkers at a given time $t = nt_u$. In accordance with the central limit theorem, the distribution of x is Gaussian. In this condition, standard deviation is

$$< x^2(n) >^{1/2} \propto n^{1/2} \tag{5.10}$$

and the diffusion equation is

$$\frac{\partial}{\partial n}p(x, n) = D\frac{\partial^2}{\partial x^2}p(x, n), \tag{5.11}$$

which gives the ordinary diffusion.

It is assumed that t_u is the minimum possible time, and that the experimental time t is much larger than t_u. Let us now make also the crucial assumption that the time distance between the occurrence of the nth event, occurring at time t_n, and the occurrence of the $(n+1)$th event, occurring at time t_{n+1}, rather than being fixed, fluctuates. The assumption that the time distance between two nearest neighbor events fluctuates is physically plausible. In fact, if the ordinary diffusion generating fluctuations are a consequence of the collision between the particle of interest and the bath molecules, it is reasonable that these collisions do not occur at regular but at erratic times. Thus the quantity

$$\tau_n = t_{n+1} - t_n \tag{5.12}$$

is a stochastic variable with the distribution density $\psi(\tau)$.

The vector $\mathbf{p}(t)$ is related to the vector $\mathbf{p}(0)$ by means of

$$\mathbf{p}(t) = \sum_{n=0}^{\infty} \int_0^t \psi_n(\tau)\Psi(t-\tau)\mathbf{M}^n\mathbf{p}(0)d\tau. \tag{5.13}$$

Note that the function $\psi_n(t)$ denotes the probability density for a sequel of n event to occur, the last of which occurs exactly at t. Due to the statistical independence of these events (App. G), the Laplace transform of $\psi_n(t)$ is $(\hat{\psi}(u))^n$, with $\hat{\psi}(u)$ denoting the Laplace transform of $\psi(t) \equiv \psi_1(t)$, namely the probability density for one event to occur at time t. The function $\Psi(t)$ is the probability that no event occurs up to time t, and it is defined by

$$\Psi(t) \equiv \int_t^{\infty} dt'\psi(t'). \tag{5.14}$$

The physical meaning of Eq. 5.13 is made evident by the following remarks. The specific state $\mathbf{p}(t)$ is determined by the last of a sequel of collisions occurring prior to time t. The number of collisions is arbitrary, thereby explaining the index n running from 0 to ∞. No further event occurs between τ and t. This is taken into account by multiplying $\psi_n(\tau)$ by $\Psi(t-\tau)$.

It is a straightforward to prove that Eq. 5.13 is equivalent to (App. J)

$$\frac{\partial}{\partial t}\mathbf{p}(t) = -\int_0^t d\tau\Phi(\tau)\mathbf{K}\mathbf{p}(t-\tau), \tag{5.15}$$

with

$$\mathbf{K} = 1 - \mathbf{M}. \tag{5.16}$$

The memory kernel $\Phi(t)$ is related to $\psi(t)$ in the Laplace domain through

$$\hat{\Phi}(u) = \frac{u\hat{\psi}(u)}{1-\hat{\psi}(u)}. \tag{5.17}$$

These results are obtained by comparing the Laplace transform of Eq. 5.15 to the Laplace transform of Eq. 5.13.

With the choice of Eq. 5.6, the result of Eq. 5.15 can be expressed in a form equivalent to that proposed by Kenkre and Knox in Ref. [35]. In fact, if the choice of

Eq. 5.6 applies, it becomes

$$-\mathbf{Kp}|_i = -(\mathbf{1}-\mathbf{M})\mathbf{p}|_i = -p_i + \frac{p_{i+1}}{2} + \frac{p_{i-1}}{2} = \frac{1}{2}\frac{\partial^2}{\partial x^2}p(x,t). \tag{5.18}$$

Thus, Eq. 5.15 is rewritten as follows

$$\frac{\partial}{\partial t}p(x,t) = D\int_0^t d\tau\Phi(\tau)\frac{\partial^2}{\partial x^2}p(x,t-\tau). \tag{5.19}$$

Notice that if the value a is assigned to the distance between the nearest neighbor sites of the model here under discussion, the diffusion coefficient D reads $D = a^2/2$.

It is worth mentioning that the GDE of Eq. 5.19 drives the density of the diffusion process described by

$$\frac{d}{dt}x(t) = \xi_R(t), \tag{5.20}$$

where $\xi_R(t)$ is a fluctuation almost always vanishing but in the correspondence of a collision, where it takes the value 1 or -1, according to the coin tossing prescription.

The diffusion equation of Eq. 5.19 in the time asymptotic limit yields scaling. This means:

$$p(x,t) = \frac{1}{t^\delta}F(\frac{x}{t^\delta}), \tag{5.21}$$

with δ called scaling coefficient, and $F(y)$ being a function of y, different in general from a Gaussian function. This is a formal but rigorous way of assessing that in the time asymptotic condition $x \propto t^\delta$. The deviation from ordinary diffusion is signaled by $\delta \neq 0.5$ and/or $F(y)$ departing from the Gaussian form.

It is evident that the departure from ordinary diffusion, when it occurs, takes the form of sub-diffusion, namely, with $\delta < 0.5$: this is so because the longer the recrossing time in one site, the slower the diffusion process. To make the recrossing in one site as long as possible, set

$$\psi(\tau) = (\mu-1)\frac{T^{\mu-1}}{(\tau+T)^\mu}, \tag{5.22}$$

with the power index μ meeting the condition

$$1 < \mu < 2, \tag{5.23}$$

so that the mean recrossing time in one site is infinite.

To evaluate the scaling in the case of Eq. 5.19 it is convenient to study the Fourier-Laplace transform of $p(x, t)$, with k and u being the variables conjugated to x and t, respectively. The Fourier-Laplace transform of $p(x, t)$ is denoted $\hat{p}(k, u)$. Its explicit form is

$$\hat{p}(k, u) = \frac{1}{u + k^2 D \hat{\Phi}(u)}. \tag{5.24}$$

Using Eq. 5.17 and the limiting condition $u \to 0$ of $\psi(\tau)$ of Eq. 5.22 as in App. H, when the condition of Eq. 5.23 applies,

$$\hat{\psi}(u) = 1 - \Gamma(2 - \mu)(uT)^{\mu - 1}, \tag{5.25}$$

we obtain

$$\hat{p}(k, u) = \frac{1}{u + \frac{k^2 u^{2-\mu} D}{\Gamma(2-\mu)}}. \tag{5.26}$$

To determine the unknown scaling coefficient δ, let us set $k \propto u^{\delta}$ and plug it into Eq. 5.26. The value of δ making $\hat{p}(u^{\delta}, u)$ proportional to $1/u$ is

$$\delta = \frac{(\mu - 1)}{2}, \tag{5.27}$$

which is in fact smaller than $1/2$, when condition (5.23) applies.

5.2. Auxiliary Fluctuation

In this section, the memoryless trajectories behind Eq. 5.1, namely, the time convoluted diffusion equation generated by the CTRW perspective will be illustraded. The hypothesis of instantaneous collision made in Section 5.1 is not essential to generate the sub-diffusional process there described. To double check the theoretical arguments by means of numerical simulation, it is convenient to adopt a fluctuation with the time

interval between two consecutive renewal events filled with auxiliary events. This fluctuation is called $\xi_A(t)$. This section is devoted to illustrating a dynamic model producing this kind of fluctuation.

Let us imagine a particle with coordinate y, moving within the interval $I \equiv [0,1]$, with the following equation of motion (App.K)

$$\frac{d}{dt}y = \alpha y^z, \tag{5.28}$$

with $z \geq 1$, and $0 < \alpha << 1$. When the particle reaches the border, $y = 1$, is injected back to a new initial condition y_0, with uniform probability, it is easy to prove [40, 41] that the waiting time distribution is given by (5.22) with

$$\mu = \frac{z}{(z-1)}. \tag{5.29}$$

Let us now define a fluctuation $\xi_A(t)$ as follows. From time $t = 0$ to time τ_1, corresponding to the particle reaching the border, the fluctuation $\xi_A(t)$ is identical to the velocity dy/dt of the particle, with a sign $\pm$ depending on the coin tossing prescription, namely,

$$\xi_A(t) = \mathcal{R}\frac{\alpha y_0^{\mu/(\mu-1)}}{\left[1 - y_0^{1/(\mu-1)}\frac{\alpha}{(\mu-1)}t\right]^{\mu}}, \tag{5.30}$$

where y_0 is a random number of the interval I and $\mathcal{R}$ is ± 1 randomly. This means that the system is prepared in such a way that at time $t = 0$ all the systems of the ensemble are at the beginning of the deterministic dynamic process, at the end of which a new back injection will occur. Of course y_0 is selected randomly, with uniform distribution within the interval I. Thus, the time of the second back injection changes from system to system, and the probability of the first sojourn time, τ_1, is given by Eq. 5.22. From time $t = \tau_1$, corresponding to the first jump after preparation to time $t = \tau_1 + \tau_2$, at which the second jump occurs, the fluctuation $\xi(t)$ goes as follows:

$$\xi_A(t) = \mathcal{R}\frac{\alpha y_1^{\mu/(\mu-1)}}{\left[1 - y_1^{1/(\mu-1)}\frac{\alpha}{(\mu-1)}(t-\tau_1)\right]^{\mu}}, \tag{5.31}$$

where y_1 denotes the initial condition after the first back injection, again selected randomly with uniform probability in the interval I, and so on.

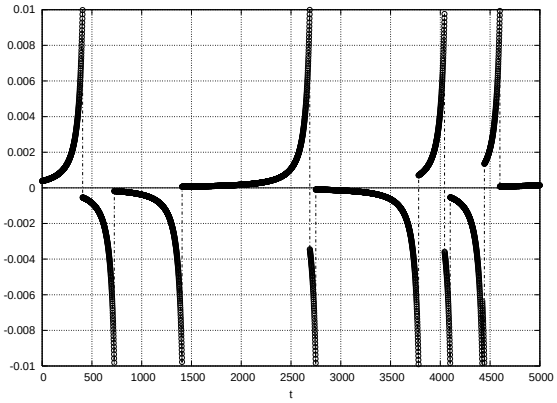

Figure 5.1. Auxiliary fluctuation $\xi_A(t)$ for $\mu = 1.666$ and $\alpha = 0.01$.

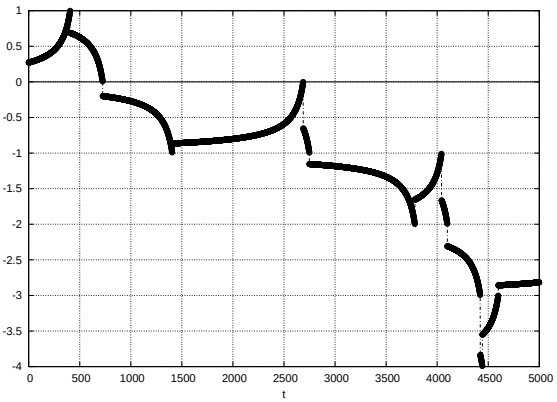

Figure 5.2. Plot of the motion in Eq. 5.32 for $\mu = 1.666$ and $\alpha = 0.01$.

Let us focus now our attention on the diffusion process described by

$$\frac{d}{dt}x(t) = \xi_A(t). \tag{5.32}$$

Figs. 5.1 and 5.2 show example functions $x(t)$ and $\xi_A(t)$. In this case, it is expected that the fluctuation $\xi_A(t)$ will produce a sub-diffusion process with the anomalous scaling of Eq. (5.27) with μ meeting the condition of (5.23).

Let us explain the intuitive reasons that lead us to make the prediction of Eq. (5.27). As explained by the arguments of Section 5.1, the generalized diffusion equation of Eq.

(5.1) is derived from ordinary diffusion, by assuming that the time distance between two consecutive jumps of the random walker is given by the waiting time distribution $\psi(\tau)$. When the mean recrossing time in one site is infinite, the process of ordinary diffusion is turned into a process of sub-diffusion with the anomalous scaling δ of Eq. (5.27). For the attainment of this result it does not matter whether the walker position remains rigorously unchanged in the time interval between two abrupt jumps, or not. The adoption of the fluctuation $\xi_A(t)$ rather than of the idealized picture to which Eq. (5.1) refers, is useful for the practical purpose of numerical simulation. In fact, it assigns to the time size of the critical events a finite rather than a vanishing measure. The idealized condition would be realized by decreasing the time size of the critical events, but increasing at the same time the computational time, which would become infinite to reproduce the idealized condition.

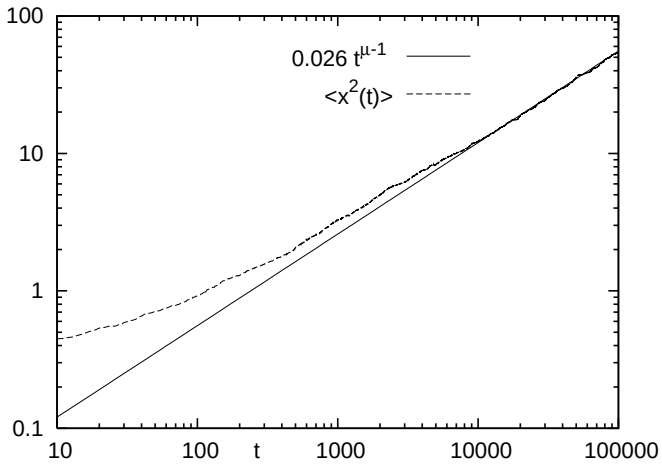

Figure 5.3. The time evolution of the second moment of $x(t)$ for CTRW, generated by the diffusion process of Eq. (5.20). The dashed curve is the numerical result and the solid curve represents the theoretical prediction of Eq. (5.27) with $\mu = 1.666$.

To check the theoretical prediction, let us look at the result of this numerical simulation in Fig. 5.3. The anomalous scaling of the diffusion process generated by the

fluctuation $\xi_A(t)$ is evaluated through the second moment of the probability distribution density, which shows that, in the asymptotic limit, the numerical scaling becomes identical to the theoretical scaling of Eq. (5.27).

Eq. (5.1), which is an evident expression of density memory emerges from the time evolution of a bunch of trajectories, with no memory. After a jump, the quantity $\xi_A(t)$ undergoes a time evolution determined by a random choice of initial condition, with no memory whatsoever of the time evolution of $\xi_A(t)$ prior to the last jump.

5.3. On the Dynamical Nature of the Memory Kernel of the Ctrw Generalized Diffusion Equation

This Section shows that the memory kernel $\Phi(t)$ of the generalized diffusion equation of Eq. (5.1) is not an equilibrium correlation function. Eq. (5.32) gives

$$x(t) = \int_0^t \xi_A(t')dt'. \tag{5.33}$$

This means that, as in the earlier section, all the walkers move from $x = 0$ at $t = 0$. The second moment of this diffusion process reads

$$< x(t)^2 >= \int_0^t dt' \int_0^t dt'' < \xi_A(t')\xi_A(t'') > . \tag{5.34}$$

Since the correlation function of ξ_A is not stationary, the integrand can not be written in terms of $t - t'$ as in Eq.2.8. By differentiating Eq. (5.34) twice with respect to time, we obtain

$$\frac{d^2}{dt^2} < x^2(t) >= 2 < \xi_A^2(t) > +2 \int_0^t dt' \frac{d}{dt} < \xi_A(t)\xi_A(t') > . \tag{5.35}$$

On the other hand, using Eq. (5.19) (App. L), we get

$$\frac{d^2}{dt^2} < x^2(t) >= 2D\Phi(t). \tag{5.36}$$

By comparing Eq. (5.35) to Eq. (5.36) we arrive at the important equality

$$D\Phi(t) =< \xi_A^2(t) > + \int_0^t dt' \frac{d}{dt} < \xi_A(t)\xi_A(t') > . \tag{5.37}$$

This relation shows that $\Phi(t)$ is *not* a correlation function. $\Phi(t)$ is related to a true correlation function, $< \xi_A(t)\xi_A(t') >$, by a functional relation, and the true correlation function is not stationary.

Let us try to find the functional form of the memory kernel, $\Phi(t)$. As shown in Section 5.2, all the systems of the Gibbs ensemble are prepared in the condition where $\xi(0) = y_0^{\mu/(\mu-1)}$, where y_0 is the initial random position. After this initial value, which is equivalent to the condition created by a jump occurring at $t = 0$, a long time is required to meet again another jump. Let us discuss here the ideal condition where the time interval between two significant fluctuations is really empty. To fill it, infinitely many other trajectories must be generated to produce significant fluctuations in this empty time interval. In the book of Feller [42] (see also Ref. [43]), it is shown that the density of events goes as $t^{2-\mu}$, which gives

$$< \xi_A^2(t) >= \frac{C}{(t+T)^{2-\mu}}, \tag{5.38}$$

and

$$< \xi_A(t)\xi_A(t') >= \frac{C}{(t+T)^{2-\mu}} F(t-t'), \tag{5.39}$$

respectively. With some algebra (App. M), we find

$$D\Phi(t) = -\frac{(2-\mu)C\hat{F}(0)}{(T+t)^{3-\mu}} + \frac{C}{(T+t)^{2-\mu}} F(t). \tag{5.40}$$

The adoption of fractional [47, 48] rather than integer derivatives is becoming more and more popular to address the study of complex systems. An interesting recent example is given by the work of Sokolov and KlafterRef in [33]. It is written here with a notation change so as to make it easier to see the connection with the other results.

$$\frac{\partial}{\partial t} p(x,t) = \frac{1}{\Gamma(2-\mu)} \frac{d}{dt} \int_0^t d\tau \frac{1}{(t-\tau)^{2-\mu}} \frac{\partial^2}{\partial x^2} p(x,\tau), \tag{5.41}$$

with the power index μ meeting the condition of Eq. 5.23. The term on the right-hand side of this equation can be expressed by means of the Riemann-Liouville fractional

derivative [47, 48] defined in general by

$$\frac{d^\alpha}{dt^\alpha} f(t) = \frac{1}{\Gamma(n-\alpha)} \frac{d^n}{dt^n} \int_0^t (t-t')^{n-\alpha-1} f(t') dt', \tag{5.42}$$

with n being the smallest integer exceeding α. With this definition, Eq. 5.41 reads

$$\frac{\partial}{\partial t} p(x,t) = \frac{\Gamma(\alpha)}{\Gamma(2-\mu)} \frac{d^{1-\alpha}}{dt^{1-\alpha}} \frac{\partial^2}{\partial x^2} p(x,t), \tag{5.43}$$

with $\alpha = \mu - 1$.

The authors of Ref. [33] found the interesting result that the same diffusion process can be expressed by means of

$$\frac{\partial^\alpha}{\partial t^\alpha} p(x,t) = \frac{\partial^2}{\partial x^2} p(x,t), \tag{5.44}$$

provided that use is made of the Caputo fractional derivative, advocated by Mainardi [47, 48], defined by

$$\frac{d^\alpha}{dt^\alpha} f(t) = \frac{1}{\Gamma(n-\alpha)} \int_0^t (t-t')^{n-\alpha-1} \frac{d^n}{dt^n} f(t') dt'. \tag{5.45}$$

Sokolov and Klafter [33] compare their GDE to the GDE of Kenkre and Knox [35], which is formally identical to Eq. 5.19, and point out as striking difference between this equation and the equation proposed by Kenkre and Knox [35] the additional time derivative in the front of the integral. Actually, their equation is equivalent to the generalized master equation of Eq. 5.15 and the additional time derivative has a physical meaning that will be properly explained.

For this purpose, let us write again Eq.5.41 in the slightly different form

$$\frac{\partial}{\partial t} p(x,t) = \frac{1}{\Gamma(2-\mu)} \frac{d}{dt} \int_0^t d\tau \frac{1}{(T+t-\tau)^{2-\mu}} \frac{\partial^2}{\partial x^2} p(x,\tau), \tag{5.46}$$

with T denoting a time interval that will be to sent to zero at a given phase of this discussion. By differentiating with respect to time, Eq. 5.46 is written in the following form

$$\begin{aligned} \frac{\partial}{\partial t} p(x,t) &= \frac{1}{\Gamma(2-\mu) T^{2-\mu}} \frac{\partial^2}{\partial x^2} p(x,t) \\ &\quad - \frac{(2-\mu)}{\Gamma(2-\mu)} \int_0^t d\tau \frac{1}{(T+t-\tau)^{3-\mu}} \frac{\partial^2}{\partial x^2} p(x,\tau). \end{aligned} \tag{5.47}$$

This means that this result can be obtained from Eq. 5.15 and so from the form of Kenkre and Knox [35] by adopting for the memory kernel $\Phi(t)$ the following expression

$$D\Phi(t) = \frac{\delta(t)}{\Gamma(2-\mu)T^{2-\mu}} - \frac{(2-\mu)}{\Gamma(2-\mu)}\frac{1}{(T+t)^{3-\mu}}. \tag{5.48}$$

A complete equivalence with the fractional derivative perspective is established by assuming

$$\frac{C}{(T+t)^{2-\mu}}F(t) = \frac{\delta(t)}{\Gamma(2-\mu)T^{2-\mu}}. \tag{5.49}$$

This is equivalent to assuming that the the decay of $F(t)/(T+t)^{2-\mu}$ is significantly faster that $1/t^{3-\mu}$.

These theoretical remarks are checked by the numerical calculation of the non-stationary correlation function $< \xi_A(t)\xi_A(t') >$. In Fig. 5.4, the plot $F(t)$ proves that it is in fact significantly faster than $1/t^{3-\mu}$.

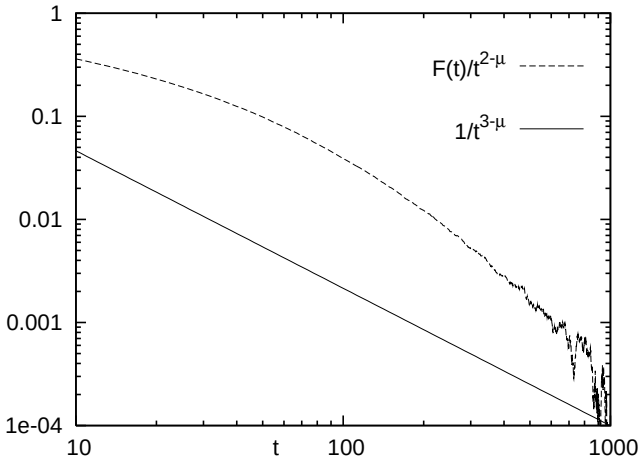

Figure 5.4. $F(t)/t^{2-\mu}$ (dashed) and $1/t^{3-\mu}$ (solid).

5.4. The Stochastic Liouville Approach

Let us now address the problem of density (Eq. 5.1) for super-diffusion. Consider the following diffusion equation

$$\frac{d}{dt}x(t) = \xi_K(t). \tag{5.50}$$

This equation is formally equivalent to Eq. (2.6), but the stochastic variable $\xi_K(t)$ is not Gaussian.

Let us adopt the Liouville formalism and let us write the time evolution of the total probability density $\rho(x, \xi_K, t)$ as follows

$$\frac{d}{dt}\rho(x, \xi_K, t) = L_T\rho(x, \xi_K, t) \equiv \left\{-\xi_K \frac{d}{dx} + L_B\right\}\rho(x, \xi_K, t). \tag{5.51}$$

The operator L_B is responsible for the time evolution of the probability density of ξ_K, namely, it is a bath operator. Following the stochastic Liouville approach of Kubo [36, 37, 38], let us consider the density $\rho(x, \xi_K, t)$ as a vector state to expand in the basis set of the eigenstates of L_B. In the stationary case the bath operator must have an eigenstate $|0>$ with vanishing eigenvalue,

$$L_B|0>= 0. \tag{5.52}$$

From within this quantum-like formalism, the out-of-equilibrium properties of the bath must be taken into account. The non-equilibrium eigenstates $|\mu>$, with $\mu \neq 0$, are defined by

$$L_B|\mu>= i\omega_\mu|\mu> . \tag{5.53}$$

With no loss of generality, let us assume

$$\omega_{-\mu} = -\omega_\mu \tag{5.54}$$

and

$$|\mu>= |\omega_\mu>= |\omega> . \tag{5.55}$$

The variable ξ_K becomes the operator defined by

$$\xi_K|0>= \sum_{\mu\neq 0} K_\mu|\mu>, \qquad \xi_K|\mu>= |0> \tag{5.56}$$

and the probabilities are set as

$$p_0(x, t) \equiv< 0|\rho(x, \xi_K, t)> \tag{5.57}$$

and

$$p_\mu(x, t) \equiv< \mu|\rho(x, \xi_K, t)> . \tag{5.58}$$

The projection over the bath eigenstates create reduced densities corresponding to the bath at equilibrium, Eq. (5.57), and to the bath in an out of equilibrium condition, Eq. (5.58). By projecting Eq. (5.51) over the bath equilibrium state and the bath excited states, we obtain

$$\frac{d}{dt}p_0(x,\,t) = -\sum_{\mu} < 0|\xi_K|\mu > \frac{d}{dx}p_\mu(x,\,t) \tag{5.59}$$

and

$$\frac{d}{dt}p_\mu(x,\,t) = i\omega_\mu p_\mu(x,\,t) - < 0|\xi_K|\mu > \frac{d}{dx}p_0(x,\,t), \tag{5.60}$$

with μ running from $-\infty$ to ∞, respectively. The formal solution of Eq. (5.60) is

$$p_\mu(x,\,t) = -\int_0^t dt' exp\left(i\omega_\mu(t-t')\right) < \mu|\xi_K|0 > p_0(x,\,t'). \tag{5.61}$$

By plugging Eq. (5.61) in Eq. (5.59) we get

$$\frac{d}{dt}p_0(x,\,t) = \int_0^t dt' \Phi_K(t-t')\frac{\partial^2}{\partial x^2}p_0(x,\,t'), \tag{5.62}$$

where

$$\Phi_K \equiv \sum_{\mu} e^{i\omega_\mu t} < 0|\xi_K|\mu >< \mu|\xi_K|0 > . \tag{5.63}$$

By moving from the discrete- to the continuous-frequency picture, and using Eq. (5.54) as well, the memory kernel of Eq. (5.62) is written under the following form

$$\Phi_K(t) = \int d\omega cos(\omega t)\Pi(\omega), \tag{5.64}$$

where

$$\Pi(\omega) = 2 < 0|\xi_K|\omega >< \omega|\xi_K|0 > . \tag{5.65}$$

Note that in this case the memory kernel $\Phi_K(t)$ is the equilibrium correlation function of the stochastic variable ξ_K.

According to the work of Ref. [39] the Generalized Diffusion Equation (GDE) of Eq. (5.62) is the exact equation of motion for the density $p(x,\,t)$ if the fourth-order

correlation functions of ξ_K fulfills the factorization condition

$$< \xi_k(t_4)\xi_k(t_3)\xi_k(t_2)\xi_k(t_1) >=< \xi_k(t_4)\xi_k(t_3) >< \xi_k(t_2)\xi_k(t_1) > \tag{5.66}$$

and the higher-order correlation functions the analogous factorization conditions, so that at equilibrium the condition

$$< \xi_k^{2n} >=< \xi_k^2 >^n \tag{5.67}$$

applies. This seems to be the natural property of a dichotomous variable, which is referred as Dichotomous Factorization (DF) property. It is important to point out that in the renewal and non-exponential case this condition is violated even if the stochastic variable has only two values [40].

It is worth making a final remark concerning the form of $\Phi_K(t)$. The model of non-Ohmic bath is discussed by several authors [44, 45, 46]. Let us select $\Pi(\omega) \propto \omega^{\eta-1}$, and see that in the time asymptotic limit

$$\Phi_K(t) \propto \frac{1}{t^\eta} \text{ for } 0 < \eta < 1 \tag{5.68}$$

and

$$\Phi_K(t) \propto -\frac{1}{t^\eta} \text{ for } 1 < \eta < 2. \tag{5.69}$$

The former state, called sub-Ohmic, is separated from the latter, called super-Ohmic, by the singular condition $\eta = 1$, corresponding the a fast relaxation, given by a delta of Dirac. In section 7, we will see that $\xi_K =$ sign ξ_G fits these properties, where ξ_G is the Gaussian fluctuation obtained by using the non-Ohmic prescription.

It is worth remarking that a GDE with the form of Eq. (5.62) was found many years ago by Kenkre and Knox [35]. These authors pointed out that this equation is exactly equivalent to the GDE generated by the adoption of the CTRW method. This is a so important observation as to force us in Section 5.1 to illustrate this argument for the sake of reader's convenience.

5.5. Dynamical Origin of the Time Convoluted Diffusion Equation

In this Section, the form of fluctuation yielding Eq. (5.62) will be illustrated. To establish this form, it is necessary to meet the constraint that the correlation function $\Phi_K(t)$ has the time asymptotic form as that discussed in Section 5.4, and the constraint that the higher-order correlation functions obey the DF property as well.

To generate the stochastic process $\xi_K(t)$, first the Gaussian fluctuation is drived which is responsible for the dynamic derivation of FBM as in chapter 3. To do that, the standard procedure is adopted as illustrated in Ref. [46],

$$\xi_G(t) = \sum_i c_i \left[x_i(0) \cos \omega_i t + v_i(0) \omega_i^{-1} \sin \omega_i t \right]. \tag{5.70}$$

This means that the fluctuation $\xi_G(t)$ is derived from the sum of infinitely many oscillator coordinates. Initial positions and velocities of the oscillators are randomly selected from a canonical distribution and $c_i^2 \propto \omega_i^{\eta-1}$, thereby making Gaussian the random variable $\xi(t)$. It is straightforward to show that the correlation function $\Phi_\xi(t)$ has the following asymptotic [45],

$$\Phi_\xi(t \to \infty) \propto \text{sign}(1-\eta)/t^\eta. \tag{5.71}$$

Actually, for computational reasons, rather than using Eq. (5.70), the fluctuation of $\xi_G(t)$ with the correlation function of Eq. (5.64) is obtained by means of the algorithm of Ref. [7]. In the numerical simulations time is discrete, $t_n = n = 1, 2, 3, \ldots$. The random variable $\xi_{eq}(n)$ with correlation function given by Eq. (5.71) with either positive or negative tail is generated with the algorithm

$$\xi_{eq}(n) = \frac{2}{\pi} \sum_{m=-\infty}^{\infty} Z_{m+n} \int_0^{\pi/2} \sqrt{\phi(y)} \cos(2my) dy \,. \tag{5.72}$$

Here, Z_n is a Gaussian ensemble of random numbers with $< Z_n >= 0$ and $< Z_n^2 >= \xi_0^2$, and the function $\phi(y)$ is determined through its Fourier series, $\phi(y) = 1 + 2 \sum_{k=1}^{\infty} \Phi_\xi(k) \cos(2ky)$.

Using algorithm (5.72), which serves the purpose of generating a fluctuation equivalent to that Eq. (5.70), it is possible for us to find the fluctuation $\xi_K(t)$, responsible for the diffusion process of Eq. (5.62).

Let us see how to derive $\xi_K(t)$ from $\xi_G(t)$, namely from $\xi_{eq}(t)$. In chapter 3, we have seen that the corresponding waiting function of the time distance between two consecutive recrossing values of $\xi_{eq}(t) = 0$ is exponential. In the renewal case, the exponential waiting time would generate a master equation with no memory. To generate the master equation of (5.62), trajectory memory is needed. To prove the existence of trajectory memory in the recrossing process, it is also showed that the correlation function of recrossing is not delta function.

The fluctuation $\xi_K(t)$ is generated by the prescription

$$\xi_K(t) \equiv sign(\xi_G(t)). \tag{5.73}$$

It is first proved that the correlation function of $\xi_K(t)$ is the same as that of $\xi_G(t)$. Fig. 5.5 shows that the time asymptotic property of the correlation function of $\xi_K(t)$ are the same as those of the original fluctuation $\xi_G(t)$. Thus, the important constraint of yielding the same correlation function as that playing the role of the memory kernel of Eq. 5.62 is fulfilled. Finally, in Fig. 5.6, we see that the DF property is fulfilled.

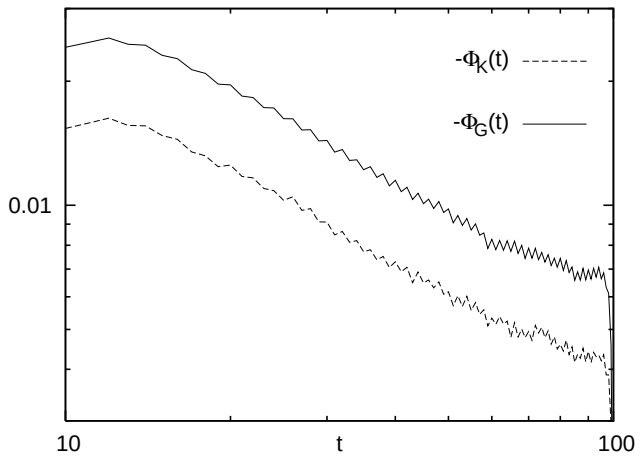

Figure 5.5. Time asymptotic properties of the correlation function of dichotomous fluctuation (dashed) and original fluctuation for $H = 1/3$ (solid).

In conclusion, to create the dichotomous fluctuation responsible for the diffusion process described by Eq. 5.62, the same Gauss fluctuation, which is generated by a non-Ohmic bath, and used in chapter 3 for the dynamic derivation of FBM, is used. It is

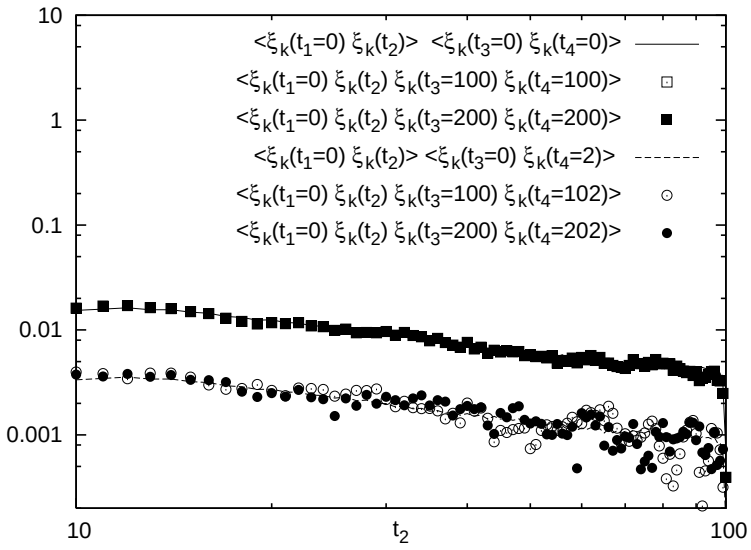

Figure 5.6. The DF property of Eq.5.66 is proved numerically. In the upper part, when $t_3 = t_4 = 100$ (empty square) and $t_3 = t_4 = 200$ (full square) the curves coincide with $< \xi\ \xi(t_2) >< \xi^2 >$ (solid). In the lower part, when $t_3 = 100$, $t_4 = 102$ (empty circle) and $t_3 = 200$, $t_4 = 202$ (full circle) the curves coincide with $< \xi\ \xi(t_2) >< \xi\ \xi(2) >$ (dashed).

proved numerically that the dichotomous signal, obtained by considering only the sign of this Gaussian fluctuation, produces a correlation function with the same fat tail as the memory kernel of Eq. 5.62. It is also proved that this dichotomous signal yields the DF property that, according to Ref. [39], the fluctuation $\xi_K(t)$ must have to be a proper generator of Eq. 5.62.

The time convoluted equation of Eq. 5.1 is formally equivalent to Eq. 5.62, and as a consequence, we would be tempted to conclude that these two equations are also physically equivalent. A recent example of this conviction is given by the interesting work of Budini [49]. Budini adopts a quantum mechanical picture that is similar to that illustrated in the classical case of Section 5.4, insofar as rather than expressing the memory kernel as the sum of many coherent components, he does express it as the sum of infinitely many exponential processes. As a result of this procedure he gets a time convoluted master equation equivalent to the adoption of the CTRW procedure, in the same way as Eq. 5.1 is formally equivalent to Eq. 5.62. The condition of sub-diffusion

makes it legitimate to claim for this equivalence, with the warning though of considering the results of Section 5.3 proving that within the Liouville perspective the memory kernel of the time convoluted equation is an equilibrium correlation function, while in the CTRW perspective is not.

In the case of super-diffusion, it is impossible to derive the time convoluted diffusion equation of Eq. 5.62 from within the CTRW perspective. This fits the conclusions of Balescu [34]. It is interesting to notice that in this case the memory density reflects correctly the trajectory density. In fact, albeit with the help of numerical rather than only by means of theoretical arguments, in Section 5.5 it is proved that the dichotomous fluctuation ξ_k, with trajectory memory, generates the diffusion process driven by Eq. 5.62. The search for the dichotomous fluctuation responsible for this kind of diffusion traces back to the work of Ref. [39] and to the earlier work of Ref. [50]. The failure of these earlier attempts is due to the fact that renewal fluctuations, namely memoryless trajectories, have been searched as generators of this diffusion process. Ref. [51] shows that the renewal condition violates the DF condition which is essential for the validity of Eq. 5.62. To solve this long-standing problem, it was necessary to shed light first of all on the confusion, existing in literature, between density and trajectory memory. The diffusion process described by Eq. 5.62 turned out to be characterized by both trajectory and density memory.

CHAPTER 6

CONCLUSION

In this work, It has been proved that the FBM fits the constraint of yielding both an infinite memory, resulting from the cooperation of the individual bath constituents, and the renewal aging. To prove that the former property is compatible with the latter it was necessary to defeat the prejudice that the FBM infinite memory establishes correlation among different recrossing of $x = 0$. The variable $x(t)$ generates non-Poisson renewal and the highly correlated nature of the variable $\xi(t)$ is a signature of cooperation. The important role of cooperation seems to be weakened by the condition $H = 0.5$, which generates non-Poisson renewal without involving any cooperation. However, it must be stress that this is a singularity, and that an even small deviation generates trajectory memory, as a reflection of cooperation.

Since FBM is a process with infinitely long range memory dependence, it is not easy to simulate numerically. The renewal and cooperation model is not successful because of limited numerical environment but it helps to explain the picture behind the FBM. There are two successful methods of generating FBM for both sub-diffusion and super-diffusion case. In the first one, using Fourier method, it was possible to generate correlated noise as much as required but the power law function has to have a cut-off value. This method is better used for getting a large enough number of recrossing times. The second one, the Voss algorithm, has no cut-off value and it gives better scaling but the trajectory length is limited.

The process of surface growth is also studied. In that case, particles obey to the sticking rule and that causes a cooperation among the columns. The study the jumps of a reference column shows that the process is close to FBM. Also, single column is able to show the cooperation among the columns.

This thesis proves that the generally accepted conviction that FBM is a process with infinite memory is incorrect. In fact, the space variable in the asymptotic time regime yields the FBM scaling in a full agreement with the renewal theory. This thesis establishes the existence of two forms of memory:

(a) The trajectory memory. The single trajectories have memory of the earlier conditions. An example of this form of memory is the velocity generated by the non-Ohmic bath. In the non-Ohmic case the time evolution of the variable velocity, described by a generalized Langevin equation, depends on the past history of the variable itself.

(b) The density memory. In this case the time evolution of a probability distribution density depends on its past history through a time convoluted structure.

In chapter 5, it has been shown that the trajectory memory does not necessarily yield density memory. In fact, the diffusion equation generating the FBM scaling has a time dependent diffusion coefficient, but does not have a time convoluted structure as seen in the diffusion equation, Eq. 5.2. FBM is compared with a different kind of diffusion, CTRW, as seen in Eq. 5.1. The subordination approach to normal diffusion, resting on trajectory without memory, has, on the contrary, a time convoluted structure. This means that a non-Poisson renewal process, although corresponding to trajectories with memory erasing jumps, yields memory at the density level. In the third case, Liouville-like approach is studied, which shows both trajectory memory and density memory as in Eqs. 5.69, 5.69 and 5.62. This last approach is used to explain dichotomized fractional Brownian motion.

APPENDIX A

SOLUTION OF THE ORDINARY DIFFUSION EQUATION

The diffusion equation can be derived from the continuity equation. It states that a change in density in any part of the system is due to inflow and outflow of material into and out of that part of the system. Effectively, no material is created or destroyed.

$$\frac{\partial}{\partial t}p(\mathbf{r}, t) + \nabla \cdot \mathbf{j} = 0, \tag{A.1}$$

where $\mathbf{j}$ is the flux of the diffusing material. The diffusion equation can be obtained easily from this when combined with the Fick's first law, which assumes that the flux of the diffusing material in any part of the system is proportional to the local density gradient.

$$\mathbf{j} = -D\ \nabla p(\mathbf{r}, t). \tag{A.2}$$

If D is a constant, the equation reduces to the following linear equation:

$$\frac{\partial}{\partial t}p(\mathbf{r}, t) = D\nabla^2 p(\mathbf{r}, t) \tag{A.3}$$

Let us start the solution with the one dimensional equation.

$$\frac{\partial p}{\partial t} = D\frac{\partial^2 p}{\partial x^2} \tag{A.4}$$

Take Fourier transform with respect to x using $p(k, t) = \int_{-\infty}^{\infty} e^{-ikx}p(x, t)dx$. And so

$$\int_{-\infty}^{\infty} e^{-ikx}\frac{\partial^2}{\partial x^2}p(x, t) = \int_{-\infty}^{\infty}(-k^2)e^{-ikx}p(x, t)dx = -k^2 p(k, t) \tag{A.5}$$

by separation by parts. The equation becomes

$$\frac{\partial}{\partial t}p(k, t) = -k^2 Dp(k, t). \tag{A.6}$$

This is an first order differential equation. The solution is simply

$$p(k, t) = C(k)e^{-Dk^2 t}. \tag{A.7}$$

First, the expression of $C(k)$ is required. For $t = 0$, $C(k) = p(k, 0)$ and

$$p(k, 0) = \int_{-\infty}^{\infty} e^{-ikx}p(x, 0)dx. \tag{A.8}$$

The initial condition is $p(x, 0) = \delta(x)$. Since it is a delta function the answer will be the Green function. So, from the above equation simply, $p(k, 0) = 1 = C(k)$. And so

$$p(k, t) = e^{-Dk^2 t}. \tag{A.9}$$

This is the solution of the diffusion equation but it must be converted back to x space.

The inverse Fourier will be

$$p(x,t) = \frac{1}{2\pi}\int_{-\infty}^{\infty} e^{ikx} p(k,t)dk. \tag{A.10}$$

So,

$$p(x,t) = \frac{1}{2\pi}\int_{-\infty}^{\infty} e^{ikx} e^{-Dk^2 t} dk = \frac{1}{2\pi}\int_{-\infty}^{\infty} e^{-Dk^2 t + ikx} dk. \tag{A.11}$$

Let's play a little with the exponential part

(A.12)

$$-Dk^2 t + ikx = -Dt(k^2 - \frac{ikx}{Dt}) = -Dt\left[(k - \frac{ix}{2Dt})^2 + \frac{x^2}{4D^2t^2}\right] = -Dt\left[(k - \frac{ix}{2Dt})^2\right] - \frac{x^2}{4Dt}.$$

and put it into the integral

$$p(x,t) = \frac{1}{2\pi} e^{-\frac{x^2}{4Dt}} \int_{-\infty}^{\infty} e^{-Dt(k-\frac{ix}{2Dt})^2} dk. \tag{A.13}$$

Set $k - \frac{ix}{2Dt} = s$ and so $dk = ds$. The integral is

$$\int_{-\infty}^{\infty} e^{-Dts^2} ds = \sqrt{\frac{\pi}{Dt}} \tag{A.14}$$

Finally, we get the well-known solution.

$$p(x,t) = \frac{1}{2\pi} e^{-\frac{x^2}{4Dt}} \sqrt{\frac{\pi}{Dt}} = \frac{1}{\sqrt{4\pi Dt}} e^{-\frac{x^2}{4Dt}} \tag{A.15}$$

APPENDIX B

SOLUTION OF THE GENERALIZED DIFFUSION EQUATION OF FBM

Here will be shown the solution of the generalized diffusion equation,

$$\frac{\partial p}{\partial t} = D\left(\int_0^t \Phi_\xi(t)dt'\right)\frac{\partial^2 p}{\partial x^2}. \tag{B.1}$$

Take Fourier transform with respect to x and the equation becomes

$$\frac{\partial}{\partial t}p(k,t) = -k^2 D\left(\int_0^t \Phi_\xi(t')dt'\right)p(k,t). \tag{B.2}$$

Similar to App.A, the solution can be obtained as follows:

$$\frac{\partial p(k,t)}{\partial t}\frac{1}{p(k,t)} = -k^2 D\left(\int_0^t \Phi_\xi(t')dt'\right) \tag{B.3}$$

$$\ln p(k,t) = -k^2 D\left(\int_0^t\int_0^{t'} \Phi_\xi(t'')dt'dt''\right) + C'(t) \tag{B.4}$$

$$\ln p(k,t) = -k^2\frac{D}{2} < x^2(t) > + C'(t) \tag{B.5}$$

$$p(k,t) = C(t)\exp\left(-k^2\frac{D}{2} < x^2(t) >\right). \tag{B.6}$$

Using Eqn. D.7, $< x^2 >= 2 < \xi^2 > \int_0^t dt' \int_0^{t'} ds\Phi_\xi(|s|)$ and since ξ is Gaussian noise with zero average and unit mean $< \xi^2 >= 1$, Again, $C(k) = 1$ for $x(t=0) = 0$ and $p(x,0) = \delta(x)$ as App. A, and $C(t) = \exp(C'(t))$. And so

$$p(k,t) = e^{-\frac{D}{2}k^2 < x^2(t) >}. \tag{B.7}$$

The inverse Fourier will be as follows:

$$p(x,t) = \frac{1}{2\pi}\int_{-\infty}^{\infty} e^{ikx}e^{-\frac{D}{2}k^2 < x^2(t) >}dk \tag{B.8}$$

$$p(x,t) = \frac{1}{2\pi}\int_{-\infty}^{\infty} e^{-\frac{D}{2} < x^2(t) >\left[k - \frac{ix(t)}{D < x^2(t) >}\right]^2 - \frac{x^2(t)}{2D < x^2(t) >}}dk \tag{B.9}$$

$$p(x,t) = \frac{1}{2\pi}e^{-\frac{x^2(t)}{2D < x^2(t) >}}\int_{-\infty}^{\infty} e^{-\frac{D}{2} < x^2(t) >\left[k - \frac{ix(t)}{D < x^2(t) >}\right]^2}dk \tag{B.10}$$

$$p(x,t) = \frac{1}{2\pi}e^{-\frac{x^2(t)}{2D < x^2(t) >}}\sqrt{\frac{\pi}{\frac{D}{2} < x^2(t) >}} \tag{B.11}$$

$$p(x,\,t) = \frac{1}{\sqrt{2\pi D < x^2(t) >}} e^{-\frac{x^2(t)}{2D<x^2(t)>}} \tag{B.12}$$

APPENDIX C

ASYMPTOTIC SOLUTION OF THE GENERALIZED DIFFUSION EQUATION OF FBM

It will be shown that, when $t \to \infty$, Eqn. 2.3 is solution of Eqn. 2.4. Diffusion equation for FBM is

$$p_t = D\ C(t)\ p_{xx} \tag{C.1}$$

where $C(t) = \int_0^t dt' \Phi(t')$, $p = p(x,t)$, $p_t = \frac{\partial p}{\partial t}$ and $p_{xx} = \frac{\partial^2 p}{\partial x^2}$.

Using

$$p = \frac{t^{-H}}{\sqrt{4\pi D}} \exp\left(-\frac{x^2}{4D} t^{-2H}\right). \tag{C.2}$$

$$p_t = -\frac{1}{\sqrt{4\pi D}} exp\left(-\frac{x^2}{4D} t^{-2H}\right)\left\{H t^{-(H+1)} + \frac{x^2}{4D} t^{-(3H+1)}\right\} \tag{C.3}$$

$$p_x = \frac{t^{-H}}{4\pi D} exp\left(-\frac{x^2}{4D} t^{-2H}\right)\left(-\frac{2x t^{-2H}}{4D}\right) \tag{C.4}$$

$$p_{xx} = -\frac{1}{\sqrt{4\pi D}} exp\left(-\frac{x^2}{4D} t^{-2H}\right)\left\{\frac{1}{2D} t^{-3H} + \frac{x^2}{4D^2} t^{-5H}\right\} \tag{C.5}$$

we get

$$C(t) = \frac{p_t}{D\ p_{xx}} = \frac{H t^{-(H+1)} + \frac{x^2}{4D} t^{-(3H+1)}}{\frac{1}{2} t^{-3H} + \frac{x^2}{4D} t^{-5H}} = t^{2H-1} \frac{H t^{2H} + \frac{x^2}{4D}}{\frac{1}{2} t^{2H} + \frac{x^2}{4D}}. \tag{C.6}$$

For $H = 1/2$, C(t)=1, and

$$\lim_{t\to\infty} \frac{H t^{2H} + \frac{x^2}{4D}}{\frac{1}{2} t^{2H} + \frac{x^2}{4D}} = 2H \text{ for } H < 1/2 \tag{C.7}$$

$$\lim_{t\to\infty} \frac{H t^{2H} + \frac{x^2}{4D}}{\frac{1}{2} t^{2H} + \frac{x^2}{4D}} = \lim_{t\to\infty} \frac{H + \frac{x^2}{4D} t^{-2H}}{\frac{1}{2} + \frac{x^2}{4D} t^{-2H}} = 2H \text{ for } H > 1/2. \tag{C.8}$$

So, from Eqn. 2.14 for $D = \langle \xi^2 \rangle$ and $H = H$,

$$\lim_{t\to\infty} \frac{d}{dt} C(t) = 2H(2H-1) t^{2H-2} = \frac{\langle \xi^2 \rangle}{D} \Phi_\xi(t) = \Phi_\xi(t). \tag{C.9}$$

APPENDIX D

RELATION BETWEEN THE VARIANCE AND THE STATIONARY CORRELATION FUNCTION OF FBM

Evaluation of Eqn. 2.10.

(D.1)

$$< x^2(t) >= \int_0^t dt' \int_0^t dt'' < \xi^2 > \Phi_\xi(t', t'') =< \xi^2 > \int_0^t dt' \int_0^t dt'' \Phi_\xi(|t' - t''|).$$

We assume that Φ_ξ is stationary so it doesn't depend on initial time but just depends on time difference.

(D.2)
$$\Phi_\xi(t, t_0) = \Phi_\xi(|t - t_0|).$$

Let us divide the integral as in the sketch

(D.3)
$$< x^2 >=< \xi^2 > \int_0^t dt' \int_0^{t'} dt'' \Phi_\xi(|t' - t''|) + < \xi^2 > \int_0^t dt' \int_{t'}^t dt'' \Phi_\xi(|t' - t''|).$$

The second integral which is upper empty triangle can be written as

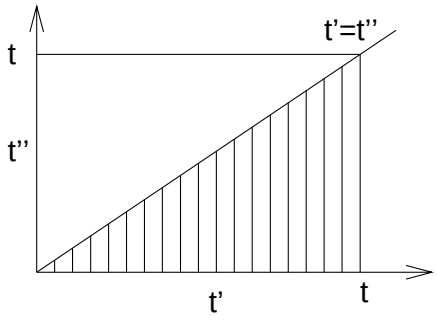

(D.4)
$$\int_0^t dt' \int_{t'}^t dt'' \Phi_\xi(|t' - t''|) = \int_0^t dt'' \int_0^{t''} dt' \Phi_\xi(|t' - t''|).$$

And transforming $t' \to t''$ and $t'' \to t'$, $\Phi_\xi(|t' - t''|)$ is unchanged.

(D.5)
$$\int_0^t dt'' \int_0^{t''} dt' \Phi_\xi(|t' - t''|) = \int_0^t dt' \int_0^{t'} dt'' \Phi_\xi(|t' - t''|).$$

Eqn. D.3 turns into

(D.6)
$$< x^2 >= 2 < \xi^2 > \int_0^t dt' \int_0^{t'} dt'' \Phi_\xi(|t' - t''|).$$

Using $s = t' - t''$ and $ds = -dt''$ for the integral inside, we get

(D.7)
$$< x^2 >= 2 < \xi^2 > \int_0^t dt' \int_0^{t'} ds \Phi_\xi(|s|).$$

Let us drive the same equation in another form. Starting with the first equation,

(D.8)
$$< x^2(t) >= \int_0^t dt' \int_0^t dt'' < \xi^2 > \Phi_\xi(t', t'') =< \xi^2 > \int_0^t dt' \int_0^t dt'' \Phi_\xi(|t' - t''|),$$

let us make the following change of integration variables:

(D.9)
$$t'' - t' = s_1, \;\; t'' + t' = s_2.$$

Note that

(D.10)
$$dt'dt'' = \begin{vmatrix} \frac{\partial t'}{\partial s_1} & \frac{\partial t'}{\partial s_2} \\ \frac{\partial t''}{\partial s_1} & \frac{\partial t''}{\partial s_2} \end{vmatrix} = \frac{1}{2} ds_1 ds_2$$

The integration domain turn to the following plot. The transformations of each corner point are as follows:

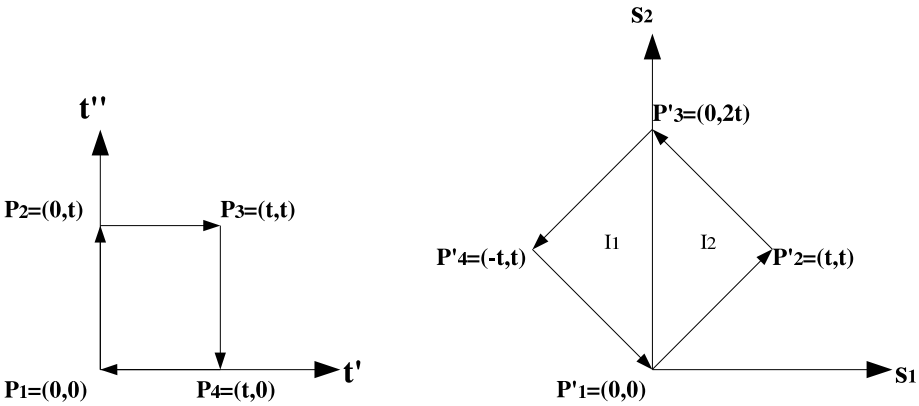

(D.11)
$$\begin{aligned}
P_1 = (0,0), &\quad t' = 0, \;\; t'' = 0 \;\; \Rightarrow \;\; s_1 = 0, \quad s_2 = 0, \quad P_1' = (0,0) \\
P_2 = (0,t), &\quad t' = 0, \;\; t'' = t \;\; \Rightarrow \;\; s_1 = t, \quad s_2 = t, \quad P_2' = (t,t) \\
P_3 = (t,t), &\quad t' = t, \;\; t'' = t \;\; \Rightarrow \;\; s_1 = 0, \quad s_2 = 2t, \quad P_3' = (0,2t) \\
P_4 = (t,0), &\quad t' = t, \;\; t'' = 0 \;\; \Rightarrow \;\; s_1 = -t, \quad s_2 = t, \quad P_4' = (-t,t)
\end{aligned}$$

The integral is divided into two parts.

$$\begin{aligned} \mathcal{I}_1 &= \int_{-t}^{0} ds_1 \int_{-s_1}^{s_1+2t} \Phi(s_1) = \int_{-t}^{0} ds_1 (2t + 2s_1)\Phi(s_1) \\ &= \int_{0}^{t} ds_1 (2t - 2s_1)\Phi(s_1) \end{aligned} \tag{D.12}$$

with $s_1 \to -s_1$ and using $\Phi(-s_1) = \Phi(s_1)$.

$$\mathcal{I}_2 = \int_0^t ds_1 \int_{s_1}^{-s_1+2t} \Phi(s_1) = \int_0^t ds_1 (2t - 2s_1)\Phi(s_1) = \mathcal{I}_1. \tag{D.13}$$

Finally, the result is

$$\begin{aligned} < x^2(t) > &= < \xi^2 > \tfrac{1}{2}[\mathcal{I}_1 + \mathcal{I}_2] = < \xi^2 > \tfrac{1}{2} 2 \int_0^t ds_1 (2t - 2s_1)\Phi(s_1) \\ &= 2 < \xi^2 > \int_0^t ds_1 (t - s_1)\Phi(s_1) \end{aligned} \tag{D.14}$$

APPENDIX E

RELATION BETWEEN THE VARIANCE AND THE SCALING OF FBM

Evaluation of the integral Eq. 2.20. More generally, Eqn. 2.3 is

$$p(x-x_0,|t-t_0|) = \frac{1}{\sqrt{4\pi D(|t-t_0|)^{2H}}} \exp\left(-\frac{(x-x_0)^2}{4D(|t-t_0|)^{2H}}\right). \tag{E.1}$$

for $x(t_0) = x_0$,then

$$< (x-x_0)^2 >= \int_{-\infty}^{\infty} (x-x_0)^2 p(x-x_0,|t-t_0|)dx \tag{E.2}$$

substitute $s = x - x_0$, $ds = dx$

$$< (x-x_0)^2 >= \int_{-\infty}^{\infty} s^2 \frac{1}{\sqrt{4\pi D(|t-t_0|)^{2H}}} \exp\left(-\frac{s^2}{4D(|t-t_0|)^{2H}}\right) ds \tag{E.3}$$

using $b = \frac{1}{4D(|t-t_0|)^{2H}}$

$$\begin{aligned} < (x-x_0)^2 > &= \textstyle\int_{-\infty}^{\infty} s^2 \sqrt{\frac{b}{\pi}} e^{-bs^2} ds \\ &= -\sqrt{\tfrac{b}{\pi}} \tfrac{\partial}{\partial b} \textstyle\int_{-\infty}^{\infty} e^{-bs^2} ds \\ &= -\sqrt{\tfrac{b}{\pi}} \tfrac{\partial}{\partial b} \sqrt{\tfrac{\pi}{b}} \\ &= -\sqrt{\tfrac{b}{\pi}} \sqrt{\pi} (-\tfrac{1}{2}) b^{-3/2} \\ &= \tfrac{1}{2b} = 2D|t-t_0|^{2H} \end{aligned} \tag{E.4}$$

If $x(t_0 = 0) = 0 = x_0$

$$< x^2(t) >= 2D|t|^{2H} \tag{E.5}$$

APPENDIX F

DIFFUSION ENTROPY

Entropy is

$$S(t) = -\int_{-\infty}^{\infty} p \ln(p) dx \tag{F.1}$$

where $p(x, t) = 1/t^{\delta} F(x/t^{\delta})$. Then,

$$S(t) = -\int_{-\infty}^{\infty} \frac{1}{t^{\delta}} F\left(\frac{x}{t^{\delta}}\right) \ln\left[\frac{1}{t^{\delta}} F\left(\frac{x}{t^{\delta}}\right)\right] dx. \tag{F.2}$$

Using $u = x/t^{\delta}$,

$$S(t) = -\int_{-\infty}^{\infty} F(u) \left[\ln F(u) - \delta \ln t\right] du. \tag{F.3}$$

$$= -\int_{-\infty}^{\infty} F(u) \ln F(u)\, du + \delta \ln t \int_{-\infty}^{\infty} F(u)\, du \tag{F.4}$$

$$= A + \delta \ln t \tag{F.5}$$

where

$$\int_{-\infty}^{\infty} p(x, t) dx = \int_{-\infty}^{\infty} \frac{1}{t^{\delta}} F\left(\frac{x}{t^{\delta}}\right) dx = \int_{-\infty}^{\infty} F(u)\, du = 1 \tag{F.6}$$

and

$$A = -\int_{-\infty}^{\infty} F(u) \ln F(u)\, du = \text{ constant.} \tag{F.7}$$

APPENDIX G

ON THE PROBABILITY OF THE RECROSSING TIMES

It is important to calculate the function $\psi_n(t)$, the probability density of occurrence of the nth recrossing at time t. The recrossing times are statistically independent so the probability of having 2 recrossing times together is $\psi_1(\tau_1)\psi_1(\tau_2) = \psi(\tau_1)\psi(\tau_2)$, where the probability of having 1 recrossing, $\psi_1(\tau)$, is just $\psi(\tau)$.

To get he probability $\psi_2(t)$, all possible intermediate time between 0 and t must be considered. Let us keep $\tau_1 + \tau_2 = t$, we have

$$\psi_2(t) = \int_0^t d\tau \psi_1(\tau)\psi_1(t-\tau). \tag{G.1}$$

Similarly, the function $\psi_n(t)$ is related to $\psi_{n-1}(t)$ by

$$\psi_n(t) = \int_0^t d\tau \psi_{n-1}(\tau)\psi_1(t-\tau), \tag{G.2}$$

Using the convolution theorem of Laplace transform, we get

$$\hat{\psi}_n(u) = \hat{\psi}_{n-1}(u)\hat{\psi}_1(u). \tag{G.3}$$

On the other hand,

$$\hat{\psi}_{n-1}(u) = \hat{\psi}_{n-2}(u)(\tau)\hat{\psi}_1(u). \tag{G.4}$$

That gives

$$\hat{\psi}_n(u) = \hat{\psi}_{n-2}(u)(\hat{\psi}_1)^2(u). \tag{G.5}$$

Bay iterating this procedure, we get

$$\begin{aligned} &\hat{\psi}_n(u) = \hat{\psi}_{n-3}(u)(\hat{\psi}_1)^3(u). \\ &\ldots \\ &\hat{\psi}_n(u) = \hat{\psi}_0(u)(\hat{\psi}_1)^n(u). \end{aligned} \tag{G.6}$$

Note that $\hat{\psi}_0(t) = \delta(t)$. That means the probability of having the 0th recrossing at $t > 0$ is zero since it is certainly at $t = 0$ that is $x(t_0 = 0) = 0$. An so $\hat{\psi}_0(t) = \mathcal{L}[\delta(t)] = 1$. Finally that gives the important result

$$\hat{\psi}_n(u) = (\hat{\psi}(u))^n. \tag{G.7}$$

APPENDIX H

LAPLACE TRANSFORM OF THE POWER LAW FUNCTION WITH SLOPE $1 < \mu < 2$

Let us consider

$$\phi(t) = \frac{(\mu-1)T^{\mu-1}}{(t+T)^{\mu}}. \tag{H.1}$$

From the work of Mauro Bologna [8]

$$\hat{\psi}(u) = \frac{(\mu-1)\Gamma(1-\mu)}{(uT)^{1-\mu}}\left[e^{uT} - E_{\mu-1}^{uT}\right], \tag{H.2}$$

where

$$E_{\mu-1}^{uT}(T) = \sum_{n=0}^{\infty}\frac{(uT)^{n+1-\mu}}{\Gamma(n+2-\mu)}. \tag{H.3}$$

Using Eqn. H.1, the Taylor series expansion of Eqn. H.3 and $\Gamma(2-\mu) = (1-\mu)\Gamma(1-\mu)$, we get:

$$\begin{aligned}\hat{\phi}(u) = -\frac{(\mu-1)\Gamma(1-\mu)}{(uT)^{1-\mu}}\Bigg\{&\frac{(uT)^{1-\mu}}{\Gamma(2-\mu)} + \frac{(uT)^{2-\mu}}{\Gamma(3-\mu)} + \frac{(uT)^{3-\mu}}{\Gamma(4-\mu)} + \cdots \\ &-1 - uT - \frac{1}{2}(uT)^2 - \frac{1}{6}(uT)^3 + \cdots\Bigg\} \\ &= \Bigg\{1 + \frac{\Gamma(2-\mu)(uT)}{\Gamma(3-\mu)} + \frac{\Gamma(2-\mu)(uT)^2}{\Gamma(4-\mu)} + \cdots \\ &-\Gamma(2-\mu)\left[(uT)^{\mu-1} + (uT)^{\mu} + \frac{1}{2}(uT)^{\mu+1} + \frac{1}{6}(uT)^{\mu+2} + \cdots\right]\Bigg\}.\end{aligned} \tag{H.4}$$

In the case of range $1 < \mu < 2$, the slowest decay is given by $(uT)^{\mu-1}$. Thus:

$$\lim_{u\to 0}\hat{\psi}(u) = 1 - \Gamma(2-\mu)T^{\mu-1}u^{\mu-1} \tag{H.5}$$

APPENDIX I

CORRELATION FUNCTION OF THE DIFFUSION VARIABLE OF FBM

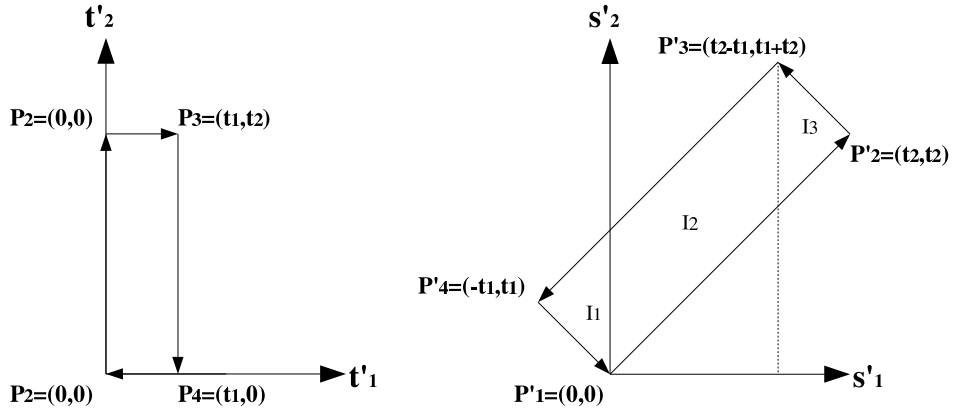

To find the correlation of $x(t)$, let consider the trajectory

$$x(t_1) = \int_0^{t_1} dt_1' \xi(t_1'). \tag{I.1}$$

The general form of the correlation is

$$\langle x(t_1)x(t_2)\rangle = \int_0^{t_1}\int_0^{t_2} dt_1' dt_2' \langle \xi(t_1')\xi(t_2')\rangle = \langle \xi^2\rangle \int_0^{t_1}\int_0^{t_2} dt_1' dt_2' \Phi_\xi(|t_2' - t_1'|). \tag{I.2}$$

Let us make the change of variable, for $0 < t_1 < t_2$,

$$\begin{aligned} s_1' &= t_2' - t_1' \\ s_2' &= t_2' + t_1' \end{aligned} \tag{I.3}$$

and so

$$dt_1' dt_2' = \begin{vmatrix} \frac{\partial t_1'}{\partial s_1'} & \frac{\partial t_1'}{\partial s_2'} \\ \frac{\partial t_2'}{\partial s_1'} & \frac{\partial t_2'}{\partial s_2'} \end{vmatrix} = \frac{1}{2} ds_1' ds_2' \tag{I.4}$$

The area of integration changes as seen in the plot. The transformations of each corner point are as follows:

(I.5)

$$\begin{array}{llllll} P_1 = (0,0), & t_1' = 0, \ t_2' = 0 & \Rightarrow & s_1' = 0, & s_2' = 0, & P_1' = (0,0) \\ P_2 = (0,t_2), & t_1' = 0, \ t_2' = t_2 & \Rightarrow & s_1' = t_2, & s_2' = t_2, & P_2' = (t_2,t_2) \\ P_3 = (t_1,t_2), & t_1' = t_1, \ t_2' = t_2 & \Rightarrow & s_1' = t_2 - t_1, & s_2' = t_2 + t_1, & P_3' = (t_2 - t_1, t_2 + t_1) \\ P_4 = (t_1,0), & t_1' = t_1, \ t_2' = 0 & \Rightarrow & s_1' = -t_1, & s_2' = t_1, & P_4' = (-t_1, t_1) \end{array}$$

After this, the integral is divided into there parts.

$$
\begin{aligned}
\mathcal{I}_1 &= \int_{-t_1}^{0} ds_1' \int_{-(s_1'+t_1)+t_1}^{(s_1'+t_1)+t_1} ds_2' \Phi_\xi(s_1') \\
&= \int_{-t_1}^{0} ds_1' 2(s_1'+t_1)\Phi_\xi(s_1') \\
&\quad \text{set } s_1' \to -s_1 \text{ and using } \Phi(-s_1) = \Phi(s_1) \\
&= -2\int_{t_1}^{0} ds_1 (t_1 - s_1)\Phi_\xi(s_1) = 2\int_0^{t_1} ds_1 (t_1 - s_1)\Phi_\xi(s_1)
\end{aligned} \tag{I.6}
$$

$$
\mathcal{I}_2 = \int_0^{t_2-t_1} ds_1' \int_{s_1'}^{s_1'+2t_1} ds_2' \Phi_\xi(s_1') = 2t_1 \int_0^{t_2-t_1} ds_1' \Phi_\xi(s_1') \tag{I.7}
$$

$$
\begin{aligned}
\mathcal{I}_3 &= \int_{t_2-t_1}^{t_2} ds_1' \int_{s_1'}^{-(s_1'-(t_2-t_1))+t_1+t_2} ds_2' \Phi_\xi(s_1') \\
&= 2\int_{t_2-t_1}^{t_2} ds_1' (t_2 - s_1')\Phi_\xi(s_1') \\
&= 2\int_0^{t_2} ds_1' (t_2 - s_1')\Phi_\xi(s_1') - 2\int_0^{t_2-t_1} ds_1' (t_2 - s_1')\Phi_\xi(s_1')
\end{aligned} \tag{I.8}
$$

Let us add the integrals to get the correlation.

(I.9)

$$
\begin{aligned}
&\langle x(t_1)x(t_2)\rangle = \tfrac{1}{2}\langle \xi^2\rangle [\mathcal{I}_1 + \mathcal{I}_2 + \mathcal{I}_3] \\
&= \langle \xi^2\rangle \left[\int_0^{t_1} ds_1' (t_1 - s_1')\Phi_\xi(s_1') + \int_0^{t_2-t_1} ds_1' t_1 \Phi_\xi(s_1') \right. \\
&\quad \left. + \int_0^{t_2} ds_1' (t_2 - s_1')\Phi_\xi(s_1') - \int_0^{t_2-t_1} ds_1' (t_2 - s_1')\Phi_\xi(s_1') \right] \\
&= \langle \xi^2\rangle \left[\int_0^{t_1} ds_1' (t_1 - s_1')\Phi_\xi(s_1') + \int_0^{t_2} ds_1' (t_2 - s_1')\Phi_\xi(s_1') - \int_0^{t_2-t_1} ds_1' (t_2 - t_1 - s_1')\Phi_\xi(s_1') \right]
\end{aligned}
$$

Repeating the same calculation for $0 < t_2 < t_1$, the same result will be obtained as t_1 and t_2 are interchanged because of the symmetry in Eqn. I.2. As a result, the correlation is

$$
\begin{aligned}
\langle x(t_1)x(t_2)\rangle &= \langle \xi^2\rangle \left[\int_0^{t_1} ds_1' (t_1 - s_1')\Phi_\xi(s_1') + \int_0^{t_2} ds_1' (t_2 - s_1')\Phi_\xi(s_1') \right. \\
&\left. - \int_0^{|t_2-t_1|} ds_1' (|t_2 - t_1| - s_1')\Phi_\xi(s_1') \right]
\end{aligned} \tag{I.10}
$$

Using Eqn.D.14, it can be written as

$$
\langle x(t_1)x(t_2)\rangle = \frac{1}{2}\left[< x^2(|t_1|) > + < x^2(|t_2|) > - < x^2(|t_1 - t_2|) > \right] \tag{I.11}
$$

and using Eqn. E.5, it becomes

$$
\langle x(t_1)x(t_2)\rangle = < \xi^2 > \left[|t_1|^{2H} + |t_2|^{2H} - |t_1 - t_2|^{2H} \right], \tag{I.12}
$$

which is the popular result found years ago by Mandelbrot and Van Ness [1].

If it is normalized to initial time, for $t_1 = t$ and $t_2 = t_0$, the result is

$$\begin{aligned} \frac{<x(t)x(t_0)>}{<x^2(t_0)>} &= (|t|^{2H} + |t_0|^{2H} - |t - t_0|^{2H})/2|t_0|^{2H} \\ &= \frac{1}{2}\left((\frac{|t|}{|t_0|})^{2H} + 1 - (\frac{|t-t_o|}{|t_0|})^{2H}\right) \\ &= \frac{1}{2}\left(\left|\frac{t}{t_0}\right|^{2H} + 1 - \left|\frac{t}{t_0} - 1\right|^{2H}\right) \end{aligned} \tag{I.13}$$

If $t_0 = -t$ and $t = t$ in Eqn. I.13, and $< x^2(-t) >=< x^2(|t|) >$, from Eqn. E.5

$$\frac{< x(t)x(-t) >}{< x^2(t) >} = \frac{1}{2}(2 - 2^{2H}) = 1 - 2^{2H-1}. \tag{I.14}$$

APPENDIX J

RELATION BETWEEN THE MEMORY KERNEL AND THE POWER LAW DISTRIBUTION OF CTRW

Let us consider the following picture

$$\mathbf{p}(t) = \sum_{n=0}^{\infty} \int_0^t \psi_n(\tau)\Psi(t-\tau)\mathbf{M}^n\mathbf{p}(0)d\tau. \tag{J.1}$$

The time convoluted structure of Eq. J.1 suggests the use of the Laplace transform method. Let us use the definition:

$$\hat{\phi}(u) = \int_0^{\infty} e^{-ut}\phi(t`)dt`. \tag{J.2}$$

Using App. G, we use the following result:

$$\hat{\psi}_n(u) = (\hat{\psi}(u))^n. \tag{J.3}$$

Given the important the fact that the last event occurred at $t` < t$, we have to make it sure that in the residual time of length $t - t`$ no event does occur. This is the reason why in Eq. J.1 we have to use the function $\Psi(t)$, whose meaning is defined by

$$\Psi(t) = \int_t^{\infty} \psi_1(t`)dt`. \tag{J.4}$$

Note that

$$\int_0^{\infty} \psi_1(t`)dt` = 1. \tag{J.5}$$

This is so because the distribution density $\psi_1(t)$ is a probability that one event occurs somewhere between $t = 0$ and $t = \infty$ must be 1. We do not know when the event occurs. We know that it does somewhere between $t = 0$ and $t = \infty$. Thus

$$\Psi(t) = \int_t^{\infty} \psi_1(t`)dt` = \int_0^{\infty} \psi_1(t`)dt - \int_0^t \psi_1(t`)dt` = 1 - \int_0^t \psi_1(t`)dt` \tag{J.6}$$

Using $\mathcal{L}[\int_0^t f(t')dt'] = \hat{f}(t)/u$ and $\mathcal{L}[1] = 1/u$ for $u > 0$, we find

$$\hat{\Psi}(t) = \frac{1 - \hat{\psi}(u)}{u}. \tag{J.7}$$

In conclusion, both $\psi_n(t)$ and $\Psi(t)$ can be expressed in terms of $\psi_1(t)$. This makes $\psi_1(t)$ so important that it is required to adopt a special notation for it, namely,

$$\psi(t) = \psi_1(t). \tag{J.8}$$

Let us evaluate the Laplace transform of Eq. J.1. We get:

$$\hat{\mathbf{p}}(t) = \sum_{n=0}^{\infty} \hat{\psi}_n(u)\hat{\Psi}(u)\mathbf{M}^n\hat{\mathbf{p}}(0). \tag{J.9}$$

Using Eq.J.3 and J.7, and assumption $\psi_0(t)\delta(t)$, we get:

$$\begin{aligned} \hat{\mathbf{p}}(t) &= \textstyle\sum_{n=0}^{\infty}(\hat{\psi}(u))^n\frac{1}{u}(1-\hat{\psi}(u))\mathbf{M}^n\hat{\mathbf{p}}(0) \\ &= \textstyle\sum_{n=0}^{\infty}(\hat{\psi}(u)\mathbf{M}^n)^n\frac{1}{u}(1-\hat{\psi}(u))\hat{\mathbf{p}}(0). \end{aligned} \tag{J.10}$$

On the other hand,

$$\sum_{n=0}^{\infty}(\hat{\psi}(u)\mathbf{M}^n)^n = \frac{1}{1-\hat{\psi}(u)\mathbf{M}}. \tag{J.11}$$

Thus Eq. J.9 becomes:

$$\hat{\mathbf{p}}(t) = \frac{1}{u}\frac{1-\hat{\psi}(u)}{1-\hat{\psi}(u)\mathbf{M}}\hat{\mathbf{p}}(0). \tag{J.12}$$

This is a way to connect the distribution at time t to the initial state $\mathbf{p}(0)$. To establish the equivalence of Eq J.1 to

$$\frac{\partial}{\partial t}\mathbf{p}(t) = -\int_0^t d\tau\Phi(\tau)\mathbf{K}\mathbf{p}(t-\tau) = -\int_0^t d\tau\Phi(t-\tau)\mathbf{K}\mathbf{p}(\tau), \tag{J.13}$$

let us evaluate Laplace transform of Eq. J.13. We get:

$$u\hat{\mathbf{p}}(u) - \mathbf{p}(0) = -\hat{\Phi}(u)\mathbf{K}\bullet\hat{\mathbf{p}}(u), \tag{J.14}$$

yielding:

$$\mathbf{p}(u) = \frac{1}{u+\hat{\Phi}(u)\mathbf{K}}\mathbf{p}(0). \tag{J.15}$$

By comparing Eq. J.12 and Eq. J.15, we get:

$$u + \hat{\Phi}(u)\mathbf{K} = \frac{u(1-\hat{\psi}(u)\mathbf{M})}{(1-\hat{\psi}(u))}. \tag{J.16}$$

Thus we get:

$$\hat{\Phi}(u)\mathbf{K} = \frac{u\hat{\psi}(u)(1-\mathbf{M})}{(1-\hat{\psi}(u))}. \tag{J.17}$$

It is convenient to get

$$\mathbf{K} = \mathbf{M} - 1 \tag{J.18}$$

and from Eq. J.17,

$$\hat{\Phi}(u) = \frac{u\hat{\psi}(u)}{(1-\hat{\psi}(u))}. \tag{J.19}$$

APPENDIX K

DERIVATION OF THE AUXILARY FUNCTION

Let us find the equation of motion of

$$\frac{dy}{dt} = \alpha y^z, \tag{K.1}$$

where $z > 1$ and $0 < \alpha \ll 1$. For $z = 1$, it is ordinary random walk and the solution is easy. Sabstitute $u = y^{1-z}$ and so $du/dt = dy/dt(1-z)y^{-z}$.

$$\frac{du}{dt}\frac{y^z}{1-z} = \alpha y^z. \tag{K.2}$$

By eliminating y^z and integrating this equation we get:

$$u = (1-z)\alpha t + C = y^{1-z}. \tag{K.3}$$

For $t = 0$, $y = y_0$ so it gives $C = y_0^{1-z}$. And final form becomes:

$$y = \left[(1-z)\alpha t + y_0^{1-z}\right]^{\frac{1}{1-z}} \tag{K.4}$$

This is the position variable. To find the velocity, which is the stochastic noise, the derivative of Eq, K.4 is needed. That gives:

$$\frac{dy}{dt} = \xi_A = \frac{\alpha y_0^z}{\left[1-(z-1)\alpha y_0^{z-1} t\right]^{\frac{z}{1-z}}}. \tag{K.5}$$

Sabstituting

$$\mu = \frac{z}{z-1}, \tag{K.6}$$

we get:

$$\xi_A(t) = \frac{\alpha y_0^{\frac{\mu}{\mu-1}}}{\left[1 - y_0^{\frac{1}{\mu-1}}\frac{\alpha}{\mu-1}t\right]^{\mu}} \tag{K.7}$$

and also for Eq. K.4

$$y(t) = \frac{y_0}{\left[1 - y_0^{\frac{1}{\mu-1}}\frac{\alpha}{\mu-1}t\right]^{\mu-1}}. \tag{K.8}$$

The initial position y_0 is chosen randomly in $[0:1]$ and when $y(t=\tau) = 1$, the motion ends and restarts with a random initial position y_0. Now let us find the distribution of

these recrossing times τ. Firstly, we know that when $y = 1$, $t = \tau$, so using Eq. K.4, we get:

$$1 = \left[(1-z)\alpha\tau + y_0^{1-z}\right]^{\frac{1}{1-z}}. \tag{K.9}$$

Inverting the equation gives:

$$\tau = \frac{\mu-1}{\alpha}\left(\frac{1}{y_0^{\frac{1}{\mu-1}}} - 1\right). \tag{K.10}$$

It shows that any random number $0 < y_0 < 1$ will give us another random number $0 < \tau < \infty$.

Let us see the way to get the random numbers with the power law distribution

$$\psi(t) = (s-1)\frac{T^{s-1}}{t+T}, \tag{K.11}$$

where time unit T and the slope $s > 1$ are constants. Since $\int_0^\infty \psi(t)dt = 1$, we have:

$$\int_0^r (s-1)\frac{T^{s-1}}{t+T}dt < 1 \tag{K.12}$$

and

$$\int_r^\infty (s-1)\frac{T^{s-1}}{t+T}dt < 1 \tag{K.13}$$

If we consider the second integral, Eq, K.13, for any random number x with the uniform probability in $[0:1]$, and set it equal to the area under the integral as

$$x = \int_r^\infty (s-1)\frac{T^{s-1}}{t+T}dt, \tag{K.14}$$

then the time value $t = r$ can be any value in $[0:\infty]$ and will have the power law distribution as Eq. K.11. Calculating the integral we get:

$$r = T(x^{\frac{1}{1-s}} - 1), \tag{K.15}$$

which is the same equation as Eq. K.10 for $s = \mu$ and $T = \frac{\mu-1}{\alpha}$, showing that Eq. K.10 give random numbers τ with power law distribution.

If we use the other integral Eq. K.12, it will give $r = T((1-x)^{\frac{1}{1-s}} - 1)$. It gives the same distribution as Eq. K.15, because if x is random in $[0:1]$ so is $1-x$.

APPENDIX L

RELATION BETWEEN THE VARIANCE AND THE MEMORY KERNEL OF CTRW

$$
\begin{aligned}
< x^2 > &= \int_\infty^\infty x^2 p(x,t)dx \\
\tfrac{d}{dt} < x^2 > &= \int_\infty^\infty x^2 \tfrac{d}{dt} p(x,t)dx \\
&= \int_\infty^\infty x^2 \left(D \int_0^t \Phi(\tau) \tfrac{d^2}{dx^2} p(x, t-\tau)d\tau \right) dx \\
&= D \int_0^t \Phi(\tau) \int_\infty^\infty x^2 \tfrac{d^2}{dx^2} p(x, t-\tau)dx\,d\tau \\
&= D \int_0^t \Phi(\tau) 2 \int_\infty^\infty p(x, t-\tau)dx\,d\tau \\
&= D2 \int_0^t \Phi(\tau) \\
\tfrac{d^2}{dt^2} < x^2 > &= 2D\Phi(\tau)
\end{aligned}
\qquad \text{(L.1)}
$$

APPENDIX M

THE FORM OF MEMORY KERNEL OF CTRW

$$
\begin{aligned}
D\Phi(t) &= <\xi_A^2(t)> + \int_0^t dt' \frac{d}{dt} <\xi_A(t)\xi_A(t')> \\
&= \frac{C}{(t+T)^{(2-\mu)}} + \int_0^t dt' \frac{d}{dt}\left[\frac{C}{(t+T)^{2-\mu}} F(t-t')\right] \\
&= \frac{C}{(t+T)^{(2-\mu)}} + \int_0^t dt' \left[\frac{(\mu-2)C}{(t+T)^{3-\mu}} F(t-t') + \frac{C}{(t+T)^{2-\mu}} \frac{dF}{dt}\right] \\
&= \frac{C}{(t+T)^{(2-\mu)}} + \int_0^t dt' \frac{(\mu-2)C}{(t+T)^{3-\mu}} F(t-t') + \int_0^t dt' \frac{C}{(t+T)^{2-\mu}} \frac{dF}{dt} \\
&= \frac{C}{(t+T)^{(2-\mu)}} + \int_0^t du \frac{(\mu-2)C}{(t+T)^{3-\mu}} F(u) + \int_0^t du \frac{C}{(t+T)^{2-\mu}} \frac{dF}{dt} \\
&= \frac{C}{(t+T)^{(2-\mu)}} - \frac{(2-\mu)C}{(t+T)^{3-\mu}} \int_0^t F(u)du + \frac{C}{(t+T)^{2-\mu}}[F(t) - F(0)] \\
&= -\frac{(2-\mu)C}{(t+T)^{3-\mu}} \hat{F}(0) + \frac{C}{(t+T)^{2-\mu}} F(t)
\end{aligned}
\tag{M.1}
$$

where we used $u = t - t'$, $F(0) = 1$ and $\hat{F}(0) = \int_0^t F(u)du$.

REFERENCES

[1] Mondelbrot B. B., Van Ness J., *The Fractinal Brownian motions, fractional noises, and applications*, SIAM Rev., 10, 422 (1968).

[2] R. Failla, M. Ignaccolo, P. Grigolini and A. Schwettmann, Phys. Rev E 70 R, 010101 (2004).

[3] Weiss U., *The Fractal Geometry of Nature*, World Scientific, Singapore (1999).

[4] Pottier N., Physics A 317, 371 (2003).

[5] Mondelbrot B. B., *Quantum Dissipative Systems*, Freeman, New York (1977).

[6] Feder J., *The Fractals*, Plenum Press, New York (1988).

[7] F. M. Izrailev, A.A. Krokhin, and S. E. Ulloa,Phys. Rev. B 63, 041102(R) (2001).

[8] Bologna M., Chem. Phys. B, 284 (2002).

[9] Godreche G., Luck J. M., J. Stat. Phys., 104, 489 (2001).

[10] Aquino G., Bologna M., Grigolini P., West B. J., Phys. Rev. E, 70, 036105 (2004.

[11] Feder J., Fractals, Plenum Press, New York, London (1988).

[12] M. Kardar, G. Parisi, and Y.-C. Zhang, Phys. Rev. Lett. 56 889 (1986).

[13] H.E. Stanley and A. L. Barabasi, *Fractal Concepts in Surface Growth*, Cambridge University Press, Cambridge (1995).

[14] S. N. Majumdar and D. Das, Phys. Rev. E 71, 036129 (2005).

[15] M. Constantin, C. Dasgupta, P. P. Chatraphorn, S. N. Majumdar, and S. Das Sarma, Phys. Rev. E 69, 061608 (2004).

[16] J. -F. Muzy, E. Bacry, Phys. Rev. E 66, 056121 (2002).

[17] R. Zwanzig, J. Chem. Phys. 33, 1338 (1960).

[18] R. Zwanzig, *Nonequilibrium Statistical Mechanics*, Oxford University Press, Oxford (2001).

[19] H. Mori, Prog. Theor. Phys. 33, 423 (1965); 34, 399 (1965).

[20] *Memory Function Approaches to Stochastic Problems in Condensed Matter*, eds. M. W. Evans, P. Grigolini, G. Pastori Parravicini, Advances in Chemical Physics, Volume 62, J. Wiley New York (1985).

[21] U. Balucani, M. H. Lee and V. Tognetti, Phys. Rep. 373, 409 (2003).

[22] R. Zwanzig, Physica 30, 1109 (1964).

[23] I. Prigogine and P. Résibois, Physica 27, 629 (1961).

[24] R. Balescu, *Equilibrium and Nonequilibrium Statistical Mechanics*, Wiley-Interscience, New York (1975).

[25] B.B. Mandelbrot, *The Fractal Geometry of Nature*, Freeman, New York (1982).

[26] S. V. Muniandy and S.C. Lim, Phys. Rev. E 66, 021114 (2002).

[27] E.W. Montroll and G. H. Weiss, J. Math. Phys. 6, 167 (1975).

[28] V. M. Kenkre, E.W. Montroll, and M. F. Shlesinger, J. Stat. Phys. 9, 45 (1973).

[29] M. Annunziato, P. Grigolini and J. Riccardi, Phys. Rev. E 61, 4801 (2000).

[30] M. O. Cáceres, Phys. Rev. E 67, 016102 (2003).

[31] P. Grigolini, Phys. Lett. A 119, 157 (1986).

[32] V.M. Kenkre, Granular Matter 3, 23 (2001).

[33] I. M. Sokolov, J. Klafter, Chaos 15, 026103 (2005).

[34] R. Balescu, *Aspects of Anomalous Transport in Plasmas*, Francis & Taylor, London (2005).

[35] V. M. Kenkre and R.S. Knox, Phys. Rev. B 9, 5279 (1974).

[36] R. Kubo, Adv. Chem. Phys. 16, 101 (1969).

[37] R. Kubo, J. Phys. Soc. (Japan) 26 Suppl, 1 (1969).

[38] P. Grigolini, Chem. Phys. 38, 389 (1979).

[39] M. Bologna, P. Grigolini and B. J. West, Chem. Phys. 284, 115 (2002).

[40] P. Allegrini, P. Grigolini, L. Palatella, and B. J. West Phys. Rev. E 70, 046118 (2004).

[41] P. Allegrini, G. Aquino, P. Grigolini, L. Palatella, and A. Rosa, Phys. Rev. E 68, 056123 (2003).

[42] W. Feller, *An Introduction to Probability and Its Applications*, vol. 2, Wiley, New York (1971).

[43] M. Ignaccolo, P. Grigolini, and A. Rosa, Phys. Rev. E 64, 026210 (2001).

[44] D. Cohen, Phys. Rev. E 55, 1422 (1997).

[45] N. Pottier, Physica A 317, 371 (2003).

[46] U. Weiss, *Quantum Dissipative Systems*, 2nd edition, World Scientific, Singapore (1999).

[47] F. Mainardi, Chaos, Solitons and Fractals, 7, 1461 (1996).

[48] F. Mainardi, in *Fractals and Fractional Calculus in Continuum Mechanics*, Springer Verlag, Wien and New York (1997) A. Carpinteri and F. Mainardi eds., downladable from http://www.fracalmo.org.

[49] A. A. Budini, Phys. Rev. E 72, 056106 (2005).

[50] P. Allegrini, P. Grigolini, B.J. West, Phys. Rev. E 54, 4760 (1996).

[51] P. Allegrini, G. Aquino, P. Grigolini, L. Palatella, A. Rosa, and B. J. West, Phys. Rev. E, 70, 046118 (2004).